The Bell System Technical Journal

Vol. XXIV *April, 1945* *No. 2*

Piezoelectric Crystals in Oscillator Circuits

By I. E. FAIR

12.00 Introduction

A STUDY or an explanation of the performance of a piezoelectric crystal in an oscillator circuit involves a study or explanation of oscillator circuits in general and a study of the crystal as a circuit element. Nicolson[1] appears to have been the first to discover that a piezoelectric crystal had sufficient coupling between electrical electrodes and mechanical vibratory movement so that when the electrodes were suitably connected to a vacuum tube circuit, sustained oscillations were produced. In such an oscillator the mechanical oscillatory movement of the crystal functions as does the electrical oscillatory circuit of the usual vacuum tube oscillator. His circuit is shown in Fig. 12.1. Cady[2] independently though later made the same discovery, but he utilized it somewhat differently and expressed it differently. He found that when the electrodes of a quartz crystal are connected in certain ways to an electric oscillator circuit, the frequency is held very constant at a value which coincides with the period of the vibrating crystal. He made the further discovery that due to the very sharp resonance properties of the quartz crystal, the constancy in frequency to be secured was far greater than could be obtained by any purely electric oscillator.

The development of analytical explanations of the crystal controlled oscillator came along rather slowly. Cady explained the control in terms of operation upon the electrical oscillator to which the crystal was attached. He said that the "capacity" of the crystal changes rapidly with frequency in the neighborhood of mechanical resonance, even becoming negative. This "capacity" connected across the oscillator tuned circuit or in other places prevented the frequency from changing to any extent, as any frequency change caused such a "capacity" change in the crystal as to tend to tune the circuit in the other direction. Cady, however, devised one circuit, Fig. 12.2, in which no tuned electrical circuit was used, but he confined his explanation to "a mechanically tuned feedback path from the plate to the grid of the amplifier". Pierce[3] came along later with a two-electrode crystal connected between plate and grid, and no tuned circuit, and also with a

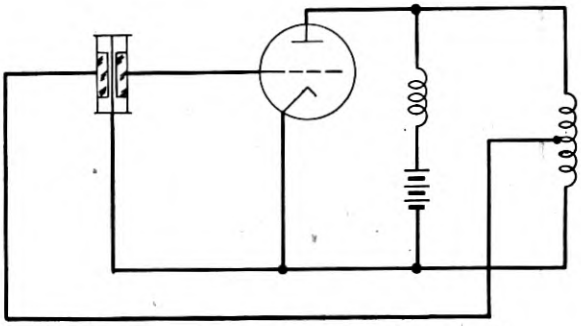

Fig. 12.1—Nicolson's crystal oscillator circuit

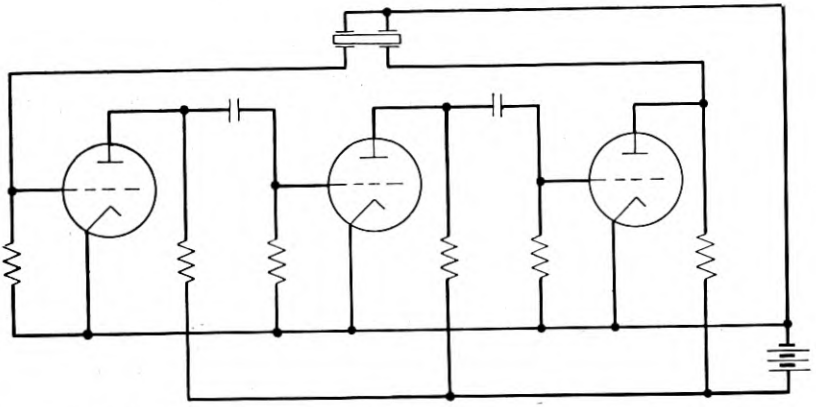

Fig. 12.2—Cady's oscillator circuit using a crystal as a "mechanically tuned feedback path"

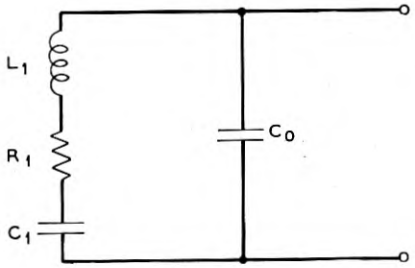

Fig. 12.3—Equivalent electrical circuit of a piezoelectric crystal near its resonant frequency

two-electrode crystal connected between grid and cathode and no tuned circuit, where the operation would not be satisfactorily explained by Cady's method. His circuits would require the crystal to exhibit inductive react-

ance, rather than the capacitance Cady spoke of. Miller[4] also produced a circuit with a two-electrode crystal connected between grid and cathode but with a tuned circuit in the plate lead, which circuit required the crystal to provide inductive reactance.

It was not until after Van Dyke[5] showed that the crystal could be represented by the circuit network of Fig. 12.3 that it was possible to explain these various phenomena. With this view of the crystal, and using the differential equation method of circuit analysis, Terry[6] pointed out that, as with electrical oscillators, the frequency is not completely governed by the resonant element, in this case the crystal, but is influenced somewhat by the circuit elements. The circuit as a whole is quite complex and the equations are difficult to use. Wright[7] and Vigoureux[8] also made analyses of the Pierce type oscillator. Because of the complexity of the equations, the frequency, amplitude, or activity are not computed directly, but the effects of the circuit variables are analyzed in a qualitative manner and the results compared with experimental data.

Oscillators employing crystals may be classified in a number of ways. One classification is based upon whether or not the circuit without the crystal is in itself an oscillator. If it is, the oscillator is called a "crystal controlled" oscillator. If it is not, it is called a "crystal" oscillator. All of Cady's oscillator circuits, except the one shown in Fig. 12.2, are of the first named class. This type of circuit will oscillate at a frequency determined by the tuned circuit if the crystal becomes broken or disconnected, or if high resistance develops in the crystal, or if the electric tuned circuit should become tuned too far from the resonant frequency of the crystal. This property at times is an advantage and at other times a disadvantage. This type of circuit will oscillate under control of the crystal with much less active crystals than most of the other types.

Nicolson's, Pierce's, Cady's of Fig. 12.2 and Miller's oscillators belong to the second named class. They will cease oscillating if the crystal breaks, develops high resistance or is disconnected. Failure of the oscillator to function at all then serves as a warning that something has happened to the crystal.

This second named class of crystal oscillators has been used much more than the first named. The crystal is the principal frequency determining element in the circuit. Often there are required only resistances, or resistances and an inductance, as the other elements to embody along with the vacuum tube and crystal. The simplicity, low costs, and usually no tuning, have made this class attractive. Most analytical studies of oscillator circuits have been made upon this class. For that reason the discussion in this chapter will be limited to this class.

An analytic study of the crystal oscillator can readily start by looking

upon the oscillator as consisting only of inductances, capacitances, and resistances, along with the vacuum tube. The crystal is replaced by the proper circuital elements arranged as in Fig. 12.3. This circuit or equivalent of the crystal is that of a series resonant circuit having capacitance paralleling it. The circuit will show both phenomena of series resonance and parallel resonance, the two frequencies being very close together. By making suitable measurements on a crystal, the magnitudes of the inductance, resistance, and the two capacitances can be determined. It is usually found that the series inductance is computed as hundreds or thousands of henries, and the series capacitance is a small fraction of a micromicrofarad. The magnitudes of the inductance and capacitance are beyond what it is possible to construct in the usual forms of building inductances and capacitances. This accounts for its superior frequency control properties.

Although reducing the crystal to an equivalent electrical circuit provides one notable step in understanding the performance of the crystal oscillator, it does not readily lead to a full understanding. The electric oscillator in itself is not fully and completely analyzed in all its ramifications, although it has been under study for over 25 years. These studies have been mathematical and experimental in character, but in all cases it appears there have been approximations of some kind, made because the variable impedance characteristics both of the plate circuit and the grid circuit of the tubes did not lend themselves readily to a rigorous analysis. The earlier investigations assumed a linear relation between grid voltage and plate current and assumed constant plate impedance. Later investigations brought in further elements and further variables, the different investigators attacking the problem in different ways and attempting to prove different points. By this means a large number of factors in oscillators have been ascertained to a first degree of approximation so that a qualitative review of the performance of the electric oscillator is very well known. It is the quantitative view upon the first order magnitude which is still difficult or uncertain. This is particularly true of the crystal oscillator because of the slightly different circuit.

It is proposed, therefore, in this paper to cover briefly a number of the studies on crystal oscillators so as to point out the different modes of attack and the different behavior points in the oscillators which the various investigators have studied. After covering these points, there will be discussed the frequency control properties of the crystal and the frequency stability of crystal oscillators. The performance of the crystal in the oscillator with respect to activity is then treated. There will be introduced two new yardsticks for measuring or indicating crystal quality, one called "figure of merit" and the other called "performance index." These are related to

the crystal constants and paralleling capacitances which are usually involved. They will be defined and their method of use and application in oscillators will be pointed out.

12.10 Solution by Differential Equations

The most direct method of determining the oscillating conditions in a circuit is to analyze the differential equation for the current in some particular branch of the circuit. The relations existing between the coefficients determine whether the current builds up, dies out, or is maintained at a constant value and frequency. Unfortunately the equations resulting from the application of this method to the crystal oscillator circuit are quite complicated. However, lower order differential equations result from the

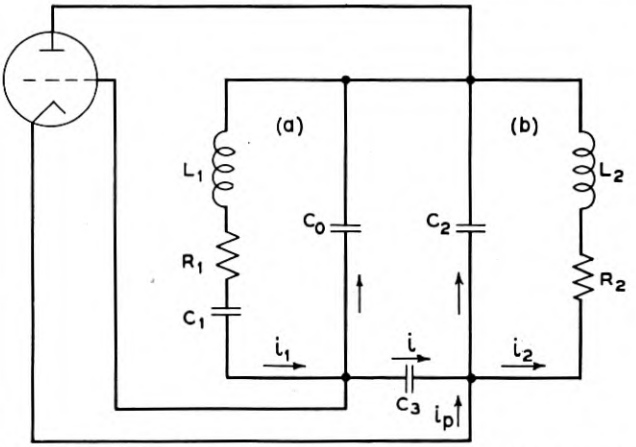

Fig. 12.4—Equivalent circuit of oscillator with crystal connected between grid and plate

application of this method to similar electric oscillator circuits, and certain qualitative information obtained from the latter is applicable to crystal oscillators. Thus Heising's[9] analysis of the Colpitts and Hartley circuits gives much information directly applicable to the Pierce and Miller types of crystal oscillators. From this the circuit conditions necessary for oscillations to exist and the effect of certain circuit variables upon the frequency are ascertained. The more complex qualitative view is given by Terry[6] who shows the relations of the coefficients of linear differential equations of the 2nd, 3rd, and 4th orders, and applies them to the analysis of three common types of crystal oscillator circuits. The resulting equations, together with certain qualitative information regarding their interpretation, are repeated here. In making this analysis the grid current is disregarded and the static tube characteristic is considered linear.

The equation is the same for the three types of circuits considered and is derived for the current i_1, in Figs. 12.4 and 12.5, although it may be set up in terms of any of the currents or voltages existing in the circuit. It is of the form

$$\frac{d^4 i_1}{dt^4} + P_1 \frac{d^3 i_1}{dt^3} + P_2 \frac{d^2 i_1}{dt^2} + P_3 \frac{di_1}{dt} + P_4 i_1 = 0 \qquad (12.1)$$

The P coefficients are functions of the circuit elements and are defined for each type of circuit in the following sections.

The solution of (12.1) normally represents a doubly periodic function arising from the two coupled antiresonant meshes (a) and (b). The normal

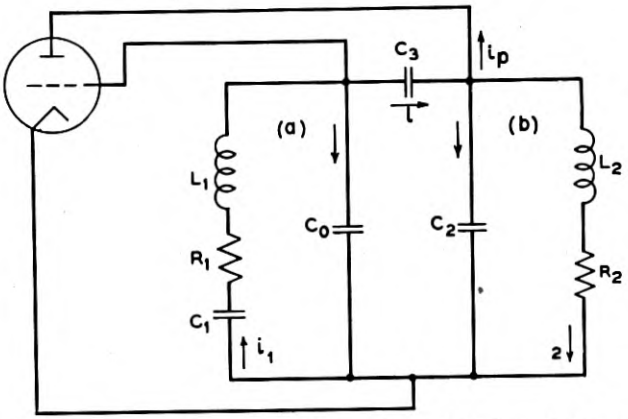

Fig. 12.5—Equivalent circuit of oscillator with crystal connected between grid and cathode

modes of oscillation consist of two currents in each mesh with frequency and damping factors β_1 and α_1, β_2 and α_2 respectively.

The conditions for undamped oscillation as derived from the general equation (12.1) are expressed in terms of the coefficients by

$$\frac{P_3}{P_1} = \frac{P_2 \pm \sqrt{P_2^2 - 4P_4}}{2} \qquad (12.2)$$

and the angular frequencies are

$$\beta^2 = \frac{P_2 \pm \sqrt{P_2^2 - 4P_4}}{2} \qquad (12.3)$$

where the plus sign gives the condition for one damping factor to be zero and the minus sign that for the other to be zero.

The frequency at which oscillations are maintained is determined by the required phase relation of voltages applied to the tube. With crystal from grid to plate, as in Fig. 12.4, the phase difference of grid and plate voltages is such that the circuit oscillates at only one of the normal modes, and with crystal connected between grid and cathode, as in Fig. 12.5, it oscillates at the other only.

12.11 Crystal Between Grid and Plate

With the crystal connected between the grid and plate of the tube, as in Fig. 12.4, the coefficients of the general equation (12.1) are

$$\left.\begin{aligned}
P_1 &= \frac{R_1}{L_1} + \frac{R_2}{L_2} + \frac{1}{R_p C_b'} \\
P_2 &= \frac{1}{L_1 C_a} + \frac{R_1 R_2}{L_1 L_2} + \frac{1}{L_2 C_b} + \frac{1}{R_p}\left(\frac{R_1}{L_1} + \frac{R_2}{L_2}\right)\frac{1}{C_b'} \\
P_3 &= \frac{R_2}{L_1 L_2 C_a} + \frac{R_1}{L_1 L_2 C_b} + \frac{1}{R_p}\left(\frac{1}{L_1 C_a C_b'} + \frac{R_1 R_2}{L_1 L_2 C_b'} - \frac{1}{L_1 C_m C_m'}\right) \\
P_4 &= \frac{1}{L_1 L_2 C_a C_b} - \frac{1}{L_1 L_2 C_m^2} + \frac{R_2}{R_p}\left(\frac{1}{L_1 L_2 C_a C_b'} - \frac{1}{L_1 L_2 C_m C_m'}\right)
\end{aligned}\right\} \tag{12.4}$$

where

$$\frac{1}{C_a} = \frac{1}{C_1} + \frac{1}{C_0} - \frac{C_x}{C_0^2} \qquad \frac{1}{C_m} = \frac{C_x}{C_2 C_0}$$

$$\frac{1}{C_b} = \frac{1}{C_2} - \frac{C_x}{C_2^2} \qquad \frac{1}{C_m'} = \frac{1}{C_m} - \frac{\mu C_x}{C_0 C_3}$$

$$\frac{1}{C_b'} = \frac{1}{C_b} + \frac{\mu C_x}{C_2 C_3} \qquad \frac{1}{C_x} = \frac{1}{C_0} + \frac{1}{C_2} + \frac{1}{C_3}$$

μ = the amplification factor of the tube.

$$R_p = \frac{\partial e_p}{\partial i_p} \quad (e_g \text{ constant})$$

The uncoupled damping factors, α_a and α_b, the uncoupled undamped angular frequencies, β_a and β_b, and the coupling coefficient τ may be introduced as follows:

$$\alpha_a = \frac{R_1}{2L_1}, \qquad \beta_a^2 = \frac{1}{L_1 C_a} \qquad \tau^2 = \frac{C_a C_b}{C_m^2}$$

$$\alpha_b = \frac{R_2}{2L_2}, \qquad \beta_b^2 = \frac{1}{L_2 C_b}$$

Note that C_a is the total capacitance across L_1 and R_1, and C_b is the total capacitance across L_2 and R_2.

The coefficients of (12.4) become

$$\left.\begin{aligned} P_1 &= 2(\alpha_a + \alpha_b) + \frac{1}{R_p C_b'} \\ P_2 &= \beta_a^2 + 4\alpha_a\alpha_b + \beta_b^2 + \frac{1}{R_p}(\alpha_a + \alpha_b)\frac{2}{C_b'} \\ P_3 &= 2(\alpha_b\beta_a^2 + \alpha_a\beta_b^2) + \frac{1}{R_p}\left[(\beta_a^2 + 4\alpha_a\alpha_b)\frac{1}{C_b'} - \frac{1}{L_1 C_m C_m'}\right] \\ P_4 &= \beta_a^2\beta_b^2\left[1 - \tau^2 + \frac{R_2}{R_p}\left(\frac{C_b}{C_b'} - \frac{C_m}{C_m'}\tau^2\right)\right] \end{aligned}\right\} \tag{12.5}$$

The coefficients as given by (12.5) satisfy (12.2) and (12.3) only when the plus sign is used.

The equations are simplified by dividing through by β_a^2 thus

$$\frac{P_3}{\beta_a^2 P_1} = \frac{\dfrac{P_2}{\beta_a^2} + \sqrt{\left(\dfrac{P_2}{\beta_a^2}\right)^2 - \dfrac{4P_4}{\beta_a^4}}}{2} \tag{12.6}$$

$$\frac{\beta^2}{\beta_a^2} = \frac{\dfrac{P^2}{\beta_a^2} + \sqrt{\left(\dfrac{P_2}{\beta_a^2}\right)^2 - \dfrac{4P_4}{\beta_a^4}}}{2} \tag{12.7}$$

which gives the ratio of driven frequency of the crystal to its undriven value. The common variable R_p must satisfy both (12.6) and (12.7). The method of computing the frequency would be to solve for R_p in (12.6) and substitute in (12.7). However, the equations are too complicated a function of R_p for this to be practical. Terry solved them graphically by plotting (12.6) and (12.7) as functions of R_p for assigned values of the circuit, and the intersection of these curves gave the frequency for the different circuit conditions. The results are shown in Fig. 12.6. The G-P curves show the frequency change as a function of plate circuit tuning for the grid to plate connection of the crystal.

12.12 Crystal Between Grid and Cathode

With the crystal connected between the grid and cathode of the tube, the circuit is as shown in Fig. 12.5. The coefficients of equation (12.1) are as follows:

$$\left.\begin{aligned}
P_1 &= \frac{R_1}{L_1} + \frac{R_2}{L_2} + \frac{1}{R_p C_b''} \\
P_2 &= \frac{1}{L_1 C_a} + \frac{R_1 R_2}{L_1 L_2} + \frac{1}{L_2 C_b} + \frac{1}{R_p}\left(\frac{R_1}{L_1} + \frac{R_2}{L_2}\right)\frac{1}{C_b''} \\
P_3 &= \frac{R_2}{L_1 L_2 C_a} + \frac{R_1}{L_1 L_2 C_b} + \frac{1}{R_p}\left(\frac{1}{L_1 C_a C_b''} + \frac{R_1 R_2}{L_1 L_2 C_b''} - \frac{1}{L_1 C_m C_m''}\right) \\
P_4 &= \frac{1}{L_1 L_2 C_a C_b} - \frac{1}{L_1 L_2 C_m^2} + \frac{R_2}{R_p}\left(\frac{1}{L_1 L_2 C_a C_b''} - \frac{1}{L_1 L_2 C_m C_m''}\right)
\end{aligned}\right\} \tag{12.8}$$

With the substitution of uncoupled frequencies, damping factors and coupling coefficient as described in the previous section, they become

$$\left.\begin{aligned}
P_1 &= 2(\alpha_a + \alpha_b) + \frac{1}{R_p C_b''} \\
P_2 &= \beta_a^2 + 4\alpha_a\alpha_b + \beta_b^2 + \frac{1}{R_p}(\alpha_a + \alpha_b)\frac{2}{C_b''} \\
P_3 &= 2(\alpha_b\beta_a^2 + \alpha_a\beta_b^2) + \frac{1}{R_p}\left[(\beta_a^2 + 4\alpha_a\alpha_b)\frac{1}{C_b''} - \frac{1}{L_1 C_m C_m''}\right] \\
P_4 &= \beta_a^2\beta_b^2\left[1 - \tau^2 + \frac{R_2}{R_p}\left(\frac{C_b}{C_b''} - \frac{C_m}{C_m''}\tau^2\right)\right]
\end{aligned}\right\} \tag{12.9}$$

Where

$$\frac{1}{C_m''} = \frac{1}{C_m} + \frac{\mu}{C_d}$$

$$\frac{1}{C_b''} = \frac{1}{C_b} + \frac{\mu}{C_m}$$

$$\frac{1}{C_m} = \frac{C_x}{C_2 C_0}$$

$$C_b = C_2 + \frac{C_0 C_3}{C_0 + C_3}$$

$$C_d = C_0 + \frac{C_2 C_3}{C_2 + C_3}$$

μ = amplification factor of tube

$$R_p = \frac{\partial e_p}{\partial i_p} \quad (e_g \text{ constant})$$

$$\frac{1}{C_x} = \frac{1}{C_0} + \frac{1}{C_2} + \frac{1}{C_3}$$

These equations of conditions for oscillation in this case satisfy (12.4) and (12.5) only when the minus sign is used. That is

$$\frac{P_3}{P_1} = \frac{P_2 - \sqrt{P_2^2 - 4P_4}}{2} \tag{12.10}$$

$$\beta^2 = \frac{P_2 - \sqrt{P_2^2 - 4P_4}}{2} \tag{12.11}$$

Again dividing by β_a^2 to obtain the frequency as a ratio of driven to undriven crystal frequency, we have

$$\frac{P_3}{\beta_a^2 P_1} = \frac{\frac{P_2}{\beta_a^2} - \sqrt{\left(\frac{P_2}{\beta_a^2}\right)^2 - \frac{4P_4}{\beta_a^4}}}{2} \tag{12.12}$$

$$\frac{\beta^2}{\beta_2^2} = \frac{\frac{P_2}{\beta_2^2} - \sqrt{\left(\frac{P_2}{\beta_a^2}\right)^2 - \frac{4P_4}{\beta_a^4}}}{2} \tag{12.13}$$

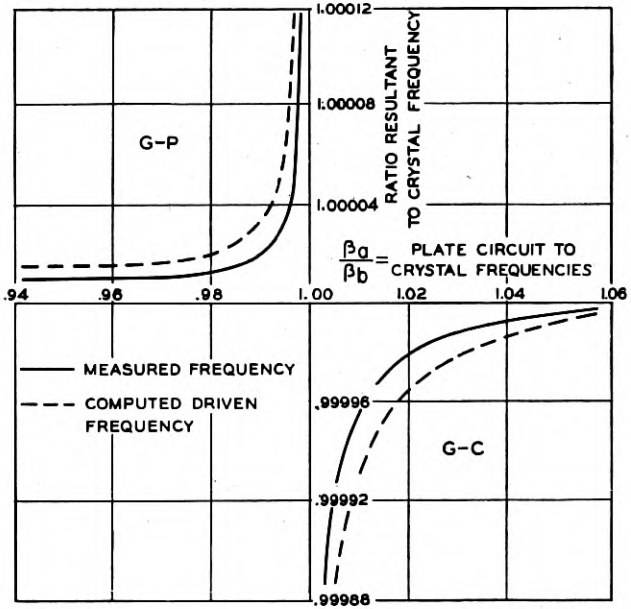

Fig. 12.6—The oscillating frequency as a function of the plate circuit frequency for the crystal connected grid to plate (G-P) and grid to cathode (G-C)

The frequency change as a function of plate circuit tuning was determined graphically in the manner described in section (12.11) and the curves are shown in Fig. 12.6 as the G-C curves.

12.13 Resistance Load Circuit

This is a special case of Plate-Grid connection of the crystal described in section (12.11) in which the plate circuit consists of a capacitance and resistance in parallel. This is a very common Pierce type of oscillator circuit and has the advantage that no tuning adjustment is necessary when using crystals of different frequencies.

Since this circuit is singly periodic, the differential equation for i_1 is of the third order and is derived from (12.1) by setting the plate inductance L_2 of the P coefficients equal to zero. The general equation then becomes

$$\frac{d^3 i_1}{dt^3} + P_1 \frac{d^2 i_1}{dt^2} + P_2 \frac{di_1}{dt} + P_3 i_1 = 0 \tag{12.14}$$

where

$$\left.\begin{aligned} P_1 &= \frac{R_1}{L_1} + \frac{1}{R_2 C_b} + \frac{1}{R_p C_b'} \\ P_2 &= \frac{1}{L_1 C_a} + \frac{R_1}{R_2 L_1 C_b} + \frac{R_1}{R_p L_1 C_b'} \\ P_3 &= \frac{1}{R_2 L_1 C_a C_b} - \frac{1}{R_2 L_1 C_m^2} + \frac{1}{R_p}\left(\frac{1}{L_1 C_a C_b'} - \frac{1}{L_1 C_m C_m'}\right) \end{aligned}\right\} \tag{12.15}$$

With the substitution of the uncoupled damping factors and frequencies, (12.15) becomes

$$\left.\begin{aligned} P_1 &= 2\alpha_a + \frac{1}{R_2 C_b} + \frac{1}{R_p C_b'} \\ P_2 &= \beta_a^2 + \frac{2\alpha_a}{R_2 C_b} + \frac{2\alpha_a}{R_p C_b'} \\ P_3 &= \frac{\beta_a^2}{R_2 C_b} - \frac{1}{R_2 L_1 C_m^2} + \frac{1}{R_p}\left(\frac{\beta_a^2}{C_b'} - \frac{1}{L_1 C_m C_m'}\right) \end{aligned}\right\} \tag{12.16}$$

The frequency as obtained from (12.14) is

$$\beta^2 = P_2 \tag{12.17}$$

with the conditions for oscillation

$$P_2 = \frac{P_3}{P_1} \tag{12.18}$$

obtained by setting the damping factor α equal to zero. The ratio of driven to undriven frequency is obtained by dividing (12.17) and (12.18) by β_a^2. That is

$$\frac{\beta^2}{\beta_a^2} = \frac{P_2}{\beta_a^2} = \frac{P_3}{\beta_a^2 P_1} \tag{12.19}$$

12.14 Interpretation of the Equations

It is learned from this analysis that the frequency of oscillation while governed principally by the frequency of the crystal also depends upon all the constants of the circuit. The effect of the plate circuit impedance is

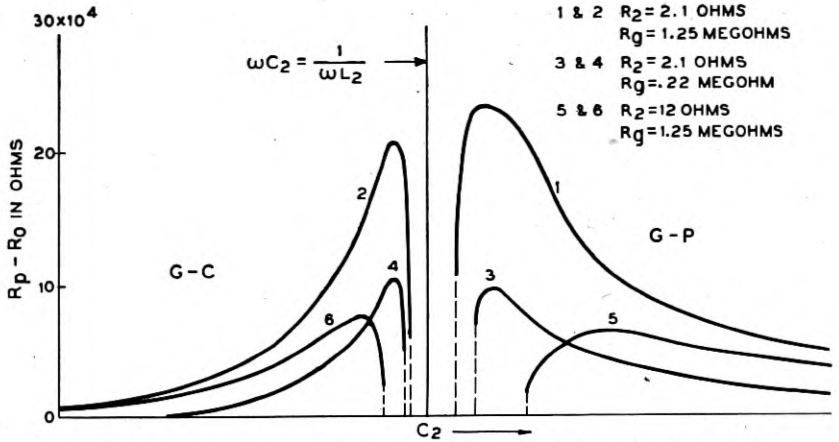

Fig. 12.7—Calculated increase in mean plate resistance against capacitance of the oscillatory circuit

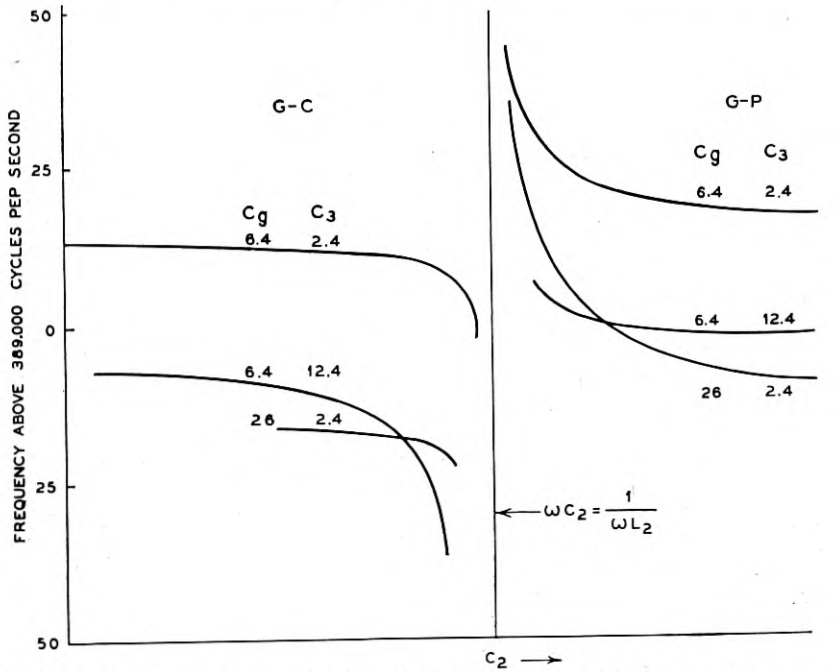

Fig. 12.8—Experimental curves, showing the influence of interelectrode capacitances on the frequency

shown in Fig. 12.6. It is pointed out that the effect of the crystal resistance R_1 is to decrease the frequency for the G-C connection and increase the frequency for the G-P connection. The discrepancy between the measured

and experimental values shown on the curves is attributed to the difference between chosen and actual value of R_1. The effect of the input loss of the tube is not shown because the grid current was disregarded; however, this loss may be reduced to an equivalent R_1. The resistance of the plate circuit R_2 affects the frequency in a similar manner. The effects of these resistances on frequency are less for low values of plate circuit impedances.

The required value of R_p gives a measure of amplitude of oscillation because it is necessary for oscillations to build up until the internal plate resistance is equal to the calculated value. It is found that R_p increases

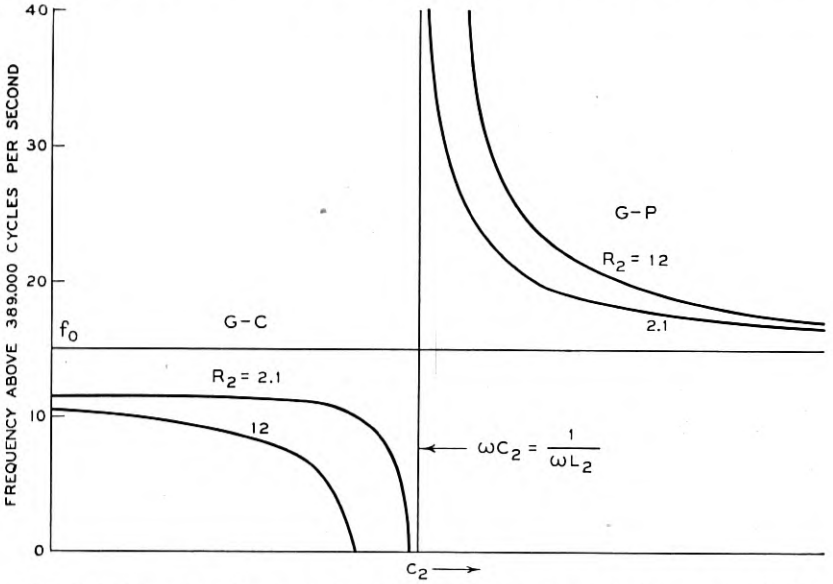

Fig. 12.9—Experimental curves, showing the relation between the frequency and the resistance of the oscillatory circuit

gradually to a maximum as the common frequency for the two types of circuits is approached then abruptly drops.

Vigoureux[8] analyzes the crystal oscillator in a manner similar to Terry and correlates his interpretations of the equations with considerable experimental data, some of which are shown in Figs. 12.7, 12.8, 12.9 and 12.10. He points out that there is an optimum value of grid capacitance with the crystal connected between grid and plate and a certain amount of grid-plate capacitance is required when the crystal is connected between grid and cathode.

Wheeler[10] does not assume a linear static tube characteristic but represents it by a three-term nonlinear expression. The results are more complex and it is necessary in the end to disregard certain resistance terms.

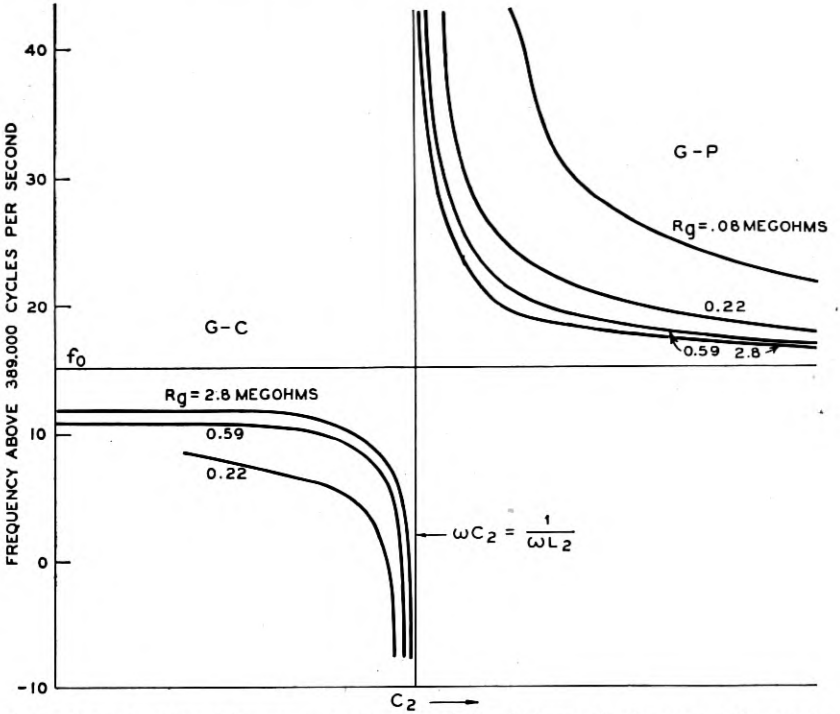

Fig. 12.10—Experimental curves, showing the relation between the frequency of a quartz oscillator and the capacitance of the oscillatory circuit for various values of the grid leak

12.20 Solution by Complex Functions

The analysis of oscillator circuits may be simplified when only steady state conditions are of interest, all circuit elements are considered linear, and certain requirements which define the conditions necessary for oscillations are known. Under these conditions the common circuit equations of complex numbers give the information desired. In this method the voltage induced in the plate circuit is considered the driving voltage which produces a current in the grid circuit (see Fig. 12.11). The network be-

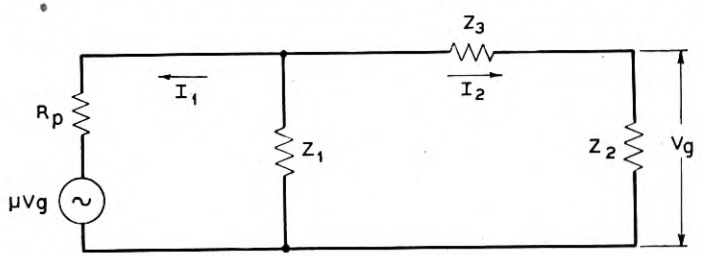

Fig. 12.11—Equivalent circuit of Pierce and Miller types of oscillators shown in Fig. 12.12

tween plate and grid may be of any type and oscillations are maintained when the total gain through the circuit is unity (gain of tubes = attenuation through circuit) and the phase relation between the induced plate voltage (μV_g) and the grid voltage (V_g) is 180° (the phase shift is zero when μ is considered negative). The expression $\mu\beta = 1$ defines these requirements. Llewellyn[11] applies this method to oscillator circuits in general and Koga[12] uses it to study the crystal oscillator in particular.

The equations are developed on the assumption that the grid-voltage vs. plate-current characteristic of the tube is linear. The fundamental equation of $\mu\beta$ is given by the ratio of the voltage developed across the grid

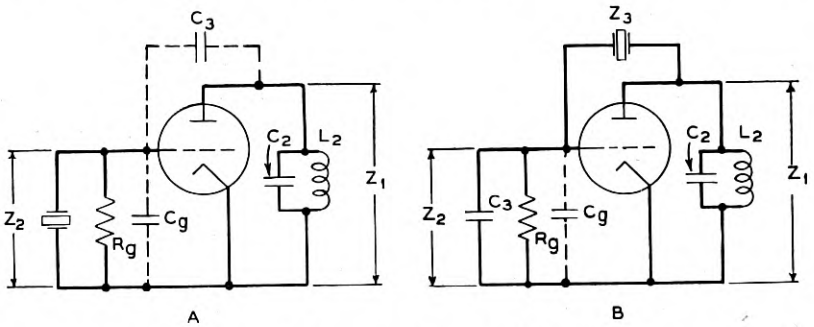

Fig. 12.12—Circuit diagrams of crystal oscillators with crystal connected from grid to cathode (A) and grid to plate (B)

circuit by the fictitious driving voltage μV_g to the voltage V_g. For the general circuit, Fig. 12.11, it is

$$\mu\beta = \frac{I_2 Z_2}{V_g} = \frac{-\mu Z_1 Z_2}{R_p Z_s + Z_1(Z_2 + Z_3)} \tag{12.20}$$

where

$$Z_s = Z_1 + Z_2 + Z_3$$

It is more convenient to write this in the reciprocal form

$$\frac{1}{\mu\beta} = \frac{R_p Z_s + Z_1(Z_2 + Z_3)}{-\mu Z_1 Z_2} = 1 \tag{12.21}$$

In applying this to the crystal oscillator, the additional assumptions made are that the grid current is negligible and the resistance in the plate impedance Z_1 is zero.

12.21 Crystal Grid to Cathode

With the assumptions made above and the crystal connected from grid to cathode of the tube according to Fig. 12.12A, the impedances are

$$Z_1 = jX_1 \qquad Z_2 = R_{cg} + jX_{cg} \qquad Z_3 = jX_3$$

where R_{cg} is the effective resistance and X_{cg} the effective reactance of the crystal, the grid resistance R_g and the circuit capacitance C_g in parallel at the oscillating frequency. Upon substitution of these in (12.21)

$$\frac{1}{\mu\beta} = \frac{[R_{cg}R_p - X_1(X_{cg} + X_3)] + j(X_1R_{cg} + R_pX_s)}{\mu X_1X_{cg} - j\mu X_1R_{cg}} = 1 \tag{12.22}$$

where

$$X_s = X_1 + X_{cg} + X_3$$

Thus $\frac{1}{\mu\beta}$ is of the form

$$\frac{1}{\mu\beta} = P + jQ$$

which means that $P = 1$ and $Q = 0$.

This results in the following two equations obtained from the real and imaginary parts of (12.22) both of which must be satisfied for oscillations to be maintained.

The real part of (12.22) gives

$$-R_p = \frac{X_1(\mu + 1)(R_{cg}^2 + X_{cg}^2) + X_{cg}X_3}{R_{cg}(X_1 + X_3)} \tag{12.23}$$

and from the imaginary part is obtained

$$X_s = \frac{X_1X_3 - R_{cg}R_p}{R_p\phi_{cg}} \tag{12 24}$$

where $\phi_{cg} = \frac{X_{cg}}{R_{cg}}$ (This ratio of reactance to resistance of the crystal circuit will appear in various equations later.)

Equation (12.24) may be said to define the oscillating frequency and is in a convenient form to examine the effect of the various circuit variables upon the frequency. The impedances X_1, R_{cg}, X_{cg} and X_3 may be thought of as forming an oscillating loop (See Fig. 12.11). For oxcillations to be maintained in such a loop the sum of the reactances must equal zero and the sum of the resistances must equal zero. But the sum of the resistances cannot equal zero since R_{cg} is the only resistance in the loop and it is positive. It is therefore necessary for the driving voltage μV_g to act upon the circuit and supply the energy dissipated by the resistance R_{cg} (and also R_p through which the energy is supplied). This alters the frequency somewhat and it is no longer determined by setting the three reactances equal to zero as may be seen by equation (12.24). Nevertheless, the right side of this equation is small and approaches zero when R_{cg} approaches zero. It also becomes very small when the reactance X_1 becomes small and R_{cg} is not too great. This is the same condition as found by the differential

equation method and illustrated in Fig. 12.6 by the *G-C* curves. As the plate reactance X_1 is made small the frequency increases and approaches a limiting value but does not quite reach it. This limiting value is the frequency at which $X_s = 0$. The dotted *G-C* curve shows that R_{cg} tends to lower the frequency and determines how close the limiting frequency is approached. The plate circuit resistance R_2 (component of Z_1), if considered, would have a similar effect as shown by the experimental curves 12.9. The grid resistance R_g (component of Z_2) has an opposite effect as shown in Figure 12.10 because increasing R_g is equivalent to decreasing the effective resistance R_{cg}.

The effect of the various constants of the crystal and circuit upon the oscillating frequency may be obtained from (12.24) upon substitution of these constants for the reactances and resistance R_{cg}. The equation is put in a more convenient form for this purpose by Koga.[12] Equation (12.21) is written,

$$\frac{1}{Z_2} + \frac{1}{Z_3} + \frac{\mu}{Z_3\left(1 + R_p/Z_1 + \dfrac{R_p}{Z_2 + Z_3}\right)} = 0 \tag{12.25}$$

It is assumed that the current in the grid branch is small compared to the plate current. This reduces the equation to

$$\frac{1}{Z_2} + \frac{1}{Z_3} + \frac{\mu}{Z_3(1 + R_p/Z_1)} = 0 \tag{12.26}$$

The admittance expression for the crystal is

$$\frac{1}{Z_c} = \frac{R_1 - j\left[\omega L_1 - \dfrac{1}{\omega C_1} - \dfrac{1}{\omega(C_0 + C_4)}\right]}{R_1^2 + \left[\omega L_1 - \dfrac{1}{\omega C_1} - \dfrac{1}{\omega(C_0 + C_4)}\right]^2}\left(\frac{C_4}{C_0 + C_4}\right)^2 + j\omega\frac{C_0 C_4}{C_0 + C_4} \tag{12.27}$$

Note that Koga considers the air gap capacitance C_4 as a separate factor but it may be included in the other constants of the crystal in which case the equivalent circuit is as shown in Fig. 12.3. With the crystal connected between grid and cathode the various circuit admittances are:

$$\frac{1}{Z_1} = \frac{1}{j\omega L_2} + j\omega C_2$$

$$\frac{1}{Z_2} = \frac{1}{Z_c} + \frac{1}{R_g} + j\omega C_g$$

$$\frac{1}{Z_3} = j\omega C_3$$

After substitution of these values of the admittances in (12.26) and setting the real and imaginary parts equal to zero, the following two equations are obtained:

$$\frac{R_1}{R_1^2 + \left[\omega L_1 - \frac{1}{\omega C_1} - \frac{1}{\omega(C_0 + C_4)}\right]^2}\left(\frac{C_4}{C_0 + C_4}\right)^2 + \frac{1}{R_g} - \mu\omega C_3 \frac{R_p\left(\frac{1}{\omega L_2} - \omega C_2\right)}{1 + R_p^2\left(\frac{1}{\omega L_2} - \omega C_2\right)^2} = 0 \tag{12.28}$$

and

$$\frac{\omega L_1 - \frac{1}{\omega C_1} - \frac{1}{\omega(C_0 + C_4)}}{R_1^2 + \left[\omega L_1 - \frac{1}{\omega C_1} - \frac{1}{\omega(C_0 + C_4)}\right]^2} = \omega\left(\frac{C_0 + C_4}{C_4}\right)^2 \left[C_g + \frac{C_0 C_4}{C_0 + C_4} + C_3 + \frac{\mu C_3}{1 + R_p^2\left(\frac{1}{\omega L_2} - \omega C_2\right)^2}\right] \tag{12.29}$$

Equation (12.28) gives the conditions necessary for oscillations and (12.29) gives the oscillating frequency as explained below:

12.22 Frequency of Oscillations for G-C Connection of Crystal

Equation (12.29) for frequency is simplified by the fact that over the narrow frequency range considered, the reactances of L_2 and C_2 do not change appreciably. Also at the oscillating frequency,

$$R_1^2 \ll \left[\omega L_1 - \frac{1}{\omega C_1} - \frac{1}{\omega(C_0 + C_4)}\right]^2$$

With these approximations (12.29) may be written

$$\omega^2 = \frac{1}{L_1 C_1} + \frac{1}{L_1 C_0}\left[1 - \frac{1}{\frac{C_0 + C_t}{C_t} + \frac{C_0}{C_4}}\right] \tag{12.30}$$

where

$$C_t = C_g + C_3 + \frac{\mu C_3}{1 + R_p^2\left(\frac{1}{\omega_0 L_2} - \omega_0 C_2\right)^2}$$

and ω_0 is a constant approximating the oscillating frequency.

Since the frequency is a function of the internal plate resistance of the tube (R_p) and this is in turn a function of the other circuit variables, the frequency equation (12.30) is not sufficient to calculate the frequency. However, qualitative effects of the various circuit components upon frequency are obtained by assuming R_p an independent variable. It is readily seen that an increase in R_p increases the frequency. The effect of the air gap between crystal and electrodes, which is represented by the capacitance C_4, and the effect of the capacitance across the crystal C_g are illustrated in Fig. (12.13).* To determine the frequency change caused by tuning of

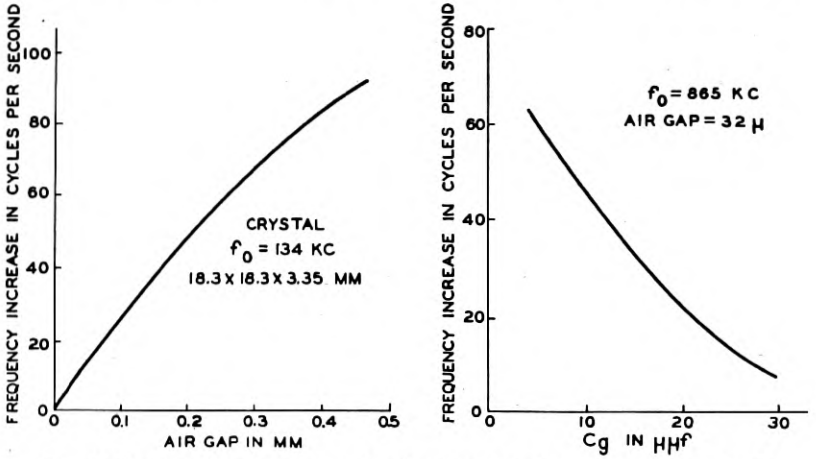

Fig. 12.13—Experimental curves, showing the effect of crystal air gap and grid capacitance on the frequency of oscillations

the plate circuit (variations of C_2) requires the calculation of the change of the variable part of C_t. This quantity is

$$C_v = \frac{\mu C_3}{1 + R_p^2 \left(\frac{1}{\omega_0 L_2} - \omega_0 C_2\right)^2} \tag{12.31}$$

The plot of C_v is shown in Fig. (12.14A). The frequency decrease is proportional to the increase in C_v. This is indicated in Fig. (12.14B). Oscillations stop before the point $\omega_0 C_2 = \frac{1}{\omega_0 L_2}$ is reached. The frequency thus varies in the same manner as shown in Fig. (12.6) but the curve is reversed because of the fact that the independent variable is taken as C_2 instead of the frequency function of C_2.

The frequency change resulting from variations in the grid-plate capacitance C_3 depends also upon the value of C_v as seen from (12.31). It is also

* See also: "The Piezoelectric Resonator and the Effect of Electrode Spacing upon Frequency," Walter G. Cady, *Physics*, Vol. 7, July 1936.

seen that the smaller the value of C_2 (lower the plate reactance) the less effect will the tube constants μ, R_p and C_3 have upon the frequency. The circuit is therefore more stable. For this reason it has become customary to measure the frequency of crystals with the capacitance C_2 reduced to a value below that which gives maximum amplitude of oscillations.

12.23 Amplitude of Oscillations for G-C Connection of Crystal

A measure of the amplitude of oscillations is obtained from (12.28) which expresses the necessary conditions for oscillations to be maintained. In order for oscillations to start the expression must be negative, and, as the amplitude builds up, R_p increases which reduces the negative terms

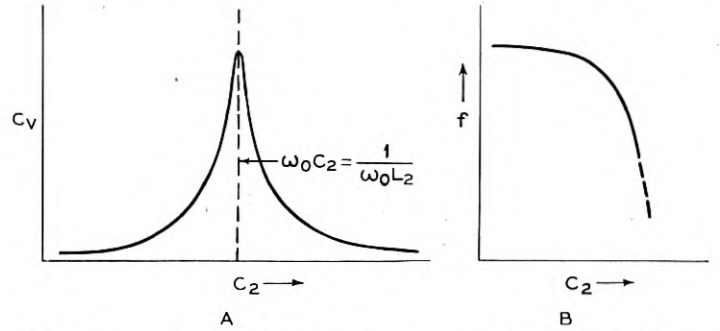

Fig. 12.14—The variation of grid to cathode capacitance (A) and oscillator frequency (B) with change in plate circuit capacitance. Crystal connected grid to cathode

until the equality is satisfied. The difference between the positive and negative terms is therefore a measure of the amplitude of oscillations.

Equation (12.28) may be written

$$\psi - \left[\Phi_0 + \frac{1}{R_g}\right] = A \tag{12.32}$$

where A is a measure of the amplitude,

$$\psi = \mu C_3 \omega_0 \frac{R_p\left(\frac{1}{\omega_0 L_2} - \omega_0 C_2\right)}{1 + R_p^2\left(\frac{1}{\omega_0 L_2} - \omega_0 C_2\right)^2} \tag{12.33}$$

and

$$\Phi_0 = R_1 \omega_0^2 \left(\frac{C_0 + C_4}{C_4}\right)^2 \left[\frac{C_0 C_4}{C_0 + C_4} + C_g + C_3 + \frac{\mu C_3}{1 + R_p^2\left(\frac{1}{\omega_0 L_2} - \omega_0 C_2\right)^2}\right]^2 \tag{12.34}$$

where again R_1^2 is assumed small compared to

$$\left[\omega_0 L_1 - \frac{1}{\omega_0 C_1} - \frac{1}{\omega_0(C_0 + C_4)}\right]^2$$

and ω_0 is considered a constant.

Equation (12.32) shows that in order to obtain a large amplitude ψ should be large and Φ_0 should be small. With this in mind equations (12.33)

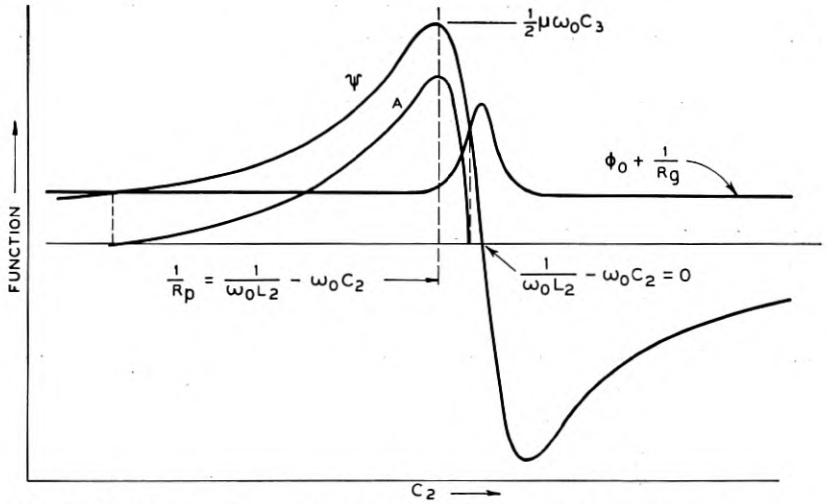

Fig. 12.15—Functions from which the activity variations (A) are determined as the plate circuit capacitance is varied. Crystal connected grid to cathode

and (12.34) may be analyzed to determine the relation between the circuit components and amplitude. It is found that for maximum amplitude

C_g and R_1 should be small,
C_4 should be large,
C_3 has an optimum value, and
R_g should be large.

As to the plate circuit, the amplitude is maximum when $\frac{1}{R_p} = \frac{1}{\omega_0 L_2} - \omega_0 C_2$. A plot of ψ and $\Phi_0 + \frac{1}{R_g}$ is shown in Fig. 12.15. The difference between these two curves is a measure of the amplitude and is shown by curve A. Oscillations can exist only where ψ lies over $\Phi_0 + \frac{1}{R_g}$. The sharpness of ψ varies considerably with the value of R_p and the resistance of the $L_2 - C_2$ circuit. The latter is disregarded for simplicity. Here again the

results can only be considered a first approximation, but agree with actual conditions sufficiently to be of considerable interest.

12.24 Crystal Grid to Plate

The equation (12.20) is general and for the condition of crystal connected between grid and plate of the tube (See Figure 12.12B) Z_3 represents the crystal impedance which will be called $Z_c = R_c + jX_c$, also: $Z_1 = jX_1$, $Z_2 = jX_2$ and $X_s = X_1 + X_2 + X_c$.

Note that R_g and C_3 are disregarded in this case because their effects are similar to those determined for the foregoing case of crystal connected grid to cathode.

After substitution of these values in (12.20) the real part is found to be

$$R_p = \frac{(\mu + 1)X_1X_2 + X_1X_c}{R_c} \tag{12.35}$$

and the imaginary part is

$$X_s = -\frac{R_cX_1}{R_p} \tag{12.36}$$

which shows the effect of the various variables on the frequency. The right hand side of equation (12.36) is comparatively small and the frequency is therefore close to a value f_0 which makes $X_s = 0$. In this case the frequency is above the limiting frequency f_0 because the right hand side is positive since X_1 is negative, whereas it was found that the frequency was below f_0 for the crystal connected between grid and cathode. As R_c and X_1 are increased the frequency will increase and as R_p increases the frequency decreases. These interpretations are verified by the *G-P* curves of Figures 12.6, 12.9 and 12.10.

The effects of the various circuit and crystal constants are determined by Koga[12] by writing the general $\mu\beta$ equation as

$$Z_3 + Z_2 + \frac{\mu Z_2}{1 + R_p/Z_1} = 0 \tag{12.37}$$

After substitution for the Z's, the real and imaginary parts are respectively,

$$\left(\frac{1}{\omega C_0}\right)^2 \frac{R_1}{R_1^2 + \left[\omega L_1 - \frac{1}{\omega C_1} - \frac{1}{\omega C_0}\right]^2} + \frac{\mu}{\omega C_g} \cdot \frac{R_p\left(\frac{1}{\omega L_2} - \omega C_2\right)}{1 + R_p^2\left(\frac{1}{\omega L_2} - \omega C_2\right)^2} = 0 \tag{12.38}$$

and

$$\frac{\frac{1}{\omega C_1}+\frac{1}{\omega C_0}-\omega L_1}{R_1^2+\left[\omega L_1-\frac{1}{\omega C_1}-\frac{1}{\omega C_0}\right]^2} = \omega C_0^2\left[\frac{1}{C_0}+\frac{1}{C_4}+\frac{1}{C_g}+\frac{\mu}{C_g}\cdot\frac{1}{1+R_p^2\left(\frac{1}{\omega L_2}-\omega C_2\right)^2}\right] \tag{12.39}$$

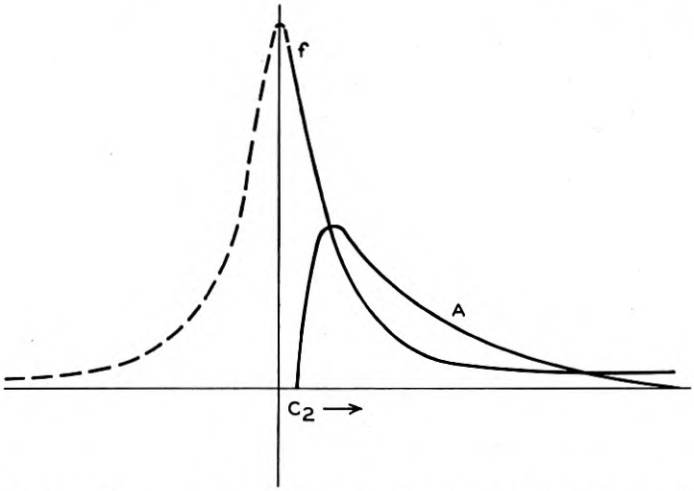

Fig. 12.16—Frequency and activity change for variations in the plate circuit capacitance. Crystal connected grid to plate

There are two values of ω which satisfy (12.39) but only one of these ω_n will satisfy (12.38). At this value of ω_n

$$R_1^2 \ll \left[\omega L_1-\frac{1}{\omega C_1}-\frac{1}{\omega C_0}\right]^2 \tag{12.40}$$

By introduction of this and the assumption that ω_0 is essentially constant, (12.38) may be written

$$R_1 C_0^2\left[\frac{1}{C_0}+\frac{1}{C_4}+\frac{1}{C_g}+\frac{\mu}{C_g}\cdot\frac{1}{1+R_p^2\left(\frac{1}{\omega_0 L_2}-\omega_0 C_2\right)^2}\right]^2 + \frac{\mu}{\omega_0 C_g}\cdot\frac{R_p\left(\frac{1}{\omega_0 L_2}-\omega_0 C_2\right)}{1+R_p^2\left(\frac{1}{\omega_0 L_2}-\omega_0 C_2\right)^2} = 0 \tag{12.41}$$

This is an approximation for the conditions for oscillation and relative amplitude.

The frequency equation (12.39) becomes

$$\omega_n^2 = \frac{1}{L_1}\left[\frac{1}{C_1} + \frac{1}{C_0} - \frac{1}{G}\right] \tag{12.42}$$

where

$$G = C_0^2\left[\frac{1}{C_0} + \frac{1}{C_4} + \frac{1}{C_g} + \frac{\mu}{C_g}\cdot\frac{1}{1 + R_p^2\left(\frac{1}{\omega_0 L_2} - \omega_0 C_2\right)^2}\right]$$

and ω_0 is a fixed value written in place of ω_n. Figure 12.16 shows the frequency and amplitude changes as a function of C_2 for the crystal connected between grid and plate.

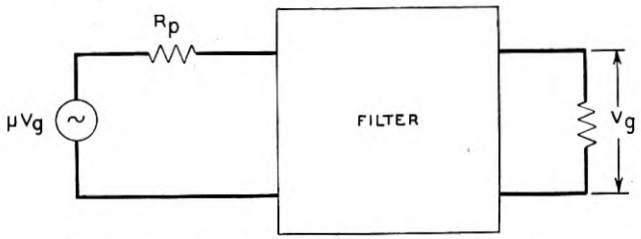

Fig. 12.17—Generalized oscillator circuit in the form of a filter network

12.25 Condition $\mu\beta = 1$ for Circuits in General

It is convenient to apply the rule $\mu\beta = 1$ as the condition for sustained oscillations to more complex oscillator circuits. The circuits may be drawn as shown in Figure 12.17 and the characteristics of the filter network between transmitting and receiving end may be analyzed by conventional filter theory to determine the conditions which fulfill the oscillation requirements. An example of this is the oscillator shown in Figure 12.18A. The equivalent configuration, Figure 12.18B, indicates that the crystal is part of a low pass filter and the frequency of operation is that at which the total phase shift is 180°.

Oscillators involving more than one tube may also be inspected in this manner. Figure 12.19 is a two tube oscillator designed to operate at a frequency close to the resonant frequency of the crystal. The proper phase shift is obtained by a two-stage amplifier and, therefore, no phase shift is required through the crystal network. The crystal thus must operate as a resistance which it can only do at its resonant or antiresonant frequency. Since the transmission through the crystal branch is very low at the antiresonant frequency of the crystal, it will oscillate only at the resonant

frequency. Heegner[13] explains a number of crystal oscillator circuits by the method briefly outlined above.

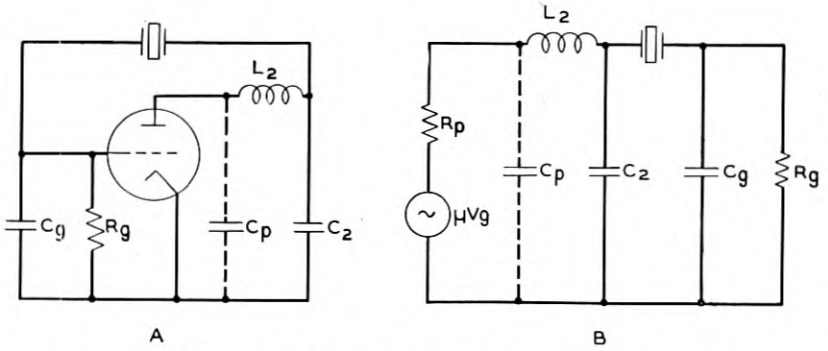

Fig. 12.18—The oscillator circuit (A) is equivalent to the filter circuit (B)

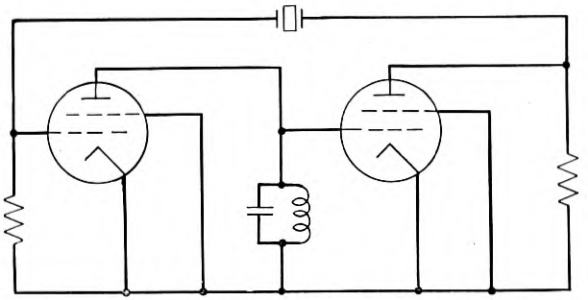

Fig. 12.19—Oscillator circuit in which the crystal operates at its series resonant frequency

12.30 Vector Method of Oscillator Analysis

A convenient method of examining the effect of certain circuit variables on frequency and the necessary conditions for oscillation is by the vector representation of the voltages and currents in the circuit. Much of Heising's[14] early work on the analysis of electric oscillators by vector methods is directly applicable to crystal oscillators. Boella[15] analyzed the crystal oscillator circuit by this method and treated in detail the effect of the decrement of the crystal on the oscillating frequency. Since some engineers prefer this method of qualitative analysis to approximate equations it will be briefly explained.

The vector diagrams for the two conditions, crystal between grid and plate and between grid and cathode, are shown in Figure 12.20A and B as applied to the circuit diagrams, Figure 12.12A and B, respectively when in the simplified form of Figure 12.11. The necessary conditions for oscilla-

tions are that V_g is in phase with and equal to μV_g (note that μ is considered negative). Like Koga, Boella assumes the current I_2 small compared to I_1, hence the voltage drop across Z_1 is approximately $Z_1 I_1$. The angle this makes with V_g is determined by the value of Z_1 and the internal plate impedance R_p. Any change in either of these requires a change in the angles ψ and ψ' in order that V_g shall be in phase with μV_g. This means that the frequency must vary to produce this change in ψ and ψ'. Because of the rapid change in the reactance and resistance of the crystal with frequency, these requirements are met with very little change in frequency, which accounts for the high degree of frequency stability obtained with crystals. This is described more in detail in a later section.

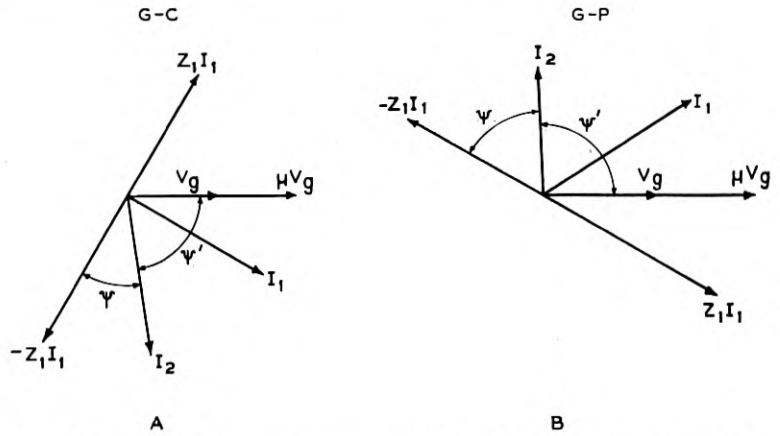

Fig. 12.20—Vector diagrams of currents and voltages in the oscillator circuit Figure 12.11 with crystal connected grid to cathode (A) and grid to plate (B)

12.31 Change in Frequency with Decrement of Crystal

It has been found that for the crystal connected from grid to cathode there is a maximum theoretical frequency at which the circuit can be made to oscillate by reducing the plate circuit impedance. This also corresponds to the minimum frequency which can be obtained with the crystal connected between grid and plate. This was called the limiting frequency f_0. It is interesting to note that f_0 is determined by the intersection of the reactance curve of the crystal plotted as a function of frequency and the reactance curve of the capacitance in series with the crystal. This series capacitance is the grid-plate capacitance for one case and the grid-cathode capacitance for the other. As illustrated in the curves Figure 12.21, the limiting frequency f_0 increases as the decrement of the crystal increases.

The difference between the true frequency of oscillations and f_0 increases

as the plate impedance is increased and as the losses in any of the circuit elements increase. This is necessary for the proper angle of $\psi + \psi'$ in the vector diagram. With the *G-P* connections, the departure from f_0 and change in f_0 as the decrement of the quartz varies are in the same direction, while for the grid-cathode connection they vary in opposite directions, and the net result will depend upon the value of the internal plate resistance and plate circuit impedance. The curves of Figure 12.21 show that the

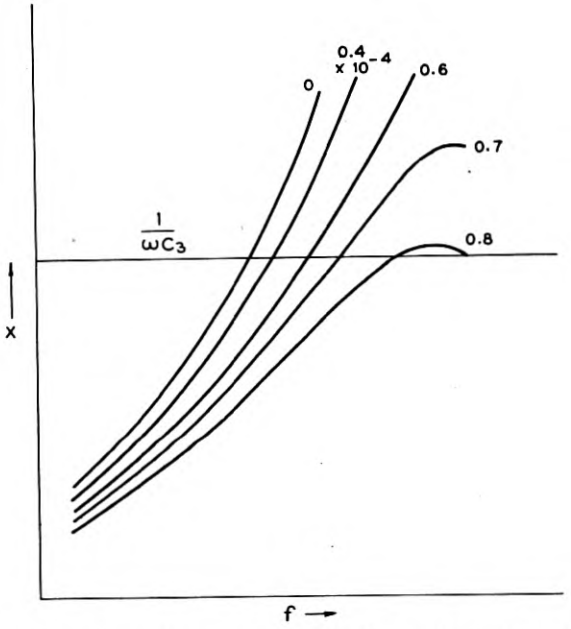

Fig. 12.21—The change in reactance characteristic of a crystal resulting from a change in decrement

change in f_0 for a given change in decrement is less for smaller values of $\frac{1}{\omega C_3}$ (larger values of series capacitance C_3). That is, the effect of the decrement of the crystal upon the oscillating frequency is small when the crystal is operated near its frequency of resonance.

12.40 Negative Resistance Method of Analysis

The methods of analyzing oscillator circuits described in the previous sections define the operation in terms of the individual circuit elements and the crystal is treated as one of the circuit elements. Certain advantages result, however, by grouping all the circuit elements, except the crystal,

into a single impedance as shown in Fig. 12.22A. Here Z_t represents the impedance looking into the oscillator from the crystal terminals.

The requirements for sustained oscillations are that the sum of the reactances around the loop equal zero and the sum of the resistances equal zero as previously stated in section 12.21. These conditions are obtained when Z_t is a negative resistance ρ in parallel with (or in series with) a capacitance C_t as shown in Fig. 12.22C. The crystal is considered to be operating as an inductance L_c and resistance R_c as determined in the pre-

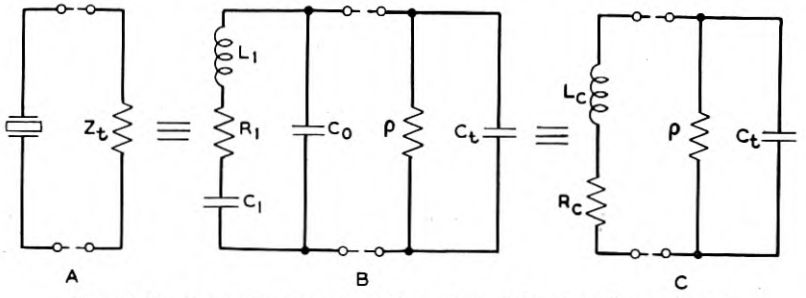

Fig. 12.22—Equivalent representations of crystal and oscillator circuit

vious sections. The frequency equation has been derived by Reich[16] from the differential equation for the current in the loop. It is

$$\omega = \sqrt{\frac{\rho + R_c}{\rho} \cdot \frac{1}{L_c C_t}} \tag{12.43}$$

and the condition for oscillation is shown to be

$$|C_t \rho| \leqq \left|\frac{L_c}{R_c}\right| \tag{12.44}$$

We shall consider the crystal connected between the grid and cathode of the tube, in which case Z_t is the input impedance of the vacuum tube. The expression for $\frac{1}{Z_t}$ was developed by Chaffee[17] from which it is possible to determine the circuit conditions necessary for the input resistance and reactance to be negative. The effect of the circuit variables upon the absolute values of ρ and C_t determines their effect upon the frequency and activity according to equations (12.43) and (12.44).

12.41 Input Admittance of the Vacuum Tube

With the assumption that the grid current is negligible and the static tube capacitances C_p and C_g are part of the external circuit, Chaffee's equation for input conductance becomes

$$g = \frac{C_3^2 \omega(K + G_1) + C_3 \omega \mu K(C_3 \omega - B_1)}{(K + G_1)^2 + (C_3 \omega - B_1)^2} \tag{12.45}$$

and for the input susceptance

$$b = -C_3\omega - \frac{C_3\omega\mu K(K + G_1) - C_3^2\omega^2(C_3\omega - B_1)}{(K + G_1)^2 + (C_3\omega - B_1)^2} \tag{12.46}$$

where K and μ are defined as follows:

$$K = \left(\frac{\partial i_p}{\partial e_p}\right) \quad (e_g \text{ constant})$$

$$\mu = -\left(\frac{\partial e_p}{\partial e_g}\right) \quad (i_p \text{ constant})$$

and G_1 and B_1 are the conductance and susceptance of the plate circuit. If we let

$$h = \frac{G_1}{|B_1|}$$

$$A = \frac{\omega C_3}{K} \quad \text{and} \quad B = \frac{B_1}{K}$$

(12.45) becomes

$$g = C_3\omega A \frac{(1 + hB) + \mu\left(1 + \frac{B}{A}\right)}{(1 + hB)^2 + A^2\left(1 - \frac{B}{A}\right)^2} \tag{12.47}$$

and (12.46) becomes

$$b = -C_3\omega\left[1 + \frac{\mu(1 + hB) - A^2\left(1 - \frac{B}{A}\right)}{(1 + hB)^2 + A^2\left(1 - \frac{B}{A}\right)^2}\right] \tag{12.48}$$

When the resistance of the plate circuit is neglected (i.e. $h = 0$), and $\mu \gg 1$ we may write

$$\frac{g}{K} = A\frac{\mu(A - B)}{1 + (A - B)^2} \tag{12.49}$$

and

$$\frac{b}{K} = -A\left[\frac{\mu - B(A - B)}{1 + (A - B)^2}\right] \tag{12.50}$$

These equations are in a convenient form to determine the effect of the plate tuning $f(B)$ and grid-plate capacitance $f(A)$ upon the resistance ρ

and capacitance C_t with the assumptions of no grid current, low plate circuit resistance, and $\mu \gg 1$.

From (12.49) it is seen that in order for g to be negative, B must be positive and greater than A, since A is normally positive. That is, the plate circuit reactance must be positive and less than the grid-plate reactance when the latter is a capacitance. Under these conditions b/K and hence the input reactance will be negative according to (12.50).

Curves of b/K are shown in Fig. 12.23 with B as independent variable and A as parameter. These curves indicate frequency change. On the

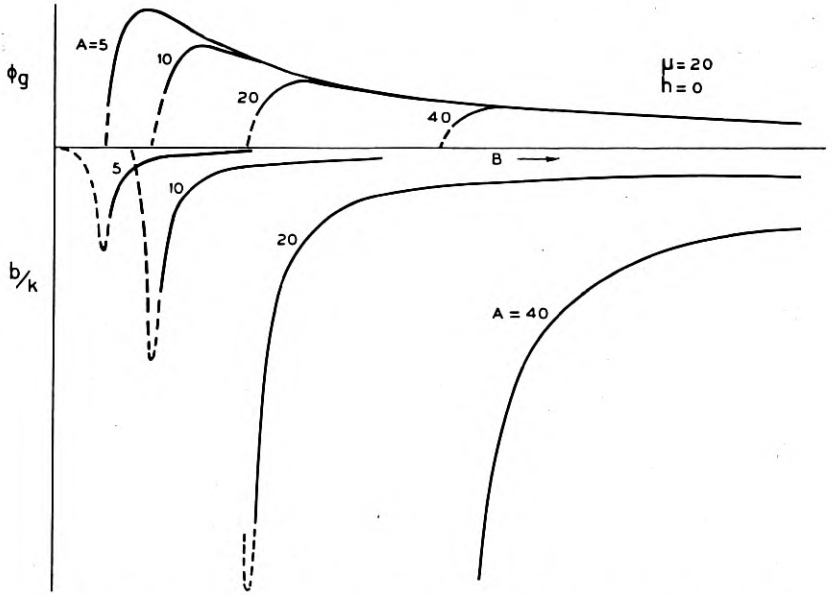

Fig. 12.23—Variations in the input impedance functions of an oscillator circuit for changes in plate circuit tuning

same figure is plotted b/g called ϕ_g. This may be considered the sensitivity of the oscillator or, for a given value of $\omega L_c/R_c$ of the crystal, it represents the activity. The similarity between these curves and the actual change in frequency and activity normally experienced is apparent.

It should be pointed out here that the presence of harmonics is effective in changing the input impedance of the vacuum tube and hence the frequency and activity of the oscillator. The presence of harmonics results from the non-linear characteristics of the vacuum tube. Llewellyn[11] explains that a non-linear resistance may be represented by a linear resistance plus a linear reactance. From what has been said concerning the

frequency of the oscillating loop, it is apparent that this effective reactance will alter the frequency. However, this reactance is small when the impedance of the circuit is low at the harmonic frequencies and is zero when the external circuit is a pure resistance.

12.50 Efficiency and Power Output of Oscillators

In many applications of crystal oscillators the efficiency and power output are important factors. These are not treated here but reference is made to the work of Heising[14] which covers this aspect for various electric oscillator circuits. Much of the analysis is directly applicable to crystal oscillators.

12.60 Frequency Stability of Crystal Oscillators

The equations for frequency show that the frequency is governed somewhat by the amplification factor, the grid resistance and internal plate resistance of the vacuum tube. Since these factors are functions of voltages applied to the tube and amplitude of oscillation, they cannot be considered fixed. If the frequency change resulting from these variables is great, the frequency stability is said to be low, and if very little frequency change takes place the frequency is determined principally by the circuit constants and the frequency stability is said to be high.

Llewellyn[11] shows how it is possible to compensate for the change in plate resistance by the proper value of circuit elements. This was done by determining the relations necessary for R_p to be eliminated from the frequency equation. It is sometimes helpful in designing very stable oscillators for frequency standards to select circuit elements which will reduce the effect of plate voltage changes on the frequency. It is more the purpose of this section, however, to show Llewellyn's derivation of the equations for frequency stability which have not heretofore been published and from them point out the characteristic of crystals which enable them to stabilize oscillators.

12.61 The Frequency Stability Equation

The steady state oscillating condition is

$$\mu\beta = 1 \tag{12.51}$$

In general β is a function of the frequency, the amplitude of oscillations, and of some independent variable V. This independent variable is the one for which it is desired to stabilize the frequency. It may be the potential applied to the tube, or it may be a capacitance located somewhere in the circuit. β depends upon these three variables thus:

$$\mu\beta = f(p\,,\, a\,,\, V) \tag{12.52}$$

Instead of the frequency, a more general symbol p is used and may be thought of as the differential operator d/dt which occurs in the fundamental linear differential equations taken as describing the oscillatory system. That is

$$p = \frac{d}{dt} = \alpha + i\omega \tag{12.53}$$

The function $\mu\beta$ may have the form

$$\mu\beta = Ae^{i\theta} \tag{12.54}$$

The result of taking a general variation δ of (12.54) is then

$$\frac{\delta A}{A} + i\delta\theta = 0 \tag{12.55}$$

Since (12.54) is a function of the three variables p, a, and V the variational equation (12.55) may be expressed in terms of partial derivatives with respect to these three variables. That is

$$\frac{1}{A}\left[\frac{\partial A}{\partial p}\delta p + \frac{\partial A}{\partial a}\delta a + \frac{\partial A}{\partial V}\delta V\right] + i\left[\frac{\partial \theta}{\partial p}\delta p + \frac{\partial \theta}{\partial a}\delta a + \frac{\partial \theta}{\partial V}\delta V\right] = 0 \tag{12.56}$$

The solution of (12.56) for the variation in p is

$$\delta p = -\frac{\frac{1}{A}\left(\frac{\partial A}{\partial V}\delta V + \frac{\partial A}{\partial a}\delta a\right) + i\left(\frac{\partial \theta}{\partial V}\delta V + \frac{\partial \theta}{\partial a}\varepsilon a\right)}{\frac{1}{A}\frac{\partial A}{\partial p} + i\frac{\partial \theta}{\partial p}} \tag{12.57}$$

It is a property of functions of complex variables that, provided they possess derivatives at all, then the value of the derivative is the same regardless of the direction in which the limiting point is approached. This fact is expressed by

$$\left.\begin{aligned} \frac{\partial A}{\partial p} &= \frac{\partial A}{\partial \alpha} = i\frac{\partial A}{\partial \omega} \\ \frac{\partial \theta}{\partial p} &= \frac{\partial \theta}{\partial \alpha} = i\frac{\partial \theta}{\partial \omega} \\ \text{and } \delta p &= \delta\alpha + i\delta\omega \end{aligned}\right\} \tag{12.58}$$

and provides means by which the real and imaginary parts of (12.57) may be separated to yield the two equations

$$\delta\alpha = \frac{\left[\frac{1}{A}\frac{\partial A}{\partial \omega}\left(\frac{\partial \theta}{\partial V}\delta V + \frac{\partial \theta}{\partial a}\delta a\right) - \frac{\partial \theta}{\partial \omega}\left(\frac{1}{A}\frac{\partial A}{\partial V}\delta V + \frac{1}{A}\frac{\partial A}{\partial a}\delta a\right)\right]}{\left(\frac{1}{A}\frac{\partial A}{\partial \omega}\right)^2 + \left(\frac{\partial \theta}{\partial \omega}\right)^2} \tag{12.59}$$

and

$$\delta\omega = \frac{-\left[\frac{1}{A}\frac{\partial A}{\partial \omega}\left(\frac{1}{A}\frac{\partial A}{\partial V}\delta V + \frac{1}{A}\frac{\partial A}{\partial a}\delta a\right) + \frac{\partial \theta}{\partial \omega}\left(\frac{\partial \theta}{\partial V}\delta V + \frac{\partial \theta}{\partial a}\delta a\right)\right]}{\left(\frac{1}{A}\frac{\partial A}{\partial \omega}\right)^2 + \left(\frac{\partial \theta}{\partial \omega}\right)^2} \tag{12.60}$$

The variable p in general may be written as the sum of α and $i\omega$. With the remembrance that p is the differential operator d/dt and that a set of linear equations expresses the transient condition, it is evident that the current will have the form Ie^{pt} which is equivalent to $Ie^{(\alpha+i\omega)t}$. Inspection of this shows that the real part of p, namely α, determines whether the currents in the system are going to build up with time, or die away with time, or remain constant, depending respectively upon whether α is greater than zero, is less than zero, or is actually equal to zero. With this in mind we see that (12.59) and (12.60) state the change in α and ω respectively which would result from some change in the circuit condition. Initially the circuit was oscillating in a steady manner so that α was zero and ω had some particular value. A change in V then occurred. This produced a change in the amplitude accompanied by a change in the frequency as expressed by (12.60) and a change in the transient term α. Suppose now that the change in V were very small. Then in order for oscillations again to assume a steady value it is necessary for the amplitude "a" to change a sufficient amount to cause α to become zero. Thus in (12.59) we put $\delta\alpha$ equal to zero and solve for the required amplitude change. This may then be eliminated from (12.60) resulting in the final expression

$$\delta\omega = \frac{\frac{1}{A}\frac{\partial A}{\partial V}\frac{\partial \theta}{\partial a} - \frac{1}{A}\frac{\partial A}{\partial a}\frac{\partial \theta}{\partial V}}{\frac{1}{A}\frac{\partial A}{\partial \omega}\frac{\partial \theta}{\partial a} - \frac{1}{A}\frac{\partial A}{\partial a}\frac{\partial \theta}{\partial \omega}}\delta V \tag{12.61}$$

which gives the frequency change $\delta\omega$ in terms of the change of the independent variable δV.

12.62 Frequency Stability of Conventional Oscillator

In applying this equation to the oscillator circuit, Fig. 12.24, we must first set up the conditions for oscillations. The $\mu\beta$ equation is

$$\mu\beta = \frac{\mu X_1 X_2 R_g}{i[X_s R_p R_g - X_1 X_2 X_3] - [R_p X_2(X_1 + X_3) + R_g X_1(X_2 + X_3)]} \tag{12.62}$$

The oscillating conditions $\mu\beta = 1$ requires

$$X_s R_p R_g = X_1 X_2 X_3$$

and

$$\mu X_1 X_2 R_g + R_p X_2 (X_1 + X_3) + R_g X_1 (X_2 + X_3) = 0 \qquad (12.63)$$

It will be assumed that the following relations exist:

$$\mu = f_1(V),\ R_g = f_2(a),\ X_s = X_1 + X_2 + X_3 = f_3(\omega),\ R_p = \text{a constant}$$

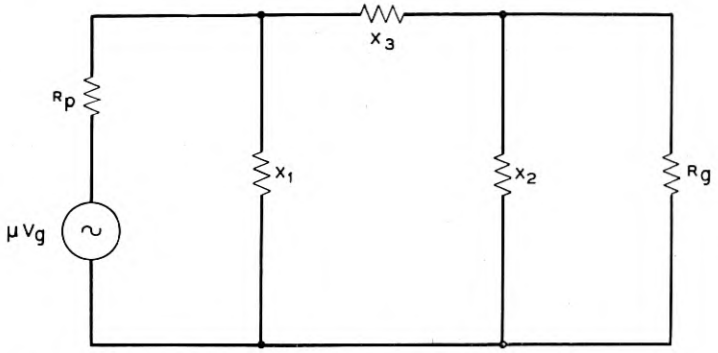

Fig. 12.24—Equivalent oscillator circuit analyzed for frequency stability

Then we obtain from (12.63)

$$\frac{1}{A}\frac{\partial A}{\partial V} = \frac{1}{\mu}\frac{\partial \mu}{\partial V} \qquad \frac{\partial \theta}{\partial V} = 0$$

$$\frac{1}{A}\frac{\partial A}{\partial a} = \frac{1}{R_g}\frac{\partial R_g}{\partial a}\left[1 + \frac{X_2 + X_3}{\mu X_2}\right] \qquad \frac{\partial \theta}{\partial a} = -\frac{1}{R_g}\frac{\partial R_g}{\partial a}\frac{X_0 R_p}{\mu X_1 X_2}$$

$$\frac{1}{A}\frac{\partial A}{\partial \omega} = \frac{1}{X_1}\frac{\partial X_1}{\partial \omega}\left[1 + \frac{R_p X_2 + R_g(X_2 + X_3)}{\mu R_p X_2}\right]$$

$$+ \frac{1}{X_2}\frac{\partial X_2}{\partial \omega}\left[1 + \frac{R_p(X_2 + X_3) + R_g X_1}{\mu R_p X_1}\right] \qquad (12.64)$$

$$+ \frac{1}{X_3}\frac{\partial X_3}{\partial \omega}\left[\frac{X_3(R_p X_2 + R_g X_1)}{\mu R_p X_1 X_2}\right]$$

$$\frac{\partial \theta}{\partial \omega} = -\frac{R_p}{\mu X_1 X_2}\left[(X_1 - X_s)\frac{1}{X_1}\frac{\partial X_1}{\partial \omega} + (X_2 - X_s)\frac{1}{X_2}\frac{\partial X_2}{\partial \omega}\right.$$

$$\left. + (X_3 - X_s)\frac{1}{X_3}\frac{\partial X_3}{\partial \omega}\right]$$

By substitution of these values in (12.61) and disregard of X_s in comparison with all other X's the equation for frequency stability is obtained as

$$\frac{d\omega}{dV} = \frac{\frac{1}{\mu}\frac{\partial \mu}{\partial V} X_1 X_2 X_3}{\left(1 - \frac{X_1}{\mu X_2}\right)\left(\frac{\partial X_1}{\partial \omega} + \frac{\partial X_2}{\partial \omega} + \frac{\partial X_3}{\partial \omega}\right) R_p R_g} \tag{12.65}$$

From this we learn that the values of the reactances X_1, X_2, and X_3 should be small and the values of R_p and R_g large to give small changes in ω when V is varied. These variables are more or less limited, however, by the conditions necessary for sustained oscillations according to equation (12.63). It is important to notice that the denominator of (12.65) contains functions which do not appear in equation (12.63) and hence may be of any value. These factors are the rates of change of the various reactances with frequency. For given values of circuit constants, the equation shows that the *frequency stability increases as these rates of change increase.*

12.63 Frequency Stability Coefficient of Crystals

The rate of change of the reactance of an element is referred to as the "frequency stability coefficient"* of the element. Expressed in per cent, we have for the frequency stability coefficient of a reactance

$$F(X) = \frac{dX}{d\omega} \cdot \frac{\omega}{X} \tag{12.66}$$

Let us now examine the frequency stability coefficient of a crystal which is used as the reactance X_2 when connected between grid and cathode of the tube and as X_3 when connected between grid and plate (See Fig. 12.24). The resistance of the crystal will be assumed to equal zero due to the negligible effect of the resistance variations upon the reactance for crystals with average Q and operated at a frequency not too near the anti-resonant frequency. (This may be observed in Fig. 12.21.)

The reactance of the crystal then is

$$X_c = -\frac{j}{\omega C_0} \frac{\omega^2 - \omega_1^2}{\omega^2 - \omega_2^2} \tag{12.67}$$

where

$\omega = 2\pi \times$ frequency
$\omega_1 = 2\pi \times$ resonant frequency
$\omega_2 = 2\pi \times$ anti-resonant frequency

* First suggested by N. E. Sowers.

By substitution of the relations

$$\frac{C_1}{C_0} = \frac{\omega_2^2 - \omega_1^2}{\omega_1^2} \quad \text{and} \quad -\frac{j}{\omega C_0} = X_0$$

into (12.67) we obtained

$$X_c = X_0\left[1 - \frac{C_1}{C_0}\frac{\omega_1^2}{\omega_2^2 - \omega^2}\right] \tag{12.68}$$

and by differentiation

$$\frac{dX_c}{d\omega} = -\frac{X_0}{\omega}\left[1 - \frac{C_1}{C_0}\frac{\omega_1^2}{\omega_2^2 - \omega^2}\right] - X_0\frac{C_1}{C_0}\left[\frac{\omega_1^2 2\omega}{(\omega_2^2 - \omega^2)^2}\right] \tag{12.69}$$

Multiply by $\frac{\omega}{X_c}$ to obtain the stability coefficient

$$F(X_c) = \frac{\omega}{X_c}\frac{dX_c}{d\omega} = -\frac{X_0}{X_c}\left[1 - \frac{C_1}{C_0}\cdot\frac{\omega^2}{\omega_2^2 - \omega^2}\right] - \frac{X_0}{X_c}\cdot\frac{C_1}{C_0}\cdot\frac{\omega^2}{\omega_1^2}\cdot\frac{2\omega_1^4}{(\omega_2^2 - \omega^2)^2} \tag{12.70}$$

and eliminate ω by substituting in (12.70) the relations obtained from equation (12.68). These are

$$\left.\begin{aligned} \frac{\omega_1^2}{\omega_2^2 - \omega^2} &= \left(1 - \frac{X_c}{X_0}\right)\frac{C_0}{C_1} \\ \text{and} \\ \frac{\omega^2}{\omega_1^2} &= \frac{C_1}{C_0} + 1 - \frac{C_1}{C_0}\frac{1}{1 - \frac{X_c}{X_0}} \end{aligned}\right\} \tag{12.71}$$

Thus

$$F(X_c) = -1 - 2\frac{X_0}{X_c}\left(1 - \frac{X_c}{X_0}\right)^2\left[1 + \frac{C_0}{C_1} - \frac{1}{1 - \frac{X_c}{X_0}}\right] \tag{12.72}$$

which may be written

$$F(X_c) = -\frac{X_c}{X_0}\left[1 + \left(1 - \frac{X_0}{X_c}\right) + 2\frac{C_0}{C_1}\left(1 - \frac{X_0}{X_c}\right)^2\right] \tag{12.73}$$

The stability coefficient of a coil and condenser $F(X)'$ may be obtained from (12.73) by letting $C_1 = \infty$. Then

$$F(X)' = -\frac{X_c}{X_0}\left[1 + \left(1 - \frac{X_0}{X_c}\right)\right] \tag{12.74}$$

The comparative stability of the crystal and tuned circuit is given by the ratio

$$\frac{F(X_c)}{F(X)'} = 1 + 2\frac{C_0}{C_1}\cdot\frac{\left(1 - \frac{X_0}{X_c}\right)^2}{1 + \left(1 - \frac{X_0}{X_c}\right)} \qquad (12.75)$$

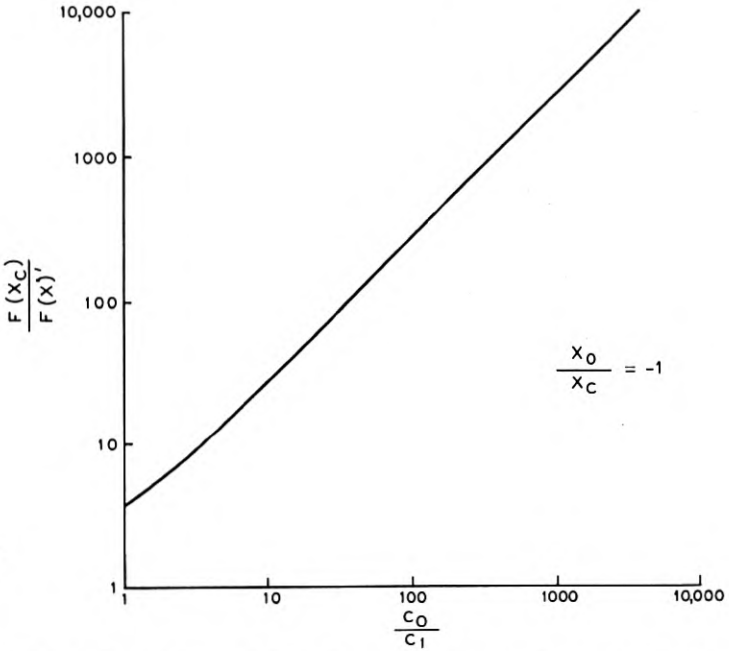

Fig. 12.25—The stability coefficient of a crystal as compared to a coil and condenser for variations of the ratio of capacitances

This ratio is plotted in Fig. 12.25 for $\frac{X_0}{X_c} = -1$ and with $\frac{C_0}{C_1}$ the independent function. It is apparent that the value of $\frac{C_0}{C_1}$ of a crystal is the factor which determines its frequency stability for given operating conditions. For an AT crystal in an air gap holder, the ratio of capacitances is of the order of 10^3 and its stability coefficient is therefore 2.6×10^3 greater than for a simple anti-resonant circuit. Since this is so much greater than the stability coefficients for the other reactances which appear in the denominator of equation (12.65) it represents the order of magnitude of improvement of the frequency stability of an oscillator obtained by the use of a crystal.

The fact that the frequency stability of a crystal oscillator is a function of $\frac{C_0}{C_1}$ explains why a BT cut crystal is in general more stable than an AT cut. The two may be made equal, however, by adding capacitance across the AT cut crystal.

Actually we have compared the frequency stability obtained by the use of one type of circuit (the equivalent crystal circuit) with one of a different configuration obtained by making $C_1 = \infty$. In practice this is usually the case since C_1 must be large to obtain oscillations when using coils and condensers. The limiting factor is therefore the value of $\frac{C_0}{C_1}$ at which oscillations stop and this is determined by the Q of the circuit elements as shown in the next section which deals with activity. It will be shown that the Q required is proportional to $\frac{C_0}{C_1}$ and therefore the maximum frequency stability that can be obtained is directly related to Q.

12.70 Relation Between Crystal Quality and Amplitude of Oscillations

The activity of a crystal is usually thought of as the relative amount of grid current produced in an oscillator circuit. This method of defining activity affords a means of comparing the quality of one crystal with another for a particular set of conditions. The disadvantages are first; it is only a relative measure, and second; it is not possible to compute the activity as thus defined by any method of oscillator analysis so far presented. Curves have been shown of amplitude of oscillations as a function of certain circuit variables, but these represent only qualitative changes associated with plate resistance variations. The first objection has been somewhat rectified by the use of reference oscillators* in which all the circuit elements including the tubes have been carefully matched. There is still the difficulty, however, of comparing crystals of different frequencies for it cannot be assumed that the measurements are independent of this variable. It would be more desirable to have some absolute measure of activity and particularly one which would lend itself to convenient computation from readily measurable constants of the crystal.

12.71 Definition of Crystal Quality for Oscillator Purposes

In deriving an expression for the quality of a crystal, it is convenient to use the negative resistance concept of the oscillator as described in section 12.40. The equations are general and in a form which admit of separating

* Developed by G. M. Thurston.

the crystal from the oscillator circuit. Equation (12.44) which gives the conditions necessary for oscillations to exist, may be written in the form

$$\omega C_t \rho \leqq \frac{\omega L_c}{R_c} \tag{12.76}$$

In order for oscillations to start, the right side of this equation must be equal to or greater than the left side. If it is greater, oscillations build up causing ρ to increase until the equality is satisfied. The difference between these two terms before oscillations start is therefore a relative measure of the final amplitude for a particular oscillator. The absolute value of amplitude cannot be obtained from equation (12.76) since we do not know the relation between ρ and amplitude. However the greater the magnitude of $\frac{\omega L_c}{R_c}$ the greater will be the amplitude of oscillations for a given set of oscillator conditions. This term may therefore be considered a measure of crystal quality. It is the effective Q of the crystal unit as measured at its two terminals and at the operating frequency. To distinguish this from the Q of the crystal as usually spoken of, it will be called φ_c.

In the same respect the left side of equation (12.76) may be thought of as a measure of quality of the oscillator circuit, that is, $\rho\omega C_t = \frac{1}{\varphi_0}$, then (12.76) becomes

$$\varphi_c \varphi_0 \geqq 1 \tag{12.77}$$

12.72 Figure of Merit of Crystals $-M$

It is very inconvenient to use φ_c as a figure of merit of the crystal because it is a complex function of the constants of the crystal circuits, Figure 12.3, and also the frequency. The computation of φ_c from such measurable characteristics as frequency of resonance f_1, frequency of anti-resonance f_2, resonant resistance R_1, and static capacity C_0, requires considerable time and effort.

It is highly desirable that a simple, easily determined expression for a figure of merit be found. The steps to indicate a suitable one are as follows:

The equation for φ_c in terms of measurable quantities for computing it is derived from equation (12.27) and given by the formula

$$\varphi_c = \frac{\omega L_c}{R_c} = \frac{-1 - \frac{\omega L_1^2}{R_1^2}\frac{(\omega^2 - \omega_1^2)(\omega^2 - \omega_2^2)}{\omega^4}}{\frac{\omega L_1}{R_1}\frac{\omega_2^2 - \omega_1^2}{\omega^2}} \tag{12.78}$$

By letting

$$M = \frac{\omega L_1}{R_1}\frac{\omega_2^2 - \omega_1^2}{\omega^2} \tag{12.79}$$

and

$$n = \frac{\omega_2^2 - \omega^2}{\omega_2^2 - \omega_1^2} \tag{12.80}$$

and with the assumption that over the narrow frequency range that the crystal will operate

$$\frac{\omega_2^2 - \omega_1^2}{\omega_1} \cong \frac{\omega_2^2 - \omega_1^2}{\omega_1 \omega} \tag{12.81}$$

equation (12.78) is reduced to

$$\varphi_c = -\frac{1 + nM^2(n-1)}{M} \tag{12.82}$$

In this equation it will be observed are only two variables, namely, n which varies widely as the frequency is varied between f_1 and f_2 and M which is substantially constant over the same range.

A set of curves is plotted in Fig. 12.26 for a hypothetical set of crystals having values of M of 1, 2, 5, and 10 with n varied over a range that falls between measured frequencies f_1 and f_2. Studies will show that whenever M increases φ_c will increase. M is readily calculated from measured constants as seen from the following: From (12.79)

$$M = \frac{\omega L_1}{R_1} \frac{\omega_2^2 - \omega_1^2}{\omega^2} = \frac{\omega_1 L_1}{R_1} \frac{\omega_2^2 - \omega_1^2}{\omega_1 \omega} \tag{12.83}$$

With the assumption in (12.81)

$$M = \frac{\omega_1 L_1}{R_1} \frac{C_1}{C_0} = \frac{1}{\omega_1 C_0 R_1} \tag{12.84}$$

which is a simple expression containing three of the four measured quantities mentioned above, and which bears a direct relation to activity for a given value of the frequency variable n. M is the new figure of merit of the crystal.

Figure 12.26 contains a further indication which is useful on occasions. Here φ_c is not positive at any frequency unless M is greater than 2. But φ_c must be positive for the crystal to oscillate in the two general types of circuits considered here.* It provides a measurable index to separate completely non-useful crystals from those that can oscillate in a given circuit.

Equation (12.84) may be written

$$M = \frac{Q}{r} \tag{12.85}$$

* For a description of oscillator circuits which do not require the crystal to exhibit a positive reactance see: "A New Direct Crystal-Controlled Oscillator for Ultra-Short-Wave Frequencies" by W. P. Mason and I. E. Fair, *Proc. I.R.E.*, Vol. 30, p. 464, Oct. 1943.

where Q is the Q of the crystal and r its ratio of capacitances. Thus the figure of merit involves the dissipation in the crystal determined by Q and the piezo-electric effect determined by r.[13]

It was pointed out in the preceding section that the frequency stability increases as r is increased. The above equation shows that Q must increase

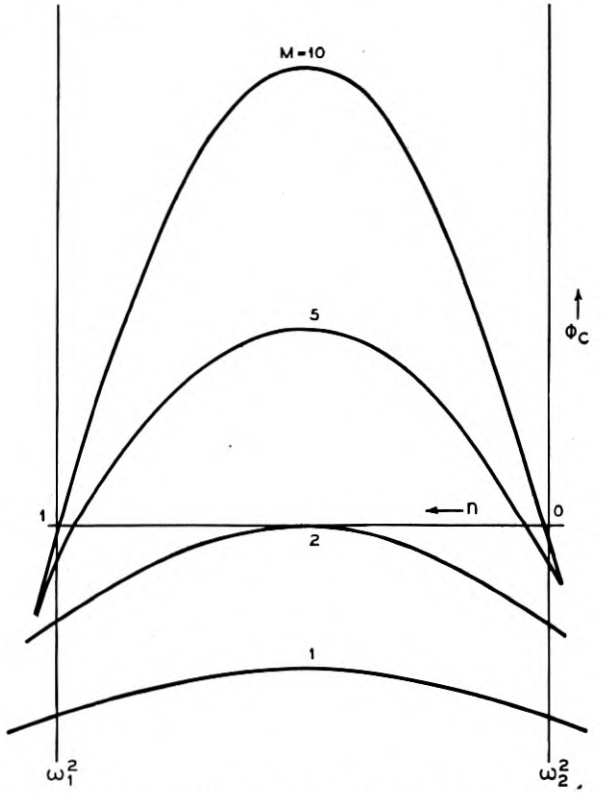

Fig. 12.26—The dependence of the quality function ϕ_c of a crystal upon frequency and figure of merit M

proportionately if the same figure of merit is to be maintained. The frequency stability obtainable in a particular oscillator is therefore limited by the Q of the crystal and the frequency stability coefficients should be compared on this basis.

12.80 Activity of Crystals

In deriving a figure of merit for crystals as oscillators, it was found that the amplitude of oscillations in a given circuit not only depends upon M but also it is a function of frequency relative to the resonant frequency

of the crystal. This may be explained by referring to Fig. 12.27 which shows curves of the reactance X_c of the crystal plotted as a function of frequency. The frequency at which oscillations occur depends principally upon the value of circuit capacitance C_t. Equation (12.43) shows that the frequency must adjust itself to a value at which C_t resonates with the reactance of the crystal. This value of reactance is represented on the curve as X_{co} and the corresponding frequency of oscillations as f_o. The

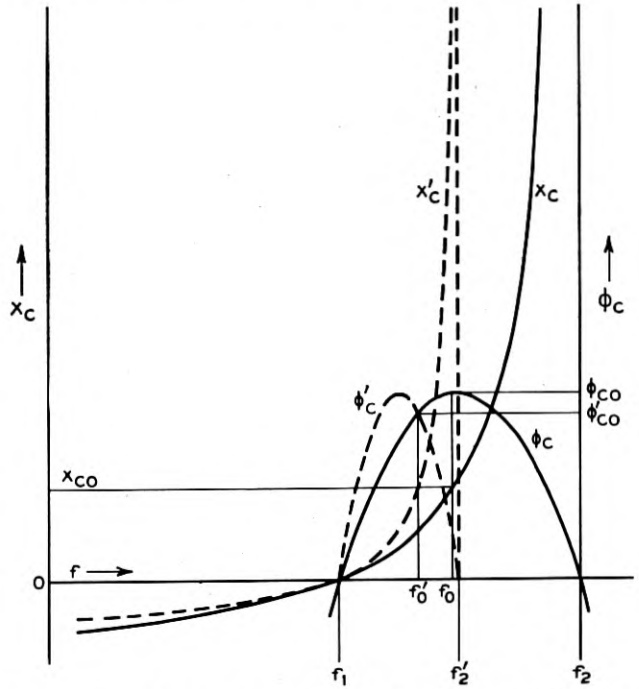

Fig. 12.27—Two crystals having the same figure of merit but with different reactance characteristics X_c and X'_c will operate with different amplitudes according to the relative values of φ_{co} and φ'_o respectively

circuit capacitance (or X_{co}) has been so chosen in the illustration that f_o lies equidistant between the resonant frequency f_1 and the anti-resonant frequency f_2. Then at this value of f_o, φ_c is a maximum, as shown by the φ_c curve, and for a given value of φ_g this will result in the greatest activity. Now let the capacitance C_0 of the crystal be increased. The frequencies f_1 and f_2 will then become closer and at the same time the height of the φ_c curve is reduced. Assume also that the Q is increased in order to maintain the same value of M and hence the same maximum value for φ_c. The reactance-frequency curve for the modified crystal and the corresponding

curve for φ_c' are represented by the dotted curves. Note that the oscillating frequency f_o' for the new curve is closer to f_2' than it is for f_1, therefore φ_{co}' is less than φ_{co} and the amplitude of oscillations will be less. Thus two crystals may have the same value of M but will not give the same output unless operated at the same relative frequency with respect to their resonant and anti-resonant frequencies. It would not have been possible to increase the oscillator output by increasing C_t so as to lower the frequency f_o' because by doing so φ_g is decreased more rapidly than φ_c' is increased, and the result would be a further decrease of activity. It is therefore necessary in deriving an expression for activity to include the variable of relative frequency or n which we have shown to be a function of the reactance of the circuit and the crystal constants.

12.81 Derivation of Performance Index of Crystals—*PI*

It will be assumed in the first derivation that the negative resistance ρ of the circuit is much greater than the effective resistance of the crystal R_c under stable oscillating conditions. Equation (12.43) which expresses the frequency then becomes

$$\omega \cong \sqrt{\frac{1}{L_c C_t}} \tag{12.86}$$

This leads to a very simple solution from which a more exact expression is later obtained.

Equation (12.44), which expresses conditions necessary for oscillations, may be written

$$|\rho| \leqq \left| \frac{\omega L_c}{\omega C_t R_c} \right| \tag{12.87}$$

As before, the numerical difference between ρ and the right side of the equation is a measure of activity. In fact, the right side of the equation may be considered to be an expression of the activity performance provided the terms are themselves independent of ρ. This is not quite true, since previous sections show that the capacitance C_t is not entirely independent of the activity. (See equations (12.30) and (12.46).) However, this effect may be considered negligible for most practical purposes and the value of the right side of (12.87) called the Performance Index (*PI*) of the crystal. From equations (12.86) and (12.87) the performance index is found to be

$$PI = \frac{1}{R_c \omega^2 C_t^2} \tag{12.88}$$

This equation may be greatly in error under operating condition which makes R_c large compared to ρ. Also R_c varies rapidly with frequency and is

difficult to evaluate. R_c is most readily eliminated from the equation by revising the picture slightly. With reference to the simplified oscillator circuit, Fig. 12.22B, it is apparent that the static crystal capacitance C_0 and the circuit capacitance C_t may be combined. This leaves for the crystal branch the inductance L_c' (different from L_c) which is a function of frequency and the resonant resistance of the crystal R_1 which is not a function of frequency. Now R_1 may be assumed small compared to ρ with considerable accuracy. It is only necessary, then, to replace C_t in equation (12.88) with $(C_0 + C_t)$ and R_c by R_1. This equation then becomes

$$PI = \frac{1}{R_1 \omega^2 (C_0 + C_t)^2} \tag{12.89}$$

An exact equation for PI is derived in section 12.83 and it is shown that the error in the simple expression above will in most cases be very small.

An approximate equation for the relation between R_1 and R_c is obtained by dividing (12.88) by (12.89). We thus find

$$1 = \frac{R_1 (C_0 + C_t)^2}{R_c C_t^2} \tag{12.90}$$

or the effective resistance of the crystal at the operating frequency is

$$R_c = R_1 \left(\frac{C_0}{C_t} + 1\right)^2 \tag{12.91}$$

Because of the approximation in equation (12.88) the equation for R_c above is accurate only when $\left(\frac{C_0}{C_t} + 1\right)^2 \ll M^2$ as will be shown in section 12.83.

The expression for PI as given by (12.89) may be written

$$PI = \frac{1}{\omega^2 C_0^2 R_1 \left(1 + \frac{C_t}{C_0}\right)^2} \tag{12.92}$$

which is the most convenient form for calculating PI from the constants of the crystal and the oscillator circuit.

12.82 Relation Between M and PI

It was found that

$$M = \frac{1}{\omega_1 C_0 R_1} \tag{12.93}$$

and this is essentially equal to $\frac{1}{\omega C_0 R_1}$ over the narrow frequency range considered. Therefore,

$$PI = \frac{M}{\omega C_0 \left(1 + \frac{C_t}{C_0}\right)^2} \tag{12.94}$$

This gives a relation between the performance index and the figure of merit of the crystal.

Another useful relation between M and PI is obtained from (12.89) and (12.93). Equation (12.93) may be written

$$M = \frac{X_0}{R_1} \tag{12.95}$$

This is of the same form as the Q of a coil when X_0 is considered to be the reactance of the coil and R_1 its resistance. Like the Q of a coil M is essen-

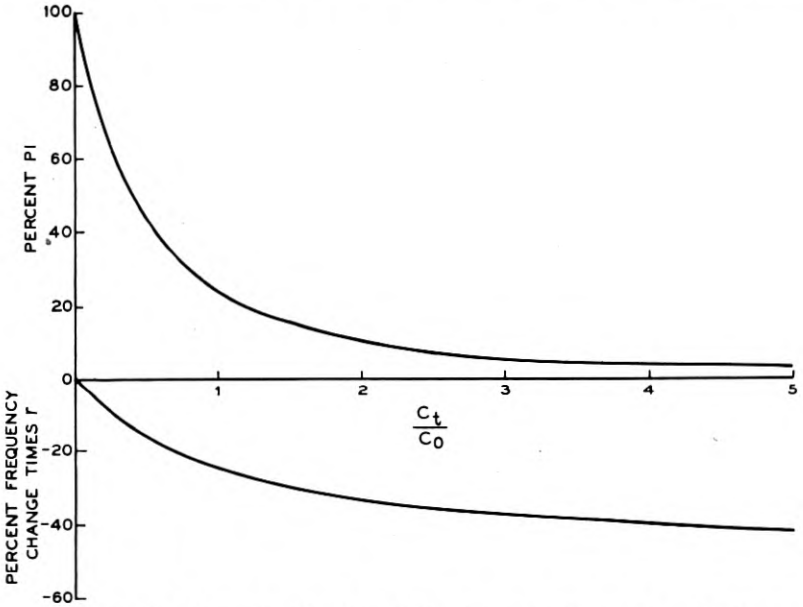

Fig. 12.28—The change in PI and oscillating frequency of a crystal as the shunt capacitance is increased

tially constant over a wide frequency range. Now if we let C_t approach zero in (12.89) it becomes

$$PI = \frac{1}{R_1 \omega^2 C_0^2} = \frac{X_0^2}{R_1} \tag{12.96}$$

This equation for PI is of the same form as the anti-resonant impedance of a coil and condenser in parallel, and like this impedance it changes rapidly with frequency. The maximum value of PI is therefore X_0 times M and is obtained when $C_t = 0$. Figure 12.28 shows a curve of % PI plotted as a function of $\frac{C_t}{C_0}$. This curve represents the change in activity as capacitance is added across the crystals (increase in C_t).

12.83 Exact Expressions for PI and R_c

The error in PI caused by the assumption that the frequency is independent of the crystal resistance R_1, that is, by use of approximate equation (12.86) for the frequency, may be investigated as follows:

The impedance of the crystal and C_t in parallel is given by

$$Z = \frac{1}{\omega(C_0 + C_t)(1 + m^2 P^2)} [P - j(1 + mP^2(m - 1))] \quad (12.97)$$

where

$$P = \frac{MC_0}{C_0 + C_t} \qquad m = \frac{\omega_3^2 - \omega^2}{\omega_3^2 - \omega_1^2}$$

ω_3 = 2π times frequency of anti-resonance of the crystal and C_t combination when $R_1 = 0$

ω_1 = 2π times frequency of resonance of the crystal and C_t combination when $R_1 = 0$

ω = 2π times operating frequency

(Note that P is the figure of merit of the crystal and C_t in parallel.) The imaginary part of Z is

$$X = -\frac{1 + mP^2(m - 1)}{\omega(C_0 + C_t)(1 + m^2 P^2)} \quad (12.98)$$

The condition for stable oscillations requires $X = 0$. For this condition

$$m = \tfrac{1}{2} \pm \sqrt{\frac{1}{4} - \frac{1}{P^2}} \quad (12.99)$$

which defines the exact frequency of oscillation. The negative sign before the radical is used since the effective resistance is greater at this frequency, thus requiring less negative conductance for oscillation.

With P large ($m \to 0$) the frequency of oscillations coincides with ω_3 which is the same as given by the approximate frequency equation (12.86). The real part of (12.97) is

$$R = \frac{P}{\omega(C_0 + C_t)(1 + m^2 P^2)} \quad (12.100)$$

and when $m = 0$

$$R = \frac{P}{\omega(C_0 + C_t)} = \frac{M}{\omega C_0 \left(1 + \frac{C_t}{C_0}\right)^2} \quad (12.101)$$

This is identical to the expression for PI of equation (12.94). *PI is therefore the anti-resonant resistance of the crystal and capacitance C_t in parallel.* Substitution of the value of m as given by (12.99) into (12.100) gives the anti-resonant resistance at the oscillating frequency. Thus

$$R_o = \frac{P}{\omega(C_0 + C_t)}\left[1 - \frac{1 - \sqrt{1 - \frac{4}{P^2}}}{2}\right] \tag{12.102}$$

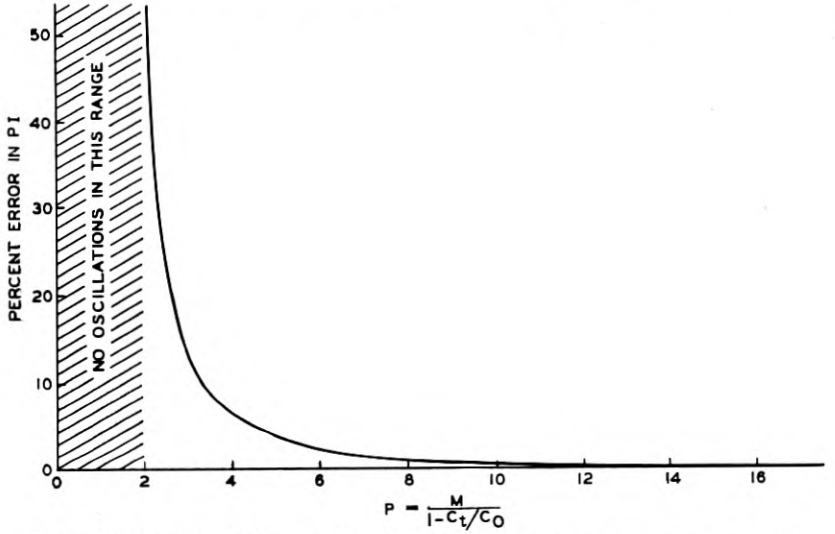

Fig. 12.29—The error in PI resulting from the use of approximate equation (12.94)

which is the exact expression for PI. The differential error resulting from the use of approximate equation (12.94) is then

$$\frac{PI - R_o}{R_o} = \frac{1 - \sqrt{1 - \frac{4}{P^2}}}{1 + \sqrt{1 - \frac{4}{P^2}}} \tag{12.103}$$

The per cent error as a function of P is shown in Fig. (12.29). The error diminishes rapidly with increase in P and is negligible for crystals that are of sufficient quality for most oscillator purposes.

Equation (12.91) for R_e is also approximate because of the assumption that the frequency is independent of R_e. A more exact expression will be derived.

The impedance of the crystal alone is

$$Z_c = \frac{1}{\omega C_0(1 + n^2 M^2)}\left[M - j(1 + nM^2(n - 1))\right] \tag{12.104}$$

where

M = the figure of merit of the crystal

$$n = \frac{\omega_2^2 - \omega^2}{\omega_2^2 - \omega_1^2}$$

ω_1 = 2π times frequency of resonance of the crystal
ω_2 = 2π times frequency of anti-resonance of the crystal
ω = the independent variable, 2π times frequency
C_0 = the static capacitance of the crystal

The resistive component of Z_e is

$$R_e = \frac{M}{\omega C_0(1 + n^2 M^2)} = \frac{R_1}{\frac{1}{M^2} + n^2} \tag{12.105}$$

In order to express R_e in terms of C_0 and C_t, the quantity n must be expressed in terms of these variables which define the oscillating frequency. This is accomplished as follows:

The equation of ratio of capacitances of a crystal is

$$\frac{C_1}{C_0} = \frac{\omega_2^2 - \omega_1^2}{\omega_1^2} \tag{12.106}$$

Similarly, when the capacitance C_t is placed across the crystal

$$\frac{C_1}{C_0 + C_t} = \frac{\omega_3^2 - \omega_1^2}{\omega_1^2} \tag{12.107}$$

where ω_3 is 2π times the anti-resonant frequency of the crystal and C_t in parallel. The ratio of (12.107) and (12.106) is

$$\frac{C_0}{C_0 + C_t} = \frac{\omega_3^2 - \omega_1^2}{\omega_2^2 - \omega_1^2} \tag{12.108}$$

The oscillating frequency is given by (12.99) in which m is as defined under (12.97). The oscillating frequency ω is therefore given by

$$\frac{\omega_3^2 - \omega^2}{\omega_3^2 - \omega_1^2} = \frac{1 - \sqrt{1 - \frac{4}{P^2}}}{2} \tag{12.109}$$

or

$$-\frac{\omega_1^2 - \omega^2}{\omega_3^2 - \omega_1^2} = \frac{1 + \sqrt{1 - \frac{4}{P^2}}}{2} \tag{12.110}$$

The angular frequency ω_3 is eliminated by multiplying this by (12.108). Thus

$$\frac{\omega_1^2 - \omega^2}{\omega_2^2 - \omega_1^2} = \frac{-C_0}{C_0 + C_t}\left[\frac{1 + \sqrt{1 - \frac{4}{P^2}}}{2}\right] \tag{12.111}$$

or

$$\frac{\omega_2^2 - \omega^2}{\omega_2^2 - \omega_1^2} = \frac{-C_0}{C_0 + C_t}\left[\frac{1 + \sqrt{1 - \frac{4}{P^2}}}{2}\right] + 1 \tag{12.112}$$

This is the value for n at the oscillating frequency and may be reduced to the form,

$$n = \left[\frac{1 - \sqrt{1 - \frac{4}{P^2}}}{2} + \frac{1 + \sqrt{1 - \frac{4}{P^2}}}{2\left(\frac{C_0}{C_t} + 1\right)}\right] \tag{12.113}$$

When this value of n is substituted in (12.105), the value of R_c is found to be

$$R_c = \frac{R_1}{\frac{1}{M^2} + \left[\frac{1 - \sqrt{1 - \frac{4}{P^2}}}{2} + \frac{1 + \sqrt{1 - \frac{4}{P^2}}}{2\left(\frac{C_0}{C_t} + 1\right)}\right]^2} \tag{12.114}$$

For crystals of usable quality $\frac{4}{P^2} << 1$ and by this assumption the equation reduces to

$$R_c = \frac{R_1}{\frac{1}{M^2} + \frac{1}{\left(\frac{C_0}{C_t} + 1\right)^2}} \tag{12.115}$$

This again reduces to (12.91) when $M^2 >> \left(\frac{C_0}{C_t} + 1\right)^2$.

12.84 Frequency Change Resulting from Paralleling Capacitance

It is often desirable to know how much the frequency of an oscillator may be changed by varying the capacitance C_t across the crystal. This is determined from (12.112) which gives the oscillating frequency as a function

of C_t. For practical considerations we may assume $\frac{4}{P^2} \ll 1$ which reduces the equation to

$$\frac{\omega_2^2 - \omega^2}{\omega_2^2 - \omega_1^2} = \frac{C_t}{C_0 + C_t} \tag{12.116}$$

From this and (12.106) we obtain

$$\frac{\omega_2^2 - \omega^2}{\omega_1^2} = \frac{C_1 C_t}{C_0 (C_0 + C_t)} \tag{12.117}$$

Since

$$\frac{\omega_2^2 - \omega^2}{\omega_1^2} = \frac{(\omega_2 - \omega)(\omega_2 + \omega)}{\omega_1^2} \simeq \frac{2(\omega_2 - \omega)}{\omega_1}$$

then

$$\frac{\omega - \omega_2}{\omega_1} \simeq \frac{-1}{2r\left(\frac{C_0}{C_t} + 1\right)} \tag{12.118}$$

where r is the ratio of the capacitances of the crystal.

A curve of per cent frequency change multiplied by r as a function of $\frac{C_t}{C_0}$ is shown on Fig. 12.28 for comparison with the associated PI change.

12.85 Relation between PI and Oscillator Activity

The relation between PI and activity obtained in a particular oscillator will now be examined. Let the curves of Fig. 12.30 represent the variations of ρ with amplitude for two oscillators A and B, or they might be for the same oscillator at widely different frequencies. These are characteristics of the oscillator circuits and may be of any shape. However, for oscillators with grid leak bias, the curves normally have no negative slopes. The rate of change of ρ depends upon the rate of change of μ and plate resistance of the vacuum tube as shown by (12.45) for input conductance.* Since ρ builds up to a value equal to PI we may plot PI for ρ. The grid current I_g is usually taken as a measure of amplitude. Therefore, Fig. 12.30 may be plotted as shown in Fig. 12.31 where PI is the independent variable. These curves are the characteristics of the oscillator circuits A and B with PI defining the quality of the crystal when used with a particular value of C_t. It is characteristic of oscillators to "saturate" as shown by the curves.

* It is also a function of grid resistance but this does not appear in the approximate equation (12.45) because of the assumption of no grid current. See Chaffee's[17] complete equation for input admittance.

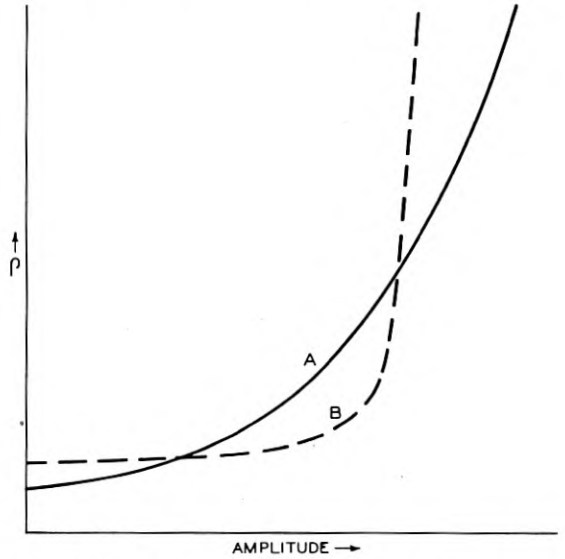

Fig. 12.30—Hypothetical curves illustrating the normal relation between the negative resistance of oscillator circuits and the amplitude of oscillations

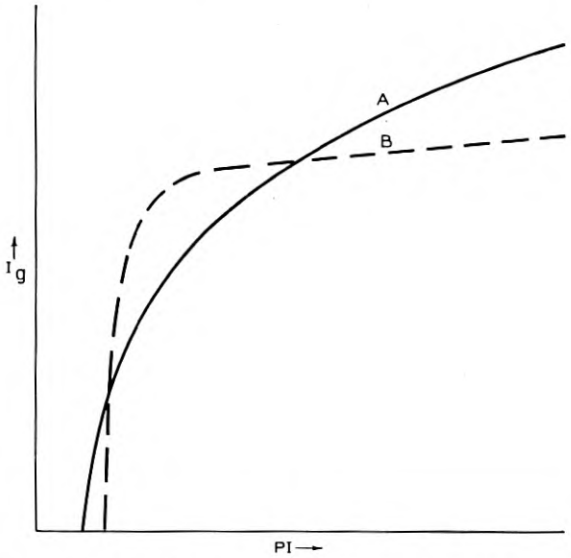

Fig. 12.31—By interchanging the coordinates of Figure 12.30 the curves will represent the relation between *PI* and oscillator grid current

Some oscillators saturate very rapidly and completely according to curve B and no further output is obtained regardless of the improvement in the crystal quality. For this reason it has not been possible in the past to separate the performance of the oscillator and the crystal since both were based upon the grid current as a measure of quality. By defining crystal activities and oscillator sensitivity in the manner outlined, the crystal and circuit can be studied separately. The per cent of crystals obtainable with PI above a certain value will be known and the design and improvement of oscillator circuits will be facilitated.

12.86 Use of PI in Crystal Design

The expression of PI in terms of the crystal constants and C_t as given by equations (12.89) or (12.92) assists in the design of crystals. As an example, the effect of changing the area of the crystal electrodes will be computed. The Q of a crystal is defined as

$$Q = \frac{1}{\omega_1 C_1 R_1} \tag{12.119}$$

By introduction of the ratio of capacitances of the crystal $r = \frac{C_0}{C_1}$ equation (12.119) becomes

$$Q = \frac{r}{\omega_1 C_0 R_1} \tag{12.120}$$

or

$$\frac{Q}{r} = \frac{1}{\omega_1 C_0 R_1} = M \tag{12.121}$$

Assuming Q and r do not vary, that is, disregarding effects such as secondary modes, change in damping produced by the mounting etc., and substituting (12.121) in (12.94) we obtain

$$PI = \frac{Q}{r} \cdot \frac{C_0}{\omega(C_0 + C_t)^2} \tag{12.122}$$

where $\frac{Q}{r}$ is considered constant. Differentiating (12.122) with respect to C_0 we find that PI is a maximum when $C_0 = C_t$. Since C_0 is proportional to the area of the electrodes this establishes the optimum area for a particular value of circuit capacitance.

The capacitance of BT-cut plates is 1.68 mmf. per square centimeter per megacycle.* Substitution of this for C_0 in (12.122) gives

$$PI = \frac{.268 \times 10^6 MA}{(1.68\ Af + C_t)^2} \tag{12.123}$$

* All frequencies are referred to the time interval of one second throughout this paper, i.e. *megacycles per second* is called simply *megacycles* as is customary in the radio field.

where A = the area of the crystal in square centimeters.
f = the frequency in megacycles
C_t = circuit capacitance in mmf.
M = figure of merit of the crystal (assumed constant)

Thus for crystals of a given area, the performance index should decrease as the frequency increases. Figure (12.32) shows the theoretical variations of *PI* as the function of the diameter of the electrodes of three frequencies and

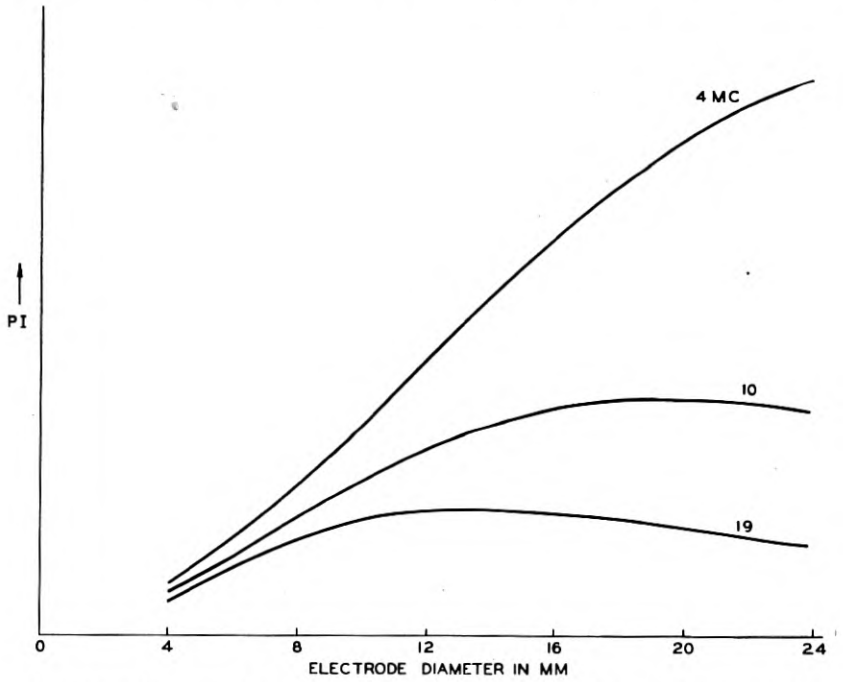

Fig. 12.32—Theoretical curves showing the relations of *PI*, electrode diameter, and crystal frequency for *BT* crystals and a circuit capacitance of 50 $\mu\mu$f

for a circuit capacitance of 50 mmf. The activity of a 4-megacycle crystal with 11-mm. diameter electrodes is about the same as a 10-megacycle crystal with 18 mm. electrodes. It must be remembered in making this comparison that it is assumed that the damping introduced by the mounting is the same in both cases. Actually the damping is much greater for low-frequency crystals of this type than for high-frequency ones and maximum *PI* occurs at some intermediate frequency as shown by the curves of Fig. 12.33. These curves show that the damping caused by the particular mounting used was small for frequencies above 6 megacycles but increases rapidly below this value.

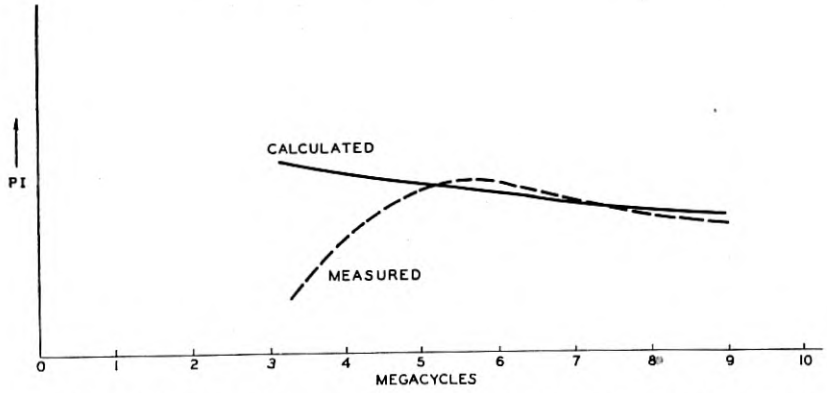

Fig. 12.33—Calculated and measured values of PI for BT crystals. The discrepancy is a measure of mounting loss

12.87 Measurement of PI and M

In all the discussions so far regarding the performance of crystals in oscillator circuits, the crystal has been represented by the equivalent circuit of Fig. 12.3 in which all the elements were considered constant. It is possible to obtain crystals in which this is essentially the case, but in general there are three secondary effects which complicate the picture. These are, first, the effect of other modes of vibration of the crystal, second, variations in the crystal constants resulting from variations in the amplitude of vibration, and third, the leakage or dielectric loss in the crystal holder. These factors will be considered in the order named.

Secondary modes of vibration affect the crystal for oscillator purposes only when the frequencies of these modes are sufficiently close to the principal one to alter its impedance characteristic in the frequency range of oscillation; that is, to alter the reactance as shown in Fig. 12.27 between the frequency f_1 and f_2 and the corresponding effective resistance between these two frequencies. With interfering modes present, the equivalent crystal circuit is so complicated as to make it impractical to compute PI or M from such measurable quantities as resonant resistance R_1, series resonant frequency f_1, anti-resonant frequency f_2, etc. For this reason it is necessary to measure the reactance and effective resistance of the crystal at the operating frequency in order to obtain a measure of crystal quality which will correlate with the crystal performance. For the same reason it is important when comparing oscillator circuits that the crystal should be operated at the same frequency in each case.

It is believed that the non-linear effect noticed in crystals when used as oscillators is produced by the changes in the mounting as the amplitude of

vibration varies. The PI of some clamped or pressure-mounted crystals has been found to vary as much as 50% with change in drive. Noticeable frequency change also occurs. A change in the nature of secondary modes as the amplitude is varied has also been observed. Some secondary modes which interfere with large amplitude of vibrations practically disappear when the amplitude is reduced. This may be explained by the fact that certain modes are damped out by the pressure of the mounting and with large amplitude of vibration the effect of the pressure is reduced.

The dielectric loss of the holder was considered negligible in the theory but it is found that certain phenolic holders have equivalent high-frequency leakage resistances less than 100,000 ohms. This resistance is in parallel with the crystal and will therefore reduce the PI according to the equation

$$PI = \frac{PI_c R_L}{PI_c + R_L} \tag{12.124}$$

where

PI = resulting PI
PI_c = calculated PI
R_L = equivalent high-frequency leakage resistance

Because of these secondary effects which are not negligible it is essential in measuring crystal activity that the frequency and voltage across the crystal be known. Standard test circuits should simulate operating conditions in this respect. With these considerations, a crystal PI meter has been developed in which the frequency and amplitude may be adjusted to correlate with various oscillators. The principle of operation and performance of this meter is described by C. W. Harrison.*

BIBLIOGRAPHY

1. A. McL. Nicolson, U. S. Patent Nos. 1495429 and 2212845, filed in 1918.
2. W. G. Cady, The Piezo-Electric Resonator. I.R.E., Vol. 10, p. 83, April, 1922.
3. G. W. Pierce, Piezo-Electric Crystal Resonators and Crystal Oscillators Applied to the Precision Calibration of Wavemeters. Proc. Amer. Acad. Arts & Sci., Vol. 59, p. 81, 1923.
4. A. Crossley, Piezo-Electric Crystal Controlled Oscillators. I.R.E., Vol 15, p. 9, Jan., 1927.
5. K. S. Van Dyke, The Electrical Network Equivalent of a Piezo-Electric Resonator. Physical Rev., Vol. 25, p. 895, 1925.
   The Piezo-Electric Resonator and Its Equivalent Network. I.R.E., Vol. 16, p. 742, June, 1928.
6. E. M. Terry, The Dependence of the Frequency of Quartz Piezo-Electric Oscillators Upon Circuit Constants. I.R.E., Vol. 16, p. 1486, Nov., 1928.
7. J. W. Wright, The Piezo-Electric Crystal Oscillator. I.R.E., Vol. 17, p. 127, Jan. 1929.

* "The Measurement of the Performance Index of Quartz Plates," this issue of the *B.S.T.J.*

8. P. Vigoureux, Quartz Resonators and Oscillators. Published by H. M. Stationery Office, Adastral House, Kingsway, London, W.C. 2.
9. R. A. Heising, The Audion Oscillator. The Physical Review, N. S., Vol. XVI, No. 3, Sept. 1920.
10. L. P. Wheeler, An Analysis of a Pieze-Electric Oscillator Circuit, I.R.E., Vol. 19, p. 627, April 1931.
11. F. B. Llewellyn, Constant Frequency Oscillators. I.R.E., Vol. 19, p. 2063, Dec. 1931; B.S.T.J., Jan. 1932.
12. Issac Koga, Characteristics of Piezo-Electric Quartz Oscillators. I.R.E., Vol. 18, p. 1935, Nov. 1930.
13. K. Heegner, Gekoppelte Selbsterregte Kreise und Kristallozillatorën. E.N.T., Vol. 15, p. 364, 1938.
14. R. A. Heising, The Audion Oscillator, Journal of the American Institute of Electrical Engineers. April and May, 1920.
15. M. Boella, Performance of Piezo-Oscillators and the Influence of the Decrement of the Quartz on the Frequency of Oscillations. I.R.E., Vol. 19, p. 1252, July 1931.
16. H. J. Reich, Theory and Application of Electron Tubes. Page 313.
17. E. L. Chaffee, Equivalent Circuits of an Electron Triode and the Equivalent Input and Output Admittances, I.R.E., Vol. 17, p. 1633, Sept. 1929.
18. W. P. Mason, An Electromechanical Representation of a Piezo-Electric Crystal Used as a Transducer. I.R.E., Vol. 23, p. 1252, Oct. 1935.

The Measurement of the Performance Index of Quartz Plates

By C. W. HARRISON

15.00 Introduction

THE theory of the general behavior of crystals in oscillator circuits has been described by I. E. Fair[1]. In Fair's paper as well as in others[2], it has been pointed out that in the neighborhood of the operating frequency a crystal is equivalent to the circuit shown in Fig. 15.1A. The crystal possesses two resonant frequencies, a series resonant frequency determined by the effective inductance, L_1, and effective capacitance, C_1, and an anti-resonant frequency determined by these same elements plus the paralleling capacitance, C_0. This paralleling capacitance is the static capacitance between electrodes of the crystal and any capacitance connected thereto by the crystal holder and lead wires within the holder. The dotted resistor, R_L, shunting the equivalent crystal circuit represents the effective shunt loss of the holder. In the ideal case and in many practical instances this loss is negligible.

It is rather difficult to express the circuital merit of a crystal quantitatively in a single term such as has been found useful for inductances and capacitances. It is customary to express the circuital merit of these two elements in the form of the ratio of reactance to resistance. That is, for an inductance

$$Q = \frac{\omega L}{R} \tag{15.1}$$

and for a capacitance

$$Q = \frac{1}{\omega C R}. \tag{15.2}$$

For filter purposes, the Q of a crystal involving only the inductance, L_1, and resistance, R_1, of Fig. 15.1A is adequate to express its usefulness in certain parts of a filter network, but for oscillator purposes it is insufficient. At frequencies other than the series resonant frequency the paralleling capacitor C_0 together with the associated shunt loss of the holder enters into the determination of a crystal's performance. The term Q therefore is not completely indicative of the crystal performance. There has been devised, as pointed out in Fair's paper[1], a term called "figure of merit" for a crystal

[1] I. E. Fair, "Piezoelectric Crystals in Oscillator Circuits," this issue of the *B.S.T.J.*

[2] K. S. Van Dyke, "The Electrical Network of a Piezo-Electric Resonator", *Physical Review*, Vol. 25, pp. 895, 1925.

which involves all the elements in the effective crystal circuit, and this term is much more expressive of the quality of a crystal. The figure of merit is:

$$M = \frac{\omega L_1}{R_1}\frac{C_1}{C_0} = \frac{Q}{r} \tag{15.3}$$

where "r" is the ratio of the paralleling capacitance to the series branch capacitance. Figure of merit is useful for expressing the quality of a crystal

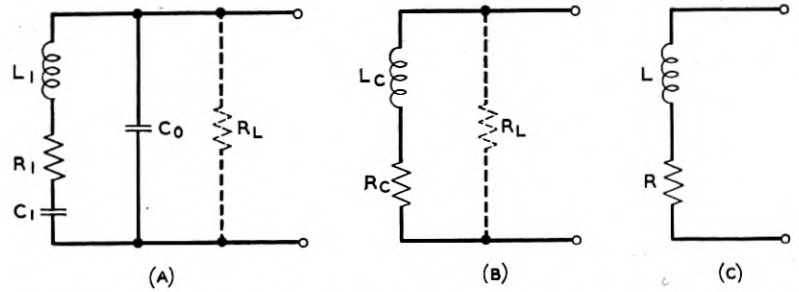

Fig. 15.1—Electrical equivalent circuits of a piezoelectric crystal—(A) At any frequency between the resonant frequency ω_1, and anti-resonant frequency ω_2; (B) and (C) at any specific frequency between ω_1 and ω_2.

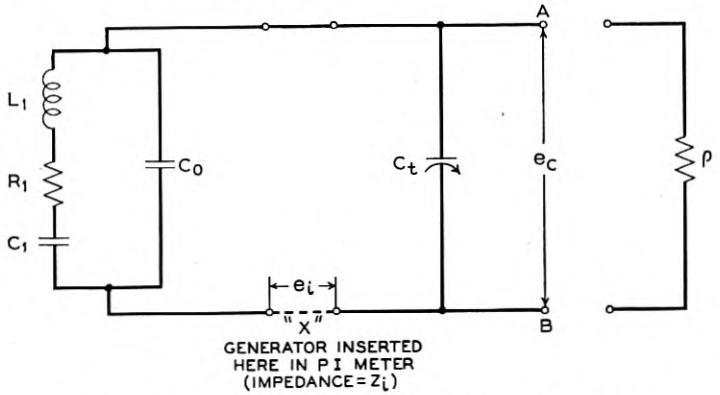

Fig. 15.2—Generalized oscillator circuit of the Pierce or Miller type.

in its holder or mount; however by definition it is independent of the value of R_L, and does not permit a ready evaluation of the performance of the crystal in an oscillator of the type that may be represented by Fig. 15.2. Any oscillator that operates the crystal in the positive region of the reactance vs. frequency characteristic exhibits capacitive reactance and negative resistance paralleled across the terminals to which the crystal is connected. The operation of the crystal when connected to an oscillator will be influenced by the magnitude of these two terms, and the combination must operate at

such a frequency that the total reactance is zero and at such an amplitude that the total resistance is zero. The performance of the crystal will therefore not depend solely upon its figure of merit, but will involve the impedance of the remainder of the oscillator. Up to the present time circuit design engineers have not devised standards or units to express the quality of their oscillator circuits without the crystal, so there are no corresponding circuital units of quality with which to correlate figures of merit of crystals to ascertain the suitability of one for the other.

It was a practice for many years for manufacturers to test crystals in a model of the oscillator in which the crystal was to be used. This required manufacturers to keep on hand models of all oscillators for which they expected to make crystals. To avoid the mounting number of such test oscillators a special test set was developed which could be adjusted to simulate any oscillator. By correlating various oscillator circuits to a set of adjustments on the test set, the actual model of the oscillator can be dispensed with. This special test set usually referred to as the '"D" spec. test set', eliminated the "file" of oscillators, and substituted a file of adjustment readings that would be their equivalent. However, the '"D" spec. test set' is still inadequate to the development engineer since it defines "activity" in terms of oscillator grid current rather than in terms of the electrical equivalent circuit of the crystal. The activity as expressed by grid current is a purely arbitrary standard and serves only as a means of determining the relative activity as against other crystals of the same frequency operated under the same circuit conditions.

The need for a system of measurement using units that are fundamental and not empirical has led to the proposal of "Performance Index". An instrument to make such measurements is to be described in this paper.

Specifically the Performance Index is

$$PI = \frac{\omega L}{\omega C_t R} \tag{15.4}$$

where C_t is the paralleling capacitance that is found in the oscillator circuit to which the crystal is attached, and L and R represent the effective inductance and resistance of the crystal as measured at the operating frequency indicated in Fig. 15.1C which is its equivalent *at that frequency*. If the loss in the holder is so low that the resistance, R_L, may be neglected, then PI may be expressed in other relations that are more useful such as,

$$\left.\begin{aligned} PI &= \frac{M}{\omega C_0 \left(1 + \frac{C_t}{C_0}\right)^2} \\ \text{or} \quad PI &= P^2 R_1 \end{aligned}\right\} \tag{15.5}$$

where the symbols R_1 and C_0 are as shown in Figs. 15.1A and 15.2 and P is expressed as

$$P = \frac{M}{1 + \frac{C_t}{C_0}} \tag{15.6}$$

With the effective capacitance, C_t, of the remainder of the oscillator added to the paralleling capacitance, C_0, in Fig. 15.2, the operating frequency will be that frequency at which the combination will exhibit a pure resistance at the terminals AB (excluding the generator "X" which is involved in the measuring technique). This leads to the definition:

The Performance Index is the anti-resonant resistance of the crystal and holder having in parallel with it the capacitance introduced by the remainder of the oscillator.

The Performance Index is therefore a term to express performance not in terms of the grid current of some particular oscillator, but in fundamental circuital units—impedance. The Performance Index is a term that may be used to compare performance of crystals at different frequencies. Its value is independent of plate voltage, grid leak resistance, or of plate impedance. It provides a measuring stick that should replace the "activity" figures of grid current in so far as the crystal is concerned. It paves the way for the oscillator circuit designers to come forth with standards of measurement for the oscillator circuit without the crystal in the hope that the two may be quantitatively associated and lend themselves to theoretical calculation of full oscillator performance.

15.10 Theory of Measurement

The problems of measurement are most readily explained by reference to Fig. 15.2. The crystal provides elements L_1, C_1, R_1 and C_0. The circuit of the oscillator provides an effective capacitance, C_t, which is composed of grid and lead wire capacitances plus capacitance introduced from the plate circuit. The frequency at which this combination exhibits anti-resonance as measured at AB is the oscillating frequency. The resistance when added to negative resistance, ρ, will be zero. Oscillations will start with ρ numerically smaller than the anti-resonant resistance measured at AB, but the amplitude of oscillations will increase causing ρ to increase until ρ and Z_{AB} are equal numerically. The primary problem is to measure the anti-resonant resistance at AB at the anti-resonant frequency with ρ disconnected.

Measurement of anti-resonant resistance directly is very difficult. The current flowing into an anti-resonant circuit is too small to measure with the usual meters. Other devices for measuring the current are likely to introduce paralleling capacitance that will vitiate the readings. The sug-

gested method of measurement utilizes a suitable driving voltage at "X" (Fig. 15.2) and a means to indicate the voltage at "X" as well as at points AB. From these and other measured constants, the anti-resonant impedance can be computed.

This method of measurement has its own difficulties, but it is believed corrections can be made to allow for errors introduced. Fundamentally, the series resonant frequency and the anti-resonant frequency are the same only when the resistances in the inductive and capacitive branches are equal. When the resistance is practically all in the inductive branch, which is true in this case, the impedance between terminals AB, at the series resonant frequency will exhibit capacitive reactance, though the total impedance will scarcely be different from that at the anti-resonant frequency. In the Performance Index meter, although the voltage is introduced in series with the circuit, the frequency is adjusted to the point of maximum voltage across AB, which further minimizes this frequency difference. A second error is inherently introduced by the loss in the crystal holder. This means that the series resonant frequency is also altered by the presence of this loss. Errors of any seriousness will result from the assumption that the series resonant and anti-resonant frequencies are identical only when the resistance in the inductive branch and loss in the crystal holder approach the effective crystal reactance in magnitude. These errors will be discussed in greater detail in a succeeding section.

The development and operation of a satisfactory meter to measure PI (Performance Index) depends upon a number of factors such as:

1. A method to determine capacitance, C_t, of the circuit (Fig. 15.2).
2. A generator "X" to produce the driving voltage e_i having variability in frequency and negligible internal impedance.
3. A current indicator that introduces a minimum of reactance and resistance.
4. A circuit or method to indicate PI directly, or with a minimum of calculations.
5. A number of other factors associated with the above which will be mentioned at the logical times.

To construct a measuring circuit to determine the anti-resonant impedance by means of a series circuit so as to avoid any unnecessary measurements and computations involves the following basic principle. Excluding ρ, Fig. 15.2 is essentially equivalent to the circuit used in Q meters. The ratio of voltage e_c to the driving voltage e_i is the voltage stepup or the Q of that part of the circuit containing the resistance. In this case, the resistance is in the crystal which at the operating frequency has an effective Q of

$$Q_1 = \frac{\omega L}{R} \tag{15.7}$$

where L and R represent the effective values of the crystal. Equation (15.4) will be found to embody the relation

$$PI = \frac{\omega L}{\omega C_t R} = Q_1 X_t \tag{15.8}$$

where X_t is the reactance of C_t, the capacitance introduced by the circuit at the operating frequency. If e_i is kept constant, e_c will at all times be proportional to Q_1. By insertion of an attenuator network, whose attenuation varies with frequency in the same manner as does the reactance of C_t, between terminals AB and the voltmeter, the meter indication will be proportional to the product of these quantities or *proportional to PI*. With

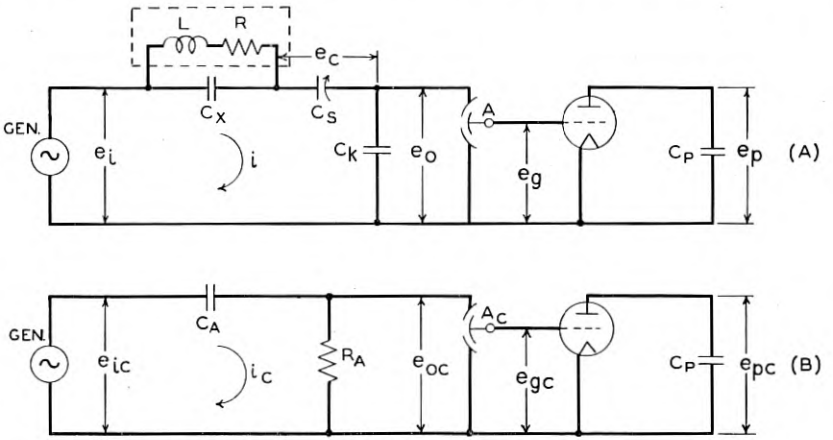

Fig. 15.3—Measuring circuits of the performance index meter.

suitable calibrations, therefore, it should be possible to get indications of *PI* as readily as is now done for Q.

The circuit shown in Fig. 15.2 is now best redrawn as in Fig. 15.3A. The crystal embodying elements L_1, C_1, R_1, and C_0 of Fig. 15.2 is now represented in Fig. 15.3A by the dotted rectangle and as having effective inductance, L, and effective resistance, R, both of which are functions of frequency. Capacitance, C_t, is simulated by capacitors C_x plus C_s and C_k in series where C_x represents the capacitance of the crystal socket. Zero internal impedance of the generator is simulated by maintaining the driving voltage constant at all times and at all frequencies. To facilitate explanation, the measured voltage e_i at the place shown is considered to be the driving voltage from a zero internal impedance generator.

Instead of using an ammeter to indicate current in the circuit, a voltmeter is utilized to measure voltage across an element under such conditions as

not to introduce disturbing capacitance. Splitting the series capacitance into two parts, C_s and C_k, the latter fixed and large compared to C_s, provides the impedance element across which the voltmeter is connected. The input capacitance of the voltmeter is incorporated in the magnitude of C_k. A capacitance attenuator, A, of known or calibrated values interposed on the input of the voltmeter enables the voltmeter to be used to indicate voltage ratios in terms of the attenuator calibration.

The measuring voltmeter and a shunting capacitance, C_p, are connected in the plate circuit of the amplifier tube, V-1. This circuit provides sufficient gain to furnish an output voltage of measurable magnitude and also provides an output voltage inversely proportional to frequency. The indication of the output voltage is proportional to PI.

The utilization of a vacuum tube in a circuit leading to a quantitative measuring instrument such as the voltmeter across C_p involves determination of tube constants or calibration. The determination of these constants is best evaluated experimentally. A calibrating circuit for that purpose is shown in Fig. 15.3B. A capacitance, C_A, of high impedance in series with comparatively negligible resistance, R_A, is connected across the driving voltage terminals of e_i with a voltmeter measuring e_i giving a reading e_{ic}. The second subscript "c" indicates calibration conditions. By connecting the input circuit of V-1 across this resistance, the attenuation variation with frequency of the $R_A - C_A$ network cancels the attenuation variation with frequency in the plate circuit of V-1. The ratio of e_{ic} to e_{pc} will then be independent of frequency. In the "calibrate" circuit (Fig. 15.3B), the capactior attenuator, A_c, interposed in the grid circuit is set at unity (minimum insertion loss) for a given deflection of the meter indicating e_p. In the operate circuit (Fig. 15.3A), the attenuator is readjusted so that voltage e_0 produces the reading of e_p as obtained in the calibrate position. The quantitative action of the amplifier then may be expressed in terms of C_p, R_A, C_A and a reading from the attenuator A, as will be shown later, and it is constant and independent of frequency. By placing this resulting constant in an equation, which will also be derived later, the value of PI may be determined in terms of such constant, of the reading of attenuator A, and of a reading on the scale of C_s that has been calibrated in terms of C_t.

To facilitate still further the operation of the PI meter, the voltage e_i is produced as shown in Fig. 15.4 by arranging for the oscillator to have its frequency controlled by the crystal through feedback from capacitor, C_k. Automatic volume control is provided such that the amplitude of e_i is essentially constant at all times and at all frequencies. The circuit is constructed to oscillate at the desired frequency, and adjustment for insuring this operation is provided in the form of a phase shifting circuit with variable

capacitor, C_r. After a crystal has been inserted in its proper place, oscillations will begin, but may be slightly above or below the resonant frequency of the crystal plus C_t. By adjustment of C_r the frequency can be shifted the slight amount necessary for resonance. This is observed by placing switch S in the PI position and making the adjustment to give maximum deflection of e_p.

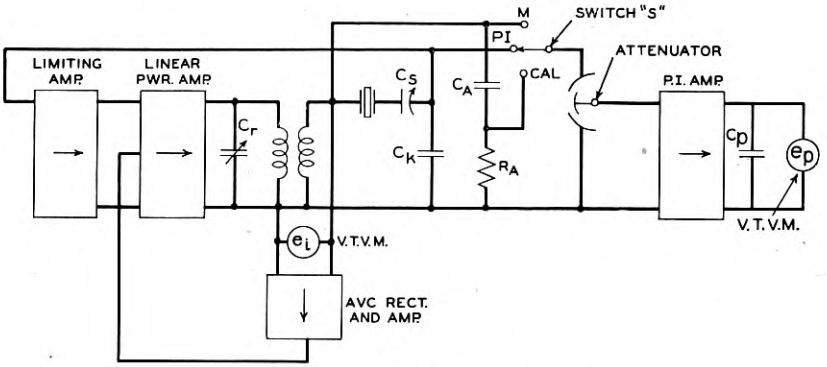

Fig. 15.4—Diagram of Performance Index meter.

15.20 Derivation of PI Circuit Equation

The following circuit relations derived from Figure 15.3 show first, that the ratio of e_p to e_i is a function of the Performance Index of the crystal, and second, that the calibration circuit permits an absolute evaluation of its magnitude.

At resonance, the effective circuit Q, designated as Q_2, is determined from

$$Q_2 = \frac{|e_c + e_0|}{e_i} = \frac{e_0}{e_i}\left(1 + \frac{C_k}{C_s}\right) \tag{15.9}$$

Since the circuit Q includes the capacitance of C_x as a part of the crystal, it is necessary to express Q_2 in terms of the crystal's properties (see Fig. 15.1). Since $Q_1\left(=\frac{X}{R}\right)$ of the crystal is independent of C_x, the relationship between Q_1 and Q_2 is readily obtained by equating the expressions for the anti-resonant impedance first, when C_x is considered to be in shunt with the series capacitor, C_t, and second, when C_x is considered as part of the crystal. This results in

$$Q_2 = Q_1 \frac{C_t - C_x}{C_t} \tag{15.10}$$

where

$$C_t = C_x + \frac{C_s C_k}{C_s + C_k} \tag{15.11}$$

enabling Q_1 to be expressed as

$$Q_1 = \frac{e_0}{e_i} \frac{C_t C_k}{(C_t - C_x)^2} \tag{15.12}$$

Expressing e_0 in terms of e_p, we have

$$|\mu e_g| = |i_p| \sqrt{r_p^2 + X_{C_p}^2} \tag{15.13}$$

$$|i_p| = \frac{e_p}{X_{C_p}} \tag{15.14}$$

hence

$$e_g = \frac{e_p \omega C_p}{G_m} \sqrt{1 + \left[\frac{X_{C_p}}{r_p}\right]^2} \tag{15.15}$$

and

$$\frac{e_0}{A} = e_g \tag{15.16}$$

With the above equations substituted in (15.12), we may express Q_1 as

$$Q_1 = \frac{e_p}{e_i} \omega \frac{C_p}{G_m} A \frac{C_k C_t}{(C_t - C_x)^2} \sqrt{1 + \left[\frac{X_{C_p}}{r_p}\right]^2} \tag{15.17}$$

Now

$$PI = \frac{Q_1}{\omega C_t} = Q_1 X_t \tag{15.18}$$

Therefore

$$PI = \frac{e_p}{e_i} A \frac{C_p}{G_m} \frac{C_k}{(C_t - C_x)^2} \sqrt{1 + \left[\frac{X_{C_p}}{r_p}\right]^2} \tag{15.19}$$

If

$$\sqrt{1 + \left[\frac{X_{C_p}}{r_p}\right]^2} \cong 1 \tag{15.20}$$

$$PI = \frac{e_p}{e_i} A \frac{C_p}{G_m} \frac{C_k}{(C_t - C_x)^2} \tag{15.21}$$

The simplified PI expression (15.21) assumes that the reactance of C_p is small compared to the plate resistance and plate load resistance of V-1. The evaluation of PI from this expression has three obvious difficulties:

(1) C_p/G_m is a quantity that is difficult to evaluate numerically, (2) the magnitude of PI is measured in terms of the ratio of the two voltages, e_i and e_p, and (3) the measurement is dependent upon the gain of a vacuum tube amplifier, V-1. These difficulties may be materially reduced in their consequence by an internal calibration circuit.

The internal calibration circuit (Fig. 15.3B) consists of a capacitor, C_A, and resistor, R_A, in series. If the reactance of C_A is very much greater than R_A, and the plate resistance of V-1 is very much greater than the reactance of C_p, the calibration is essentially independent of frequency.

The internal calibration circuit (Figure 15.3B) enables the evaluation of C_p/G_m to be carried out. The additional subscript, c, indicates "calibrate" conditions.

$$i_c = \frac{e_{ic}}{\sqrt{R_A^2 + X_{C_A}^2}} \tag{15.22}$$

$$e_{0c} = i_c R_A = \frac{e_{ic}\,\omega C_A R_A}{\sqrt{1 + \left[\frac{R_A}{X_{C_A}}\right]^2}} \tag{15.23}$$

$$\frac{e_{0c}}{A_c} = e_{g_c} \tag{15.24}$$

Equation (15.15) remains the same for both "operate" and "calibrate" conditions with the exception of the second subscript reserved for the "calibrate" operation. Therefore, by solving for C_p/G_m we find

$$\left|\frac{C_p}{G_m}\right| = \frac{e_{gc}}{e_{p_c}\,\omega \sqrt{1 + \left[\frac{X_{C_p}}{r_p}\right]^2}} \tag{15.25}$$

Equation (15.25) may be rewritten as (15.26), if (15.23) and (15.24) are substituted in (15.25)

$$\left|\frac{C_p}{G_m}\right| = \frac{e_{ic} R_A C_A}{e_{pc} A_c}\left[\frac{1}{\sqrt{1 + \left[\frac{X_{C_p}}{r_p}\right]^2}}\right]\left[\frac{1}{\sqrt{1 + \left[\frac{R_A}{X_{C_A}}\right]^2}}\right] \tag{15.26}$$

If (15.26) is substituted in (15.19), it is found that PI may be expressed as follows:

$$PI = \frac{e_p}{e_i}\frac{e_{ic}}{e_{pc}}\frac{A}{A_c} R_A C_A \left[\frac{C_k}{(C_t - C_x)^2}\right] \frac{1}{\sqrt{1 + \left[\frac{R_A}{X_{C_A}}\right]^2}} \tag{15.27}$$

The above equation involves only the original approximation that maximum current indicates resonance. If R_A and C_A are selected such that $R_A << X_{C_A}$ and if A_c equals unity, then

$$PI = \left[\frac{e_p}{e_i}\frac{e_{ic}}{e_{pc}}\right] A \frac{C_k}{(C_t - C_x)^2} R_A C_A \tag{15.28}$$

From this expression it can be seen that the PI measurement is independent of calibration of both the e_p and e_i vacuum tube voltmeters, provided that the same voltmeter scale factors are used for the "operate" and "calibrate" conditions. The absolute calibration then depends on the magnitude of A, R_A, C_A, C_k, C_t and C_x. The "multiply-by" factor that is to appear on the C_s dial is determined by the magnitude of $\frac{R_A C_A C_k}{(C_t - C_x)^2}$.

Accurate evaluation of this quantity by capacitance and resistance measurements is a little difficult since the denominator represents the square of the difference of two small capacitances. When C_t is large, the evaluation of this factor is helped considerably. This "multiply-by" factor may be experimentally determined by a voltage measuring means which permits an evaluation of this factor to a higher degree of accuracy. Substituting (15.11) in (15.28) we have

$$PI = \left[\frac{e_p}{e_{pc}}\frac{e_{ic}}{e_i}\right] A \frac{R_A C_A}{C_k}\left(1 + \frac{C_k}{C_s}\right)^2 \tag{15.29}$$

Now by shorting the crystal socket terminals (Fig. 15.3A) and applying a voltage e_1 at the e_i generator terminals of external origin (the crystal oscillator circuit itself may be used if self-excitation is provided), the current i_1 through the capacitors C_k and C_s is given as

$$i_1 = \frac{e_1 \omega C_s C_k}{C_s + C_k} = \frac{e_1 \omega C_k}{\left(1 + \frac{C_k}{C_s}\right)} \tag{15.30}$$

Now the voltage, e_2, across the series capacitor, C_k, is

$$e_2 = \frac{i_1}{\omega C_k} \tag{15.31}$$

The ratio of e_1/e_2 may be expressed as given in (15.32) when (15.31) is substituted in (15.30)

$$\frac{e_1}{e_2} = \left(1 + \frac{C_k}{C_s}\right) \tag{15.32}$$

If (15.32) is substituted in (15.29), we find

$$PI = \left[\frac{e_p}{e_{pc}}\frac{e_{ic}}{e_i}\right] A \frac{R_A C_A}{C_k}\left[\frac{e_1}{e_2}\right]^2 \tag{15.33}$$

The quantity $\frac{e_1}{e_2}$ is readily determined by the attenuator, A, when the switch, S, (Fig. 15.4) is operated between "M" and "PI" for the above described conditions. The absolute calibration then depends upon A, R_A, C_A and C_k. All four of these quantities may be determined within a few per cent.

15.30 Oscillator Correlation

The equivalent crystal circuit has been discussed in so far as the measurement of PI is concerned; however, for correlation with an oscillator, the behavior of the crystal in that oscillator must be duplicated. Correlation of the PI meter with an oscillator is a function of both amplitude and frequency. It is obviously necessary from the derivation of (15.28) that the frequency of operation be duplicated, but the necessity for amplitude correlation can only be explained from the practical consideration that the equivalent circuit components of Fig. 15.1 are parameters that may be functions of amplitude. Crystals having nonlinear characteristics of the type that necessitate amplitude correlation may in part be attributed to either the method of mounting the crystal or couplings to other modes of vibration whose coupling coefficients are functions of amplitude.

In most oscillators the voltage across the terminals of a crystal is a function of many parameters such as plate voltage, vacuum tubes, etc. With an average set of conditions, however, reasonable correlation is obtained with the PI meter for a single adjustment of the generator voltage, e_i, for all crystals. The magnitude of e_i must, of course, be chosen to produce a voltage across the crystal equal to the average value obtained in the oscillator circuit for which the crystal is intended.

Frequency correlation with an external oscillator is a function of the effective capacitance, C_t, in shunt with the crystal. In order to duplicate the oscillator frequency with the PI meter, the capacitance, C_s, (Fig. 15.4) must be adjusted until the frequency of oscillation in the PI meter is the same as that in the oscillator for a crystal having average activity. In Fig. 15.4, the capacitance, C_s, is variable, and its dial is calibrated in terms of both the total effective capacitance across the crystal, C_t, and the resulting multiplying factor $\frac{R_A C_A C_k}{(C_t - C_x)^2}$. The magnitude of C_t may be measured by means of a capacitance bridge connected across the crystal socket terminals with the generator impedance shorted.

The determination of the dynamic or effective capacitance, C_t, across the crystal for an oscillator may similarly be obtained by adjusting the magnitude of C_s in the PI meter until the frequencies of oscillation in the PI

meter and in the oscillator under test are identical for the same amplitude of oscillation. By this means, the *PI* meter directly indicates the effective oscillator capacitance, C_t. The amplitude of oscillation must be duplicated in as much as C_t is not independent of the amplitude in most oscillators.

15.40 Description of Oscillator Generating "e_i"

The generator plays no part in the theory of *PI* measurement as it could be replaced by a signal generator or any other suitable source of radio frequency energy. It is convenient, however, to utilize the voltage appearing across C_k as an input to an amplifier whose output represents the generator. This in effect constitutes a feedback oscillator whose frequency is controlled by the crystal under test. Initial consideration of the over-all characteristics of the *PI* meter oscillator leads to the following requirements. The oscillator must,

1. Be capable of oscillating all crystals usable in other oscillator circuits.
2. Be capable of operating the crystal over a wide range of shunting capacitances in order to duplicate all the frequencies of oscillators now in the field.
3. Be capable of permitting high degrees of *AVC* control in order to maintain the generator voltage constant while the frequency is adjusted for reasonance.

If the generator voltage, e_i, is constant, resonance of the crystal circuit is essentially indicated by maximum crystal current, and oscillation is maintained at that resonant frequency. The adjustment to obtain maximum current is such that the phase shift throughout the oscillator loop is $2\pi n$ where $n = 0, 1, 2, 3$, etc. As previously described the phase shift and resulting frequency of oscillation are varied by a tuned circuit. The generator voltage, e_i, is held constant by an automatic amplitude control similar to the automatic volume control which is often applied to amplifiers. The manual control of the magnitude of the generator, e_i, is provided by an adjustment of the bias voltage of the automatic amplitude control circuit. In this way the maximum or start gain is independent of the setting of the amplitude control.

Automatic amplitude control (commonly referred to as automatic volume control, *AVC*) of an oscillator may be applied by the separation of the limiter from the linear amplifier. This means that in order to apply a high degree of *AVC* to the *PI* oscillator (Fig. 15.4), the input voltage of the limiter must be above the threshold of limiting by an amount exceeding the variation in the β path caused by the *AVC* control. This enables the limiter to absorb the changes in the gain of the linear amplifier such that $\mu\beta = 1$ at all times.

The time constant of the limiter is fast compared to that of the *AVC*

circuit, a condition which permits damping of transients set up by changes in gain occurring from AVC action. The input of the linear amplifier is held constant by the limiter. Gain changes in the linear amplifier produced by the variation of C_r (Fig. 15.4) are absorbed by AVC, while the variation of activity in the crystal is absorbed by the limiting amplifier.

15.50 Evaluating Performance Index

From (15.28) it can be seen that the attenuator, A, the effective variable capacitance, C_t, together with the vacuum tube voltmeters, e_i and e_p, offer a number of possible variations in the method of evaluating the constants used to determine the PI of quartz crystals. There are, however, two principal methods—the first provides direct reading, while the second is more accurate but requires an indirect evaluation.

The first method utilizes a means of calibration of the meter scales directly in terms of PI. The attenuator is adjusted such that its indicator reading times the multiplying factor associated with the dial attached to C_s is some multiple of 10. If in the calibrate position, A_c is set at unity, and e_{pc} and e_{ic} are adjusted by varying the capacitive load to some reference deflection, then the expression for PI becomes

$$PI = \frac{e_p}{e_i} K_1 \tag{15.34}$$

where

$$K_1 = \left[\frac{e_{ic}}{e_{pc}} A \frac{C_k R_A C_A}{(C_t - C_x)^2}\right]$$

The Performance Index then is indicated by the two readings of e_p and e_i. The absolute magnitudes of e_i and e_p need not be known since it is possible to use as a reference, the arbitrary calibrating deflections of e_{ic} and e_{pc}. The magnitude of e_p indicates the significant figures while e_i is a multiplying factor.

The second method of evaluating Performance Index eliminates any calibration errors in the two vacuum tube voltmeters, e_i and e_p. This method utilizes the attenuator to adjust $\left[\frac{e_p e_{ic}}{e_i e_{pc}}\right] = 1$. In the "calibrate" operation, e_{ic} is set to equal e_i and then e_{pc} is adjusted for full scale or a convenient deflection. In the "operate" position, the attenuator is varied until e_p equals e_{pc}. In this manner, the two readings of the attenuator are used to determine the ratio of $\frac{e_p}{e_{pc}}$ and the measurement is independent

of the voltmeter calibration. The factor $R_A C_A$ is a constant; therefore, the P.I. equation (15.28) simplifies to

$$P.I. = (\Delta A)K_2 \tag{15.35}$$

where

ΔA = change in attenuator insertion loss between the "operate" and "calibrate" conditions in terms of output voltage ratio $\frac{e_p}{e_{pc}}$, given as $\frac{A}{A_c}$.

$K_2 = \frac{C_k R_A C_A}{(C_t - C_x)^2}$ where C_t is the effective capacitance in series with the crystal, C_k is the fixed series capacitance and C_x is the crystal socket capacitance. (See Fig. 15.3)

15.60 P.I. Meter Applications

The application of this instrument can be extended to determine other properties of both crystal and oscillator. With the aid of a frequency measuring means and a capacitance bridge, the P.I. meter may be used to determine all the circuit constants designated in the electrical equivalent circuit of Fig. 15.1. If the loss in the holder is negligible then the equations are considerably simplified; however, in those instances where holder loss must be considered, the approximation that $X_t \ll R_L$ which may be allowed for most cases enables an evaluation of M and Q_c that is readily computed.

The dial controlling C_s, that is calibrated in terms of the total capacitance, C_t, makes possible the calculation of the magnitude of the input impedance to the crystal circuit, R, as well as Q_1.

$$\left.\begin{aligned} R &= \frac{X_t^2}{P.I.} \\ Q_1 &= \frac{P.I.}{X_t} \end{aligned}\right\} \tag{15.36}$$

The magnitude of Q_1 may also be measured directly from equation (15.12) where Q_1 was given as

$$Q_1 = \frac{e_0}{e_i} \frac{C_k C_t}{(C_t - C_x)^2} \tag{15.12}$$

As may be seen from Fig. 15.4, e_0/e_i can be evaluated in terms of the attenuator calibration by enabling switch, S, to select the "*PI*" and "*M*" positions respectively and adjusting the attenuator such that the same output meter indication is obtained in the two cases.

The quantity Q_1 makes possible the calculation of Q_c where Q_c is defined as

$$Q_c = \frac{\omega L_c}{R_c} \cong \frac{X_t}{R_1\left(1 + \frac{C_0}{C_t}\right)^2} \tag{15.37}*$$

It can be shown that Q_c in terms of Q_1 is given by the following equation if $R_L \gg X_t$.

$$Q_c = \frac{Q_1}{1 - Q_1\frac{X_t}{R_L}} = \frac{Q_1}{1 - \frac{P.I.}{R_L}} \tag{15.38}$$

The Figure of Merit, M, defined by (15.3) at the series resonant frequency of the crystal, ω_1, becomes

$$M \cong \frac{1}{\omega_1 C_0 R_1} = \frac{X_{c_0}}{R_1} \tag{15.39}$$

The measurement of M can be determined from Q_c provided C_t and C_0 are known. M may be determined from the following expression

$$M = \frac{Q_1}{1 - \frac{P.I.}{R_L}} \frac{C_t}{C_0}\left(1 + \frac{C_0}{C_t}\right)^2 \tag{15.40}$$

If C_t is selected such that $C_t \gg C_0$, then for most cases R_L is large compared to $Q_1 X_t$. This means that $Q_1 \cong Q_c$ and $R \cong R_c$. With this approximation, (15.40) becomes

$$M = Q_1 \frac{C_t}{C_0}\left(1 + \frac{C_0}{C_t}\right)^2 \tag{15.41}$$

The relationship between R_c and R_1 as a function of frequency may be expressed directly from the input impedance expression of the equivalent circuit. This is given as

$$R_c = \frac{R_1}{\left[\frac{\omega_2^2 - \omega^2}{\omega_2^2 - \omega_1^2}\right]^2 + \frac{1}{M^2}} \tag{15.42}$$

where ω is the unity power factor frequency in the P.I. meter, neglecting R_L. If

$$\frac{1}{M} \ll \left[\frac{\omega_2^2 - \omega^2}{\omega_2^2 - \omega_1^2}\right]$$

---

* The relationship $R_c \cong R_1\left(1 + \frac{C_0}{C_t}\right)^2$ was derived in Fair's paper*[1].

which is a plausible assumption when $C_t \geq C_0$, and we assume that $\frac{\omega_1 + \omega_2}{2} = \omega_e$ then,

$$R_c = \frac{R_1}{\left[\frac{\omega_2 - \omega}{\omega_2 - \omega_1}\right]^2} \tag{15.43}$$

The relationship between R_1 and R_c does not involve R_L and may be expressed in terms of C_0 and C_t instead of frequency. Neglecting R_L to determine the relationship between capacitance and frequency in the P.I. meter as derived in Section 15.92, we find

$$\frac{\omega_2 - \omega}{\omega_2 - \omega_1} = \frac{1}{1 + \frac{C_0}{C_t}} \frac{\left[1 + \sqrt{1 + \frac{4}{P_1^2}}\right]}{2} \tag{15.44}$$

where,

$$P_1 = \frac{M}{\left(1 + \frac{C_0}{C_t}\right)} \tag{15.45}$$

If $P_1 \gg 2$ then the expression between R_c and R_1 may be written

$$R_c = R_1 \left(1 + \frac{C_0}{C_t}\right)^2 \tag{15.46}$$

The restriction that $C_t \geq C_0$ may be removed if the error between (15.42) and (15.46) is taken into account. This error may be expressed as

$$\text{Per Cent Error in } R_c = 100 \left[\frac{1}{P_1^2}\right] \left[\frac{2}{1 + \sqrt{1 + 4/P_1^2}}\right] \tag{15.47}$$

The resonant resistance, R_1, together with (15.46) provides a means of checking the P.I. meter. The magnitude of R_1 may be determined by the substitution method and from this, the value of R_c calculated. Fig. 15.5 represents the agreement between the P.I. meter and those expected from resonant frequency measurements.

The remaining crystal constants L_1 and C_1 (Fig. 15.1) may be evaluated from the measurement of ω_1, ω_2 and C_0. The resonant frequency, ω_1, is defined as

$$\omega_1^2 = \frac{1}{L_1 C_1} \tag{15.48}$$

The anti-resonant frequency, ω_2, is defined as

$$\omega_2^2 = \frac{1}{L_1} \left(\frac{1}{C_1} + \frac{1}{C_0}\right) \tag{15.49}$$

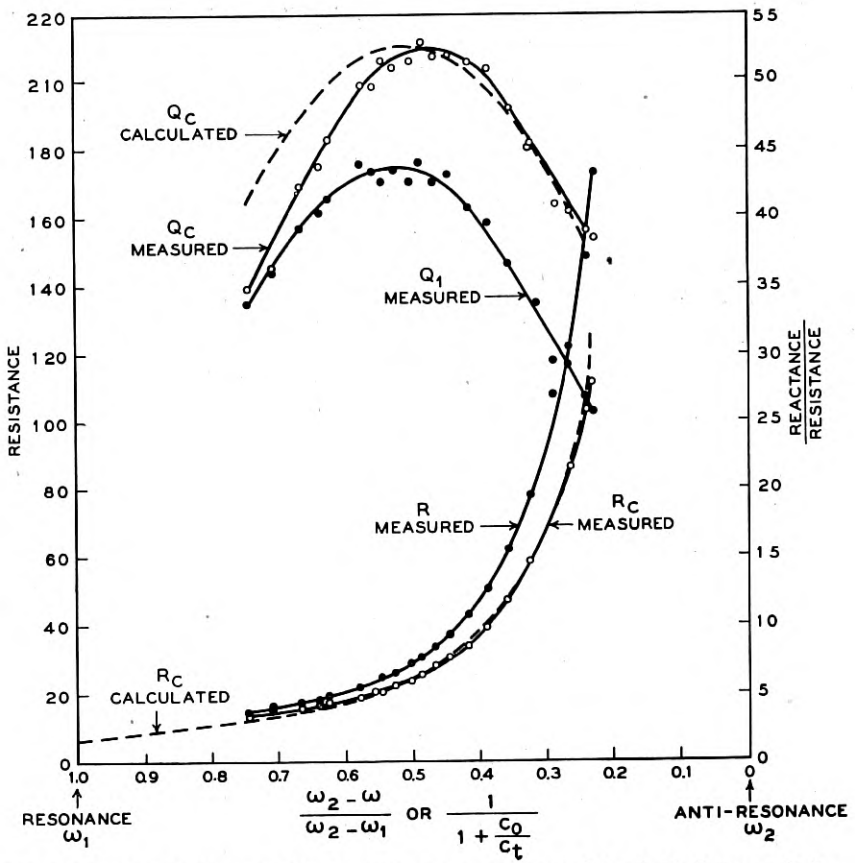

Fig. 15.5—Typical characteristic of a quartz crystal measured by the Performance Index meter.

Solving these equations simultaneously, it is found that

$$\left.\begin{aligned} L_1 &= \frac{1}{C_0(\omega_2^2 - \omega_1^2)} \eqsim \frac{1}{2\omega_e C_0(\omega_2 - \omega_1)} \\ C_1 &= \frac{C_0(\omega_2^2 - \omega_1^2)}{\omega_1^2} \eqsim \frac{2C_0(\omega_2 - \omega_1)}{\omega_1} \end{aligned}\right\} \tag{15.50}$$

15.70 Experimental Data

The performance of the P.I. meter may best be illustrated by experimental data. The following data indicate the correlation which may be obtained between the P.I. meter and various types of oscillator circuits. Experimental considerations are extended to

(1) Frequency and amplitude correlation with a "Pierce" and "Tuned-Plate" oscillator

(2) The measurement of the effective capacitance, C_t, of an oscillator as a function of tuning, and

(3) The variation of P.I. as a function of voltage across the crystal.

The results presented are not to be considered as generalized data, but are intended only to show a set of measurements obtained for a specific set of operating conditions for each type of circuit.

It has been pointed out that the frequency of oscillation is a function of R_1, ω_1, ω_2, C_0 and C_t. Since R_1, ω_1, ω_2 and C_0 are explicit parameters of the crystal, the capacitor, C_t, becomes the only frequency determining element in the P.I. meter. From analytical methods to be described in

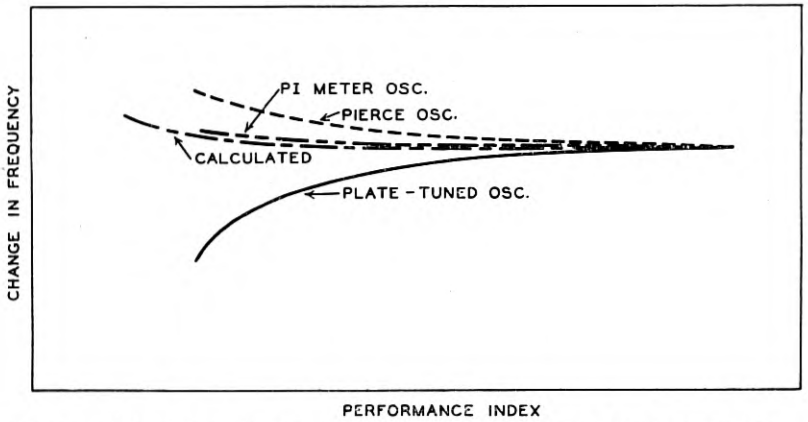

Fig. 15.6—Frequency variations in oscillators as a function of Performance Index.

Sections 15.80 and 15.92 the frequency difference between the P.I. meter and the generalized oscillator (neglecting R_L) is given as

$$\Delta\omega \cong \frac{(\omega_2 - \omega_1)}{M^2}\left(1 + \frac{C_0}{C_t}\right)\frac{2}{\left[1 + \sqrt{1 + \frac{4}{P_1^2}}\right]} - \frac{(\omega_2 - \omega_1)}{M^2}\left(1 + \frac{C_t}{C_0}\right) \tag{15.51}$$

Since the magnitude of frequency change in the above equation is small compared to the variations caused by changes in operating conditions, the P.I. meter may be used as a frequency correlation medium. Fig. 15.6 is an example of the correlation between the "Pierce" and "Tuned-Plate" oscillator and the P.I. meter. The P.I. meter falls between these two oscillators in frequency for any crystal activity. It must be recognized that Fig. 15.6 is not conclusive to the extent of generalization; however, it is indicative of possible correlation with these two popular oscillator circuits.

Figures 15.7 (A) and (B) show the amplitude correlation between the Performance Index meter and the grid current of the "Tuned-Plate" and "Pierce" oscillators, respectively. The P.I. vs. grid current characteristic was arbitrarily taken at three frequencies—4.5 mcs, 5.66 mcs and 7.81 mcs. The change in grid current of the oscillator shown in Fig. 15.7 (A) with frequency is caused by the varying *L-C* ratio in the plate circuit. (See curves *A*, *B* and *C* for constant crystal activity.) The curves *A* and *D* represent the effect of changing bands by switching coils, varying the *L-C* ratio 2 to 1 in the plate circuit for the same crystal frequency. Fig. 15.7

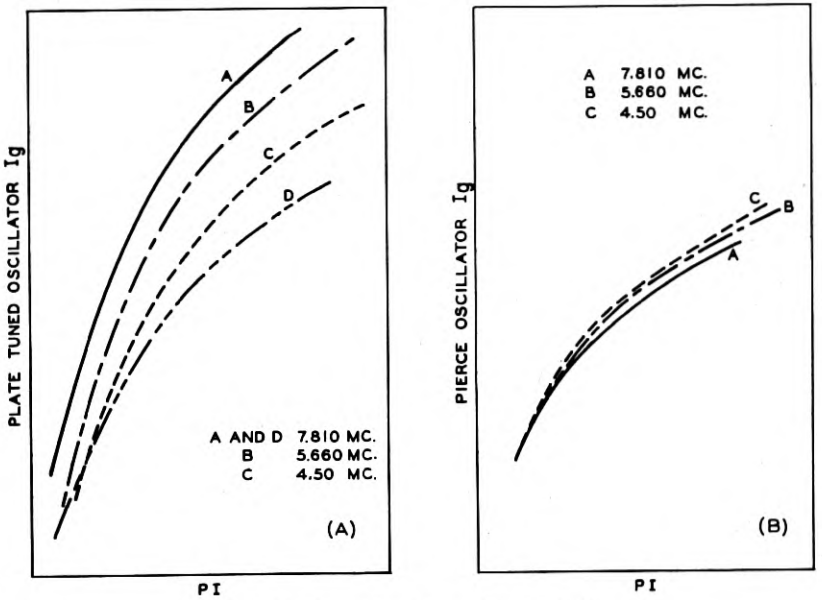

Fig. 15.7—Typical oscillator characteristics.

(B) represents the correlation between P.I. and grid current of the "Pierce" type oscillator. The results of this correlation indicate that the grid current is essentially independent of the operating frequency.

The measurement of P.I. is independent of the level of crystal vibration, provided that the electrical equivalent circuit parameters of Fig. 15.1 become constants; however, in actual practice these are not constants, particularly R_1. Variations of this type, as previously discussed, make it necessary to duplicate the amplitude of oscillation of the P.I. meter with the oscillator. Fig. 15.8 represents the variation of P.I. as a function of voltage across the crystal terminals for five crystals arbitrarily selected. It is readily observed that P.I. may be a random function of amplitude.

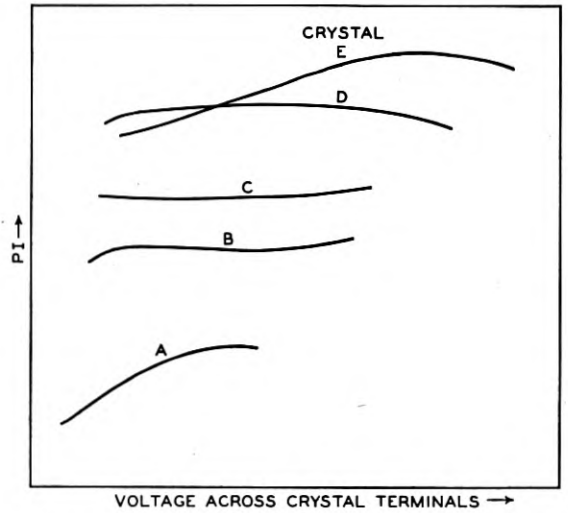

Fig. 15.8—Observed variation of Performance Index as a function of voltage across the crystal terminals.

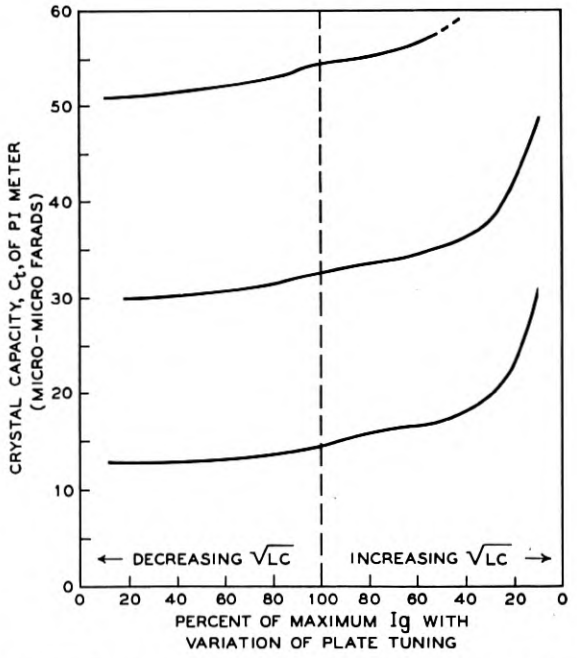

Fig. 15.9—Observed variation of effective crystal capacitance in a Miller oscillator.

Equation (15.44) indicates that the capacitance, C_t, determines the operating frequency between ω_1 and ω_2 of any given crystal. The capacitance, however, may include reflected reactances from associated circuits or possibly from circuits unintentionally coupled to the oscillator. Normally, crystals are adjusted to frequency for a specified value of C_t. This makes it of interest to measure the magnitude of C_t over the range of the manual oscillator tuning adjustments, as well as over the frequency range of the oscillator. Fig. 15.9 shows the circuit capacitance, C_t, plotted as a function of tuning of the plate circuit of a Tuned-Plate oscillator. Tuning of the plate circuit is expressed in terms of percentage of maximum grid current.

15.80 Circuit Analysis Involving the Accuracy of P.I. Measurements

The method of P.I. measurement just described involved a number of unverified approximations. These approximations under the majority of conditions will be proven to be justified and the resulting expressions for percentage error will be obtained.

It is necessary to apply a method of analysis that is most readily adaptable to the crystal circuit. The analysis described in this section involves the use of Conformal representation as a means of determining (1) the behavior of the equivalent crystal circuit, (2) the error resulting in P.I. from assuming operation at the resonant frequency rather than the frequency for minimum impedance, and (3) the comparison of frequency of oscillation in the P.I. meter with other oscillator circuits.

Generally, the variations of reactance, X, and resistance, R, of the equivalent circuit (Fig. 15.1) are plotted as a function of frequency, and the analysis of the impedance, $R + jX$, between the resonant frequency, ω_1, and anti-resonant frequency, ω_2, are handled in precisely the same way as any linear passive element. This was essentially the procedure used to derive the equations in section 15.60. The analysis required to evaluate the errors leads to rather an elaborate study; however, in Section 15.81, it will be shown that it is very helpful analytically if the impedance of the crystal is plotted in the form of a circle diagram, that is, with the ordinate representing reactance, X, and the abscissa representing resistance, R.

15.81 *Conformal Representation*

Conformal Representation or Mapping is a convenient tool which for this application enables the physical operating condition to be expressed quantitatively from its graphical counterpart. Physical interpretation also makes it possible to draw many other conclusions that by other methods prove clumsy and laborious.

The basis for this analysis depends upon the ability to utilize the following equation to represent any impedance whose frequency of operation is controlled by a crystal. This equation is known as a linear fractional transformation

$$W = \frac{\alpha + \beta Z}{\gamma + \delta Z} \tag{15.52}$$

The terms α, β, γ, and δ represent complex constants and Z represents a complex variable later to be chosen to represent a linear function of frequency. Since W and Z represent the dependent and independent variable, they may also be considered as representing two separate planes. The abscissa and ordinate of these two planes represent their real and imaginary components respectively. The planes are linked by (15.52), that is, this equation will transform a specific point from one plane to the other.

The constants α, β, γ and δ for the equivalent crystal circuit are determined by writing the expression for Z_c in the form of (15.52). For example (neglecting R_L), Z_c from Fig. 15.1 may be written as

$$Z_c = \frac{1}{j\omega C_0} \frac{\left[R_1 + j\left(\omega L_1 - \frac{1}{\omega C_1}\right)\right]}{\left[R_1 + j\left(\omega L_1 - \frac{1}{\omega}\left(\frac{1}{C_1} + \frac{1}{C_0}\right)\right)\right]} \tag{15.53}$$

By substituting (15.48) and (15.49) in (15.53), this impedance may be written as

$$Z_c = \frac{1}{j\omega C_0} \frac{[\omega R_1 + jL_1(\omega - \omega_1)(\omega + \omega_1)]}{[\omega R_1 + jL_1(\omega - \omega_2)(\omega + \omega_2)]} \tag{15.54}$$

Since the operating frequency, ω, represents some frequency between ω_1 and ω_2, and $\omega \gg \omega_2 - \omega_1$, we can make the following approximations in this operating range. The symbol ω_e is defined as the average operating radian frequency.

$$\left.\begin{aligned} \omega_e &= \frac{\omega_1 + \omega_2}{2} \\ \omega_e &\cong \omega \end{aligned}\right\} \tag{15.55}$$

If (15.55) is substituted in (15.54), factor ω_e out, add and subtract ω_2 from the imaginary component in both numerator and denominator, we may write Z_c as

$$Z_c = \frac{\left[\frac{1}{\omega_e C_0} + j\,\frac{1}{\omega_e C_0}\,\frac{2L_1}{R_1}\,(\omega_2 - \omega_1)\right] + \left[\frac{1}{\omega_e C_0}\right] j\,\frac{2L_1}{R_1}\,(\omega - \omega_2)}{[j] + [j] j\,\frac{2L_1}{R_1}\,(\omega - \omega_2)} \tag{15.56}$$

The constants α, β, γ and δ may be written immedately from (15.56); however, for purposes of simplification let

$$\left.\begin{aligned} \tau &= \frac{1}{\omega_e C_0} \\ Z &= j\frac{2L_1}{R_1}(\omega - \omega_2) \\ M &= \frac{2L_1}{R_1}(\omega_2 - \omega_1) \quad \text{(See equation 15.50)} \end{aligned}\right\} \tag{15.57}$$

then,

$$Z_c = \frac{[\tau + jM\tau] + [\tau]Z}{j + jZ} \tag{15.58}$$

Now if Z_c may be represented by W in (15.52) the remaining constants must be

$$\left.\begin{aligned} \alpha &= \tau + j\tau M \qquad \gamma = j \\ \beta &= \tau \qquad\qquad\quad \delta = j \end{aligned}\right\} \tag{15.59}$$

Now Z represents the frequency variable and graphically represents a line coincident with the Y-axis in the Z-plane, and W, the corresponding impedance variable, represents a circle in the W-plane. The coordinates of the center of the circle, W_0, in the W-plane is given by

$$W_0 = \frac{\beta}{\delta}\frac{\left[\frac{\alpha}{\beta} - \frac{\bar{\gamma}}{\bar{\delta}}\right]}{\left[\frac{\gamma}{\delta} + \frac{\bar{\gamma}}{\bar{\delta}}\right]} \tag{15.60}*$$

when $\bar{\gamma}$ and $\bar{\delta}$ represent the conjugate functions of γ and δ respectively. The radius of the circle is given by

$$\sigma = \left|\frac{\beta}{\delta}\right| \frac{\left|\frac{\alpha}{\beta} - \frac{\gamma}{\delta}\right|}{\left|\frac{\gamma}{\delta} + \frac{\bar{\gamma}}{\bar{\delta}}\right|} \tag{15.61}*$$

*E. C. Titchmarch, "Theory of Functions," Oxford 1932, pp. 191–192. Note: These equations are not derived in Titchmarch; however, by taking the limit as the diameter of the circle in the Z-plane approaches infinity, (15.60) and (15.61) result.

Now substituting the values given in (15.59) in (15.60) and (15.61) to determine the coordinates of the center of the circle and the radius respectively, we find

$$\left.\begin{aligned} W_0 &= \frac{\tau M}{2} - j\tau \\ \sigma &= \frac{M\tau}{2} \end{aligned}\right\} \tag{15.62}$$

As might be expected, the radius of the circle is equal to the real component of the coordinates of the center of the circle. This indicates that Fig. 15.10

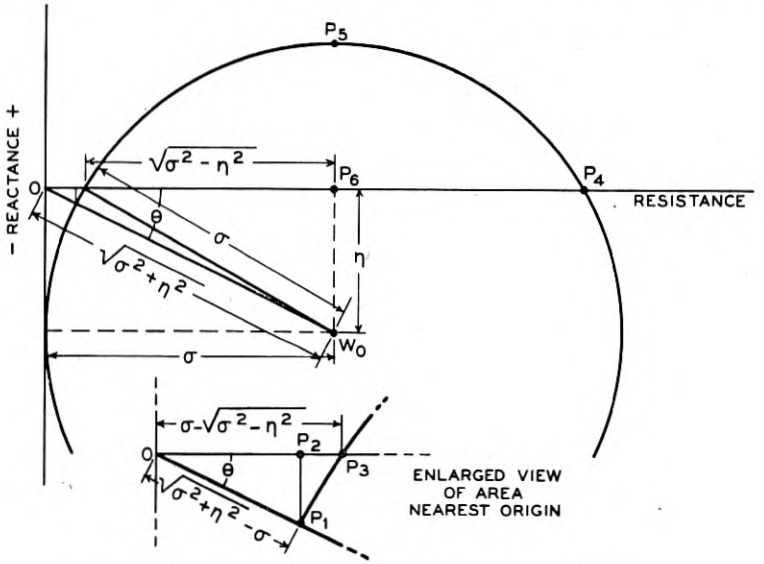

Fig. 15.10—Circle diagram for crystal circuit combinations.

graphically represents the circle diagram where $\eta \cong \tau$. The impedance, Z_c, is represented for a given frequency, as a vector from the origin to the corresponding point on the perimeter of the circle. From Fig. 15.10 the following crystal properties may be deduced.

1. The anti-resonant impedance designated as $O - P_4$ is simply $\sigma + \sqrt{\sigma^2 - \eta^2}$, and when evaluated equals $R_1(M^2 - 1) \cong R_1M^2$.
2. The resonant resistance, $O - P_3$ given by $\sigma - \sqrt{\sigma^2 - \eta^2}$ is equal to R_1.
3. The maximum positive reactance between ω_1 and ω_2 is represented by the distance from P_5 to P_6. It is given as $\sigma - \eta$ which equals $\left(\frac{R_1M^2}{2} - X_{c_0}\right)$.

4. The condition which must exist when the crystal reactance is zero between ω_1 and ω_2 occurs when $\sigma = \eta$ or $M = 2$.

It follows that the error of measuring, say the series resistance R_1, by varying the frequency for maximum transmission and assuming true resonance when the crystal is between two low non-inductive resistors is associated with the difference between the length of the two vectors $O - P_3$ and $O - P_1$. The per cent error caused by the crystal capacitor, C_0, by this method of measurement of R_1 is given as

$$\begin{aligned} \text{Per cent error of } R_1 &= 100\left[1 - \frac{O - P_1}{O - P_3}\right] \\ &= 100\left[1 - \frac{\sqrt{\sigma^2 + \eta^2} - \sigma}{\sigma - \sqrt{\sigma^2 - \eta^2}}\right] \end{aligned} \tag{15.63}$$

If σ and η are substituted in (15.63), we find

$$\text{Per cent error of } R_1 = 100\left[1 - \frac{1 + \sqrt{1 - \frac{4}{M^2}}}{1 + \sqrt{1 + \frac{4}{M^2}}}\right] \tag{15.64}$$

This difference in amplitude was caused by the difference in frequency between resonance and minimum impedance. This frequency difference may be determined by transforming the points P_1 and P_3 into the Z plane by (15.52) and subtracting them arithmetically.

In order to express the coordinates of any point in the W-plane by its real and imaginary components let

$$W = R_0 + jX_0 \tag{15.65}$$

Now the coordinates of P_3 may be expressed as,

$$R_0 = \sigma\left[1 - \sqrt{1 - \left(\frac{\eta}{\sigma}\right)^2}\right]; \qquad X_0 = 0 \tag{15.66}$$

The coordinates of P_1 are similarly given by

$$\left.\begin{aligned} R_0 &= \sigma\left[1 - \frac{1}{\sqrt{1 + \left(\frac{\eta}{\sigma}\right)^2}}\right] \\ X_0 &= -\eta\left[1 - \frac{1}{\sqrt{1 + \left(\frac{\eta}{\sigma}\right)^2}}\right] \end{aligned}\right\} \tag{15.67}$$

The coordinates of these two points represent values of W; now (15.52) may be solved for Z.

$$Z = \frac{\alpha - \gamma W}{\delta W - \beta} \tag{15.68}$$

Substituting in values for α, β, γ and δ given by (15.59), we find

$$Z = j\frac{2L_1}{R_1}(\omega - \omega_2) = j\frac{M(\omega - \omega_2)}{(\omega_2 - \omega_1)} = -j2\frac{\sigma(\eta + X_0)}{(\eta + X_0)^2 + R_0^2} \tag{15.69}$$

The real component of Z must be zero since the function of Z is coincident with the Y-axis. By substituting values of R_0 and X_0 from (15.66) and (15.67), we find

$$\omega - \omega_2 = -\frac{(\omega_2 - \omega_1)}{M}\frac{\eta/\sigma}{[1 - \sqrt{1 - (\eta/\sigma)^2}]} \tag{15.70}$$

also

$$\omega - \omega_2 = -\frac{(\omega_2 - \omega_1)}{M}\frac{\eta/\sigma}{\left[\sqrt{1 + \left(\frac{\eta}{\sigma}\right)^2} - 1\right]} \tag{15.71}$$

Subtracting (15.71) from (15.70) to get $\Delta\omega$ we have

$$\Delta\omega = \frac{\eta}{\sigma}\frac{(\omega_2 - \omega_1)}{M}A \tag{15.72}$$

where

$$A = \frac{\sqrt{1 - (\eta/\sigma)^2} - \sqrt{1 + (\eta/\sigma)^2}}{(\eta/\sigma)^2} \tag{15.73}$$

Now the $\lim_{\eta/\sigma \to 0} A = 1$. When $\frac{\eta}{\sigma} = \frac{2}{M}$ then $\Delta\omega = \frac{\omega_2 - \omega_1}{M}A$

15.82 *Circuit Analysis Involving Crystals*

The same procedure could be followed for the impedance, Z_i, in Fig. 15.3; however, the impedance expression conforming to (15.52) may be written directly if a more general expression is derived for impedances added in parallel or series.

Paralleling the impedance, W, with an impedance, T, (Fig. 15.11) modifies the constants in (15.52) but not its form providing T is essentially constant between ω_1 and ω_2. For parallel impedances the impedance equation becomes,

$$\frac{WT}{W + T} = \frac{\alpha + \beta Z}{\left(\gamma + \frac{\alpha}{T}\right) + \left(\delta + \frac{\beta}{T}\right)Z} = \frac{\alpha' + \beta' Z}{\gamma' + \delta' Z} \tag{15.74}$$

The numerator remains the same; however, the denominator has an additional term added to both γ and δ.

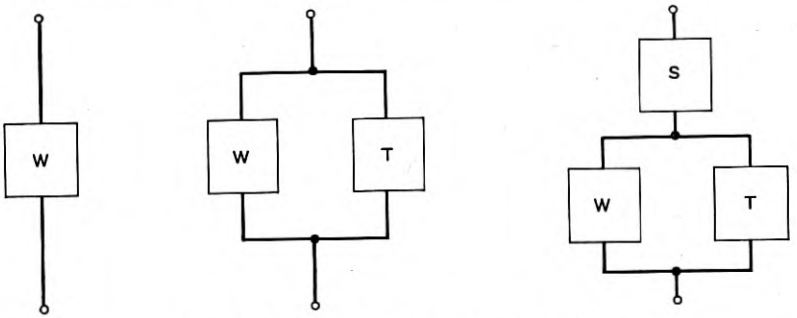

Fig. 15.11—Various crystal circuit combinations.

In the same way, a series element, S, may be added as shown in Fig. 15.11. The impedance of this combination is similarly modified and the input impedance may be expressed as

$$S + \frac{WT}{W+T} = \frac{\left[\alpha + S\left(\gamma + \frac{\alpha}{T}\right)\right] + \left[\beta + S\left(\delta + \frac{\beta}{T}\right)\right] Z}{\left(\gamma + \frac{\alpha}{T}\right) + \left(\delta + \frac{\beta}{T}\right) Z} = \frac{\alpha'' + \beta'' Z}{\gamma'' + \delta'' Z} \tag{15.75}$$

The addition of a series element leaves the denominator unchanged but adds a term to the numerator. The form of (15.75) is exactly the same as (15.52) except that the magnitudes of the constants, α, β, γ and δ have been modified.

As an example, apply (15.74) to obtain an expression for the impedance Z_{AB} (Fig. 15.2). This expression for impedance may be written directly if the following values are substituted in (15.74).

$$\left.\begin{aligned} \alpha &= \tau + jM\tau \\ \beta &= \tau \\ \gamma &= \delta = j \\ T &= \frac{1}{j\omega C_t} \end{aligned}\right\} \tag{15.76}$$

$$Z_{AB} = \frac{WT}{W+T} = \frac{[\tau + jM\tau] + [\tau]Z}{\left[-M\frac{C_t}{C_0} + j\left(1 + \frac{C_t}{C_0}\right)\right] + \left[j\left(1 + \frac{C_t}{C_0}\right)\right] Z} \tag{15.77}$$

From this expression we can again see the same form as (15.52) except that the coefficients of α, β, γ and δ are modified by the capacitance, C_t, in parallel with the equivalent crystal circuit. It has been previously explained that the frequency of oscillation in the generalized oscillator is determined by the anti-resonant frequency of the impedance, Z_{AB}, and that this impedance represents the exact definition of P.I. P.I. therefore is represented in magnitude by $O - P_4$ in Fig. 15.10.

Equation (15.75) enables us to write the expression for the input impedance, Z_i, for the P.I. meter directly and furthermore, it enables us to compute the error produced by the adjustment of C_r to minimum impedance rather than unity power factor as assumed in the derivation of (15.28). This error obviously will be a function of M, C_0, C_t and R_L. Writing the impedance expression for Z_i directly, requires a little modification in that the crystal is shunted by two elements, C_x (the crystal socket capacitance) and R_L (the holder loss) as well as having the combination in series with the capacitor, C_3, where $C_3 = \dfrac{C_s C_k}{C_s + C_k}$. Shunting the crystal with C_x modifies (15.77) only in that $C_t = C_x$; from this we can use (15.75) directly in a form readily adaptable to the determination of our original coefficients, α'', β'', γ'' and δ''. Adding a series capacitor, C_3, and a shunt resistor, R_L, modifies (15.77) in a manner specified by (15.75). Here,

$$\left.\begin{aligned} \alpha &= \tau + jM\tau & \delta &= j\left(1 + \frac{C_x}{C_0}\right) \\ \beta &= \tau & T &= R_L \\ \gamma &= -M\frac{C_x}{C_0} + j\left(1 + \frac{C_x}{C_0}\right) & S &= \frac{1}{j\omega C_3} \end{aligned}\right\} \qquad (15.78)$$

Substitute these constants given by (15.78) in (15.75) then α'', β'', γ'' and δ'' become,

$$\left.\begin{aligned} \alpha'' &= \alpha + S\left(\gamma + \frac{\alpha}{T}\right) = \left[\tau + X_{c_3}\left(1 + \frac{C_x}{C_0}\right) + \frac{M\tau X_{c_3}}{R_L}\right] \\ &\qquad + j\left[M\tau + \frac{MC_x X_{c_3}}{C_0} - \frac{\tau}{R_L}X_{c_3}\right] \\ \beta'' &= \beta + S\left(\delta + \frac{\beta}{T}\right) = \left[\tau + X_{c_3}\left(1 + \frac{C_x}{C_0}\right)\right] - j\left[\frac{X_{c_3}\tau}{R_L}\right] \\ \gamma'' &= \left(\gamma + \frac{\alpha}{T}\right) = \left[-M\frac{C_x}{C_0} + \frac{\tau}{R_L}\right] + j\left[1 + \frac{C_x}{C_0} + \frac{M\tau}{R_L}\right] \\ \delta'' &= \left(\delta + \frac{\beta}{T}\right) = \left[\frac{\tau}{R_L} + j\left(1 + \frac{C_x}{C_0}\right)\right] \end{aligned}\right\} \qquad (15.79)$$

Substitute these values in (15.60) and (15.61) to obtain the coordinates of the center of the circle, W_0, and the radius, σ.

$$W_0 = \tau \frac{\left[\left(M\frac{C_0}{C_0+C_x} + 2\frac{\tau}{R_L}\right) - 2j\left(1 + \frac{C_0+C_x}{C_3} + \frac{\tau X_{c_3}}{R_L^2} + \frac{M\tau}{R_L}\frac{C_0}{C_3}\right)\right]}{2\left[1 + \left(\frac{\tau}{R_L}\right)^2 + \frac{MC_0}{C_0+C_x}\frac{\tau}{R_L}\right]} \tag{15.80}$$

$$\sigma = \tau \frac{M\frac{C_0}{C_0+C_x}}{\left[1 + \left(\frac{\tau}{R_L}\right)^2 + \frac{MC_0}{C_0+C_x}\frac{\tau}{R_L}\right]} \tag{15.81}$$

From the above expressions, σ is not exactly equal to the real component of W_0. If however, $2\frac{\tau}{R_L} \ll \frac{MC_0}{C_0+C_x}$, then the above equations reduce to

$$W_0 = \tau \frac{\left[M\frac{C_0}{C_0+C_x} - 2j\left(1 + \frac{C_0+C_x}{C_3} + \frac{\tau MC_0}{R_L C_3}\right)\right]}{\left[2\left(1 + \frac{MC_0}{C_0+C_x}\frac{\tau}{R_L}\right)\right]} \tag{15.82}$$

and

$$\sigma = \frac{\tau\left[\frac{MC_0}{C_0+C_x}\right]}{2\left[1 + \frac{MC_0}{C_0+C_x}\frac{\tau}{R_L}\right]} \tag{15.83}$$

Now the radius, σ, equals the real component of W_0. The per cent error of P.I. resulting from tuning to minimum impedance rather than unity power-factor in terms of Fig. 15.10 is given as,

$$\text{Per Cent Error of P.I.} = 100\left[1 - \frac{O-P_3}{O-P_1}\right]$$

$$= 100\left[1 - \frac{\left[1 - \sqrt{1 - \left(\frac{\eta}{\sigma}\right)^2}\right]}{\left[\sqrt{1 + \left(\frac{\eta}{\sigma}\right)^2} - 1\right]}\right] \tag{15.84}$$

Now since η represents the imaginary component of (15.82) then

$$\frac{2\sigma}{\eta} = P_2 = \frac{M}{\left(1 + \frac{C_x}{C_0}\right)\left(1 + \frac{C_0+C_x}{C_3} + M\frac{X_{c_t}}{R_L}\right)} \tag{15.85}$$

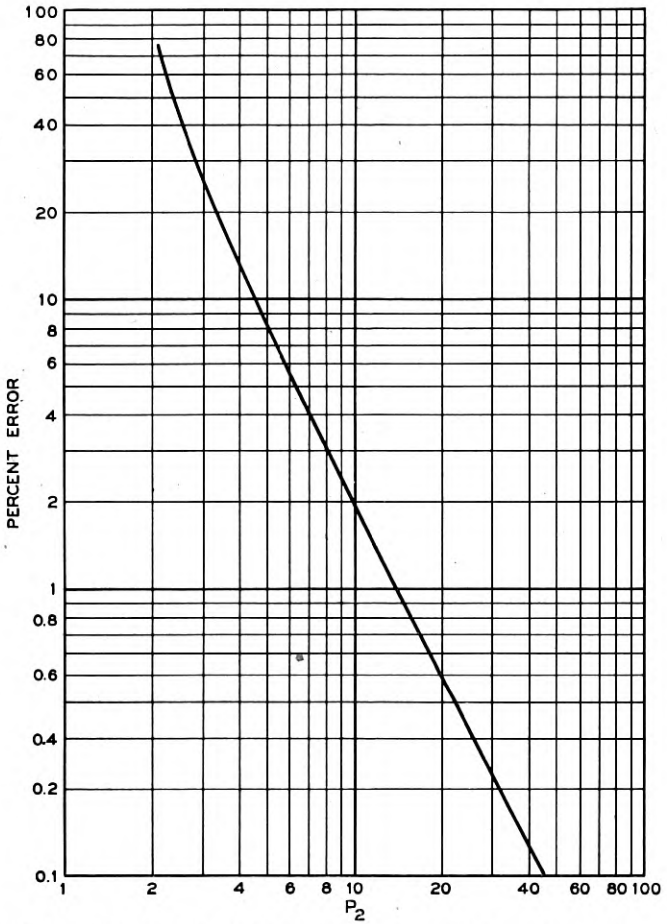

Fig. 15.12—Inherent error of the P.I. meter due to tuning for an indication of minimum impedance rather than unity power factor.

Rewriting (15.84) we have

$$\text{Per cent Error of P.I.} = 100\left[1 - \frac{\left[1 - \sqrt{1 - \frac{4}{P_2^2}}\right]}{\left[\sqrt{1 + \frac{4}{P_2^2}} - 1\right]}\right] \tag{15.86}$$

If $C_0 \gg C_x$ then

$$P_2 = \frac{M}{\left(1 + \frac{C_0}{C_t} + M\frac{X_{c_t}}{R_L}\right)} \tag{15.87}$$

The error given by (15.86) is plotted in Fig. 15.12 as a function of P_2.

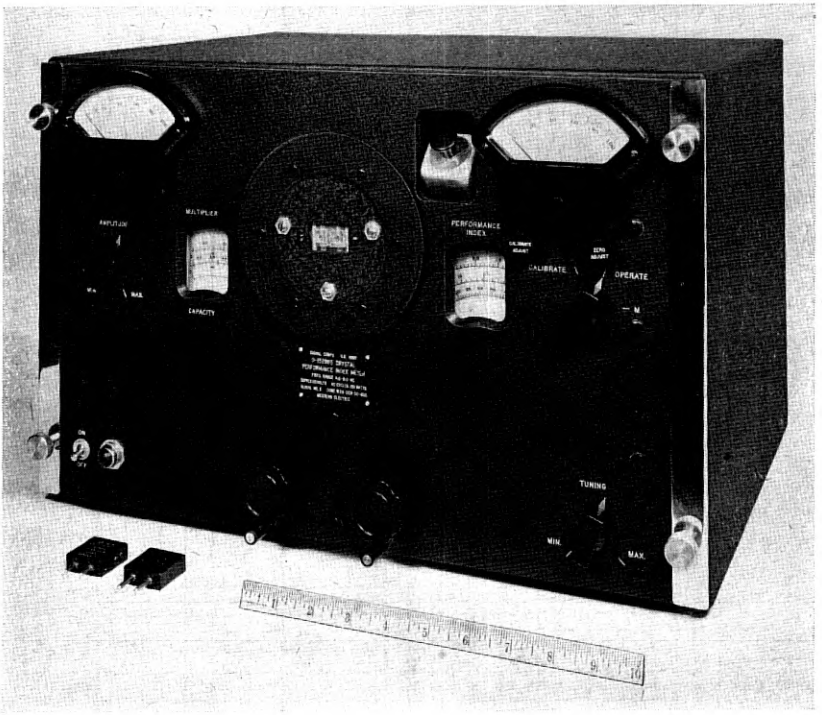

Fig. 15.13—Exterior view of crystal Performance Index meter.

15.83 *Frequency Errors*

As suggested in Section 15.81, conformal representation simplifies the mathematics required for the determination of frequency errors. In Section 15.81, the difference between the resonant frequency and the minimum impedance frequency was computed for the equivalent crystal circuit. This same procedure could be used to compute the frequency difference between the antiresonant frequency of the generalized oscillator circuit (Fig. 15.2) and the minimum impedance frequency of the P.I. meter for the same value of C_t. Comparison of the frequency of these two oscillators is plotted in Fig. 15.6 together with the measured values obtained from a "Pierce" and a "Tuned Plate" oscillator. This frequency comparison involves setting up two circle diagrams, one for Z_{AB} (Fig. 15.2) and one for the impedance, Z_i (Fig. 15.3) similar to Fig. 15.10. The impedance equations for both Z_{AB} and Z_i would be arranged such that they have the same function of Z in

order to have a common Z plane. In this way, transformation of operating points such as the "anti-resonant frequency" operating point (P_4) for the Z_{AB} impedance circle, could be subtracted from the "minimum impedance frequency" operating point (P_1) of the P.I. meter impedance circle in the common Z-plane. As in section 15.81, the frequency difference represents the arithmetic difference between P_4 and P_1 in the Z-plane in terms of $\frac{2L_1}{R_1}(\omega - \omega_2)$. As an example, look at the calculated curve in Fig. 15.6. This curve was computed for the case when R_L is negligible. The derivation of (15.51) given in section 15.92 precisely follows the procedure just described.

It is of interest to note that (15.27) may also be derived by Conformal means. It is more laborious than the usual circuit equations of section 15.2; however, it does provide a check of the methods used.

15.84 *Errors of Other Approximations*

Further consideration of P.I. meter errors leads to the assumptions made in the derivation of (15.27). The derivation of (15.27) assumed that the resistor, R_A, was non-reactive. While actually it can be made essentially noninductive, we have neglected the effect of the input capacitance of the attenuator that is shunted across its terminals. The error from neglecting this capacitance in (15.28) is given by the following expression

$$\text{Per Cent Error} = 100\left[1 - \frac{\sqrt{1 + Q_A^2}}{\omega R_A(C_u Q_A^2 + C_A)}\right] \quad (15.88)$$

Where Q_A equals the reactance of the shunt capacitance of the attenuator, C_u, divided by the magnitude of the calibration resistor, R_A.

It is interesting to note in the derivation of (15.28) that R_A was assumed to be very much less than X_{C_A} which introduces an error of,

$$\text{Per Cent Error} = 100\left[1 - \sqrt{1 + \left[\frac{R_A}{X_{C_A}}\right]^2}\right] \quad (15.89)$$

15.90 *Derivation of Circuit Equations*

15.91 *Derivation of Equation* (15.42)

Other equations used in this paper may best be developed from Fig. 15.3. By analysis of the input impedance, Z_i, the basis for the development of (15.42) is as follows:

From Fig. 15.2

$$Z_i = \frac{1}{j\omega C_t} + \frac{1}{j\omega C_0} \frac{\left[R_1 + j\left(\omega L_1 - \frac{1}{\omega C_1}\right)\right]}{\left[R_1 + j\left[\omega L_1 - \frac{1}{\omega}\left(\frac{1}{C_0} + \frac{1}{C_1}\right)\right]\right]} \tag{15.90}$$

By substituting (15.48) and (15.49) in (15.90), we find

$$Z_i = \frac{1}{j\omega}\left[\frac{1}{C_t} + \frac{1}{C_0}\left[\frac{\omega R_1 + jL_1(\omega^2 - \omega_1^2)}{\omega R_1 + jL_1(\omega^2 - \omega_2^2)}\right]\right] \tag{15.91}$$

This may be expressed in the form,

$$Z_i = \frac{\frac{\omega R_1}{H} + jL_1\left[\frac{(\omega^2 - \omega_2^2)}{C_t} + \frac{(\omega^2 - \omega_1^2)}{C_0}\right]}{-\omega L_1(\omega^2 - \omega_2^2) + j\omega^2 R_1} \tag{15.92}$$

where

$$H = \frac{C_0 C_t}{C_0 + C_t}$$

Now adding and subtracting ω_2^2 to the $\frac{\omega_2^2 - \omega_1^2}{C_0}$ term we have

$$Z_1 = \frac{\frac{\omega R_1}{H} + jL_1\left[\frac{(\omega^2 - \omega_2^2)}{C_t} + \frac{(\omega^2 - \omega_2^2)}{C_0} + \frac{(\omega_2^2 - \omega_1^2)}{C_0}\right]}{-\omega L_1(\omega^2 - \omega_2^2) + j\omega^2 R_1} \tag{15.93}$$

Rationalizing (15.93) and equating it to R_c and substituting in $L_1 = \frac{1}{C_0(\omega_2^2 - \omega_1^2)}$ (obtained from (15.50)), we find

$$R_c = \frac{R_1}{\left[\frac{\omega^2 - \omega_2^2}{\omega_2^2 - \omega_1^2}\right]^2 + \left[\frac{\omega}{\omega_1}\frac{1}{M}\right]^2} \tag{15.94}$$

15.92 *Derivation of Equations* (15.51) *and* (15.44)

Equation (15.51) makes possible the theoretical computation of the frequency difference between the generalized oscillator and the minimum impedance frequency adjustment of the *PI* meter. The derivation assumes that R_L is negligible and that the total capacitance across the crystal terminals is lumped in series with the crystal.

The impedance, Z_{AB}, in the generalized oscillator, Fig. 15.2, was given by (15.77). This equation may be expressed as follows:

$$Z_{AB}\omega_e(C_0 + C_t) = \frac{[1 + jM] + Z}{\left[-\frac{MC_t}{C_0 + C_t} + j\right] + jZ} \tag{15.95}$$

From this expression, as previously explained, (see Section 15.81), the following values for σ and η may be determined.

$$\left.\begin{aligned} \sigma &= \frac{M}{2}\,\frac{C_0}{C_0 + C_t} \\ \eta &= 1 \end{aligned}\right\} \tag{15.96}$$

The anti-resonant impedance of Z_{AB} is represented by $O - P_4$ in Fig. 15.10. The left hand term of (15.95) for the P_4 operating point becomes

$$Z_{AB}\omega_e(C_0 + C_t) = \sigma + \sqrt{\sigma^2 - 1} \tag{15.97}$$

Substituting this value in (15.95) and solving for Z, we find

$$Z = -jM\left[K_3\,\frac{C_0}{C_0 + C_t} - 1\right] \tag{15.98}$$

where

$$K_3 = \frac{1}{2} + \frac{1}{2}\sqrt{1 - \frac{1}{\sigma^2}}$$

If K_3 is expanded and all except the first two terms are neglected, Z may be expressed as

$$Z = -j\left[\frac{M}{1 + \dfrac{C_0}{C_t}} + \frac{\left(1 + \dfrac{C_t}{C_0}\right)}{M}\right] \tag{15.99}$$

The next step is to obtain a similar expression to (15.99) only for the minimum frequency impedance of Z_i in Fig. 15.3 with ρ disconnected. For this application $S = \dfrac{1}{j\omega C_t}$ and $T = \infty$. Substituting these values, as well as those in (15.59), in (15.75), we have

$$Z_i = \frac{\left[\tau + jM\tau + \dfrac{1}{\omega C_t}\right] + \left[\tau + \dfrac{1}{\omega C_t}\right]Z}{j + jZ} \tag{15.100}$$

From this equation, values for σ and η may be determined as described in Section 15.81.

$$\left.\begin{aligned} \sigma &= \frac{M\tau}{2} \\ \eta &= \frac{C_0 + C_t}{C_t}\,\tau \end{aligned}\right\} \tag{15.101}$$

By the same procedure just described for evaluating Z from the impedance expression Z_{AB}, the value of Z corresponding to the minimum impedance operating point, P_1, (Fig. 15.10) must be determined. For this operating condition Z_1 may be expressed by (15.65). The coefficients of this operating point are given by (15.67) with the above values of σ and η (Equation 15.101). Utilizing (15.68) to solve for Z, we get

$$Z_i' = -j \frac{M}{\left(1 + \frac{C_0}{C_t}\right)} \frac{\left[1 + \sqrt{1 + \frac{4}{P_1^2}}\right]}{2} \text{ (minimum impedance)} \quad (15.102)$$

now

$$Z_i - Z_i' = \frac{2L_1}{R_1} (\Delta\omega)$$

where $\Delta\omega$ = the difference in radian frequency between the frequency of oscillation in the generalized oscillator (anti-resonant frequency of the impedance, Z_{AB}) and the frequency of oscillation in the PI meter (minimum impedance frequency of the impedance, Z_i')

$$\Delta\omega = \left[\frac{\omega_2 - \omega_1}{M^2}\left(1 + \frac{C_0}{C_t}\right) \frac{2}{\left[1 + \sqrt{1 + \frac{4}{P_1^2}}\right]} - \frac{\omega_2 - \omega_1}{M^2}\left(1 + \frac{C_t}{C_0}\right)\right] \quad (15.51)$$

It is of interest to note that (15.102) becomes (15.44) when the value of Z (15.69) is introduced.

Lightning Protection of Buried Toll Cable

By E. D. SUNDE

A theoretical study of lightning voltages in buried telephone cable, of the liability of such cable to damage by lightning and of remedial measures, together with the results of simulative surge tests, oscillographic observations of lightning voltages and lightning trouble experience.

Introduction

PRACTICALLY all of the toll cable installed since 1939 has been of the carrier type and most of it has been buried in order to secure greater immunity from mechanical damage. It was realized, however, that burying the cable would not prevent damage due to lightning and that, on account of their smaller size, more damage was to be expected on the new carrier cables than on the much larger voice-frequency underground cables then in use. Moreover, when damage by lightning does occur, such as fusing of cable pairs or holes in the sheath, it is not so easy to locate and repair as on aerial cables, since excavations may have to be made at a number of points. Studies were therefore made of the factors affecting damage of buried cables by lightning and remedial measures were devised and put into effect in cases where a high rate of lightning failures was anticipated on new installations, or was experienced with cable already installed. Most of the cable installed was thus provided with extra core insulation, and shield wires were plowed in on many of the new routes.

It was recognized early in these studies that more effective lightning protection might be secured by providing the lead sheath with a thermoplastic coating of adequate dielectric strength and an outside copper shield, and that such cable might be required in territory where the earth resistivity is very high. This type of cable has recently been installed on a route in high-resistivity territory where experience has indicated that other types of construction would probably be inadequate and, since it has advantages also from the standpoint of corrosion and mechanical protection, it may be used also where lightning is not of such decisive importance.

When lightning strikes, the current spreads in all directions from the point where it enters the ground. If there are cables in the vicinity they will provide low resistance paths, so that much of the current will flow to the cables near the lightning stroke and in both directions along the sheath to remote points. The flow of current in the ground between the lightning channel and the cables may give rise to such a large voltage drop that the breakdown voltage of the soil is exceeded, particularly when the earth

resistivity is high. The lightning stroke will then arc directly to the cables from the point where it enters the ground, often at the base of a tree. Furrows longer than 100 feet have been found in the ground along the path of such arcs.

The current entering the sheath near the stroke point is attenuated as it flows towards remote points. Since a high earth resistivity is accompanied by a small leakage conductance between sheath and ground, the current will travel farther the larger the earth resistivity. The current along the sheath produces a voltage between the sheath and the core conductors, which is largest at the stroke point. This voltage is equal to the resistance drop in the sheath, between the stroke point and a point which is sufficiently remote so that the current in the sheath is negligible. Since the current travels farther along the sheath the higher the earth resistivity, this resistance drop will also increase with the earth resistivity. The maximum voltage between sheath and core is thus proportional to the sheath resistance and, as it turns out, to the square root of the earth resistivity. Carrier cables now being used are of smaller size and have a higher sheath resistance than full-size voice-frequency cables, and for this reason they are liable to have more lightning damage, particularly when the earth resistivity is high.

To secure experimental verification of certain points of the theory presented here, staged surge tests were made on the Stevens Point-Minneapolis cable, one of the first small-size buried toll cables to be installed. The results of these tests, which have already been published,[1] are here compared with those obtained theoretically, on the basis of the earth resistivity measured at the test location. Lightning voltages on this cable route were also recorded by automatic oscillographs and the results of these observations are also briefly discussed together with the rate of lightning failures experienced on this and other routes.

The first part of the paper deals with voltages between the cable conductors and the sheath due to sinusoidal currents and surge currents. The second part deals with the liability of damage due to excessive lightning voltages and with certain characteristics of lightning discharges of importance in connection with the present problem, such as the impedance encountered by the lightning channel in the ground, the rate of lightning strokes to ground and to buried structures and the crest current distribution for such strokes. In the third part remedial measures are discussed, together with lightning-resistant cable.

I. Voltages Between Cable Conductors and Sheath

1.1 *General*

Cable installed in the ground is designated "underground" when placed in duct, and "buried" when not in duct. Buried cable is sometimes pro-

vided with steel tape armor for protection against mechanical damage. While such armor may also reduce voltages due to low-frequency induction, mainly because of the high permeability of the steel, this is not true in the case of lightning voltages. The magnetic field in the armor due to lightning current in the cable is rather high, and the corresponding permeability fairly low. The armor resistance is, furthermore, quite high compared to that of the sheath, so that the effect of the armor may be neglected in considering lightning voltages. The tape or armor is usually separated from the sheath by paper and asphalt, but is bonded to the sheath at every splice point. Strokes to ground, or to the cable, may give rise to large currents in the armor and thus to excessive voltages between the armor and the sheath some distance from bonding points. The resulting arc may fuse a hole in the sheath or dent it, due to the explosive effect of the confined arc, and insulation failures may be experienced on this account. Such failures are not considered here since they are usually confined to a single point and are thus of less importance than insulation failures due to excessive voltages between the core conductors and the sheath, which may be spread for a considerable distance along the cable.

For protection against corrosion, buried cables are usually jute-covered (asphalt, paper and jute) and in some cases have thermoplastic or rubber coating. The leakance of jute-covered sheaths is usually large enough so that the cable may be assumed to be in direct contact with the earth and the leakance is, furthermore, increased at the time of lightning strokes by numerous punctures due to excessive voltage between sheath and ground. This effect is large enough so that even rubber-covered cable may be regarded as in direct contact with the soil in the case of direct strokes and sometimes also for strokes to ground in the vicinity of the cable, as discussed later.

In order to calculate the voltage between the sheath and the core conductors of a buried cable, due to a surge current entering the sheath or the ground in the vicinity of the cable, it is convenient to consider at first a sinusoidal current. The voltage due to a unit step current may then be obtained by operational solution and, in turn the voltage for a current $J(t)$ of arbitrary wave shape, by means of either one of the integrals:

$$\begin{aligned} V(t) &= \int_0^t J'(t-\tau)S(\tau)\,d\tau \\ &= \int_0^t J(t-\tau)S'(\tau)\,d\tau \end{aligned} \tag{1}$$

where $S(t)$ is the voltage due to unit step current and $S'(t)$ the time derivative of this voltage. The second of the above integrals is more convenient in the present case.

Photographic observations[2] indicate that a lightning discharge is usually initiated in the cloud by a so-called "stepped leader," except in the case of discharges to sufficiently tall structures[3] where this leader is initiated at the ground end. After the leader reaches the ground, or the cloud in the case of a tall structure, a heavy current "return stroke" proceeds from the ground toward the cloud at about $\frac{1}{10}$ the velocity of light. The main surge of current in the return stroke, which usually lasts for less than 100 microseconds, may be followed by a low current lasting for $\frac{1}{10}$ second or so.

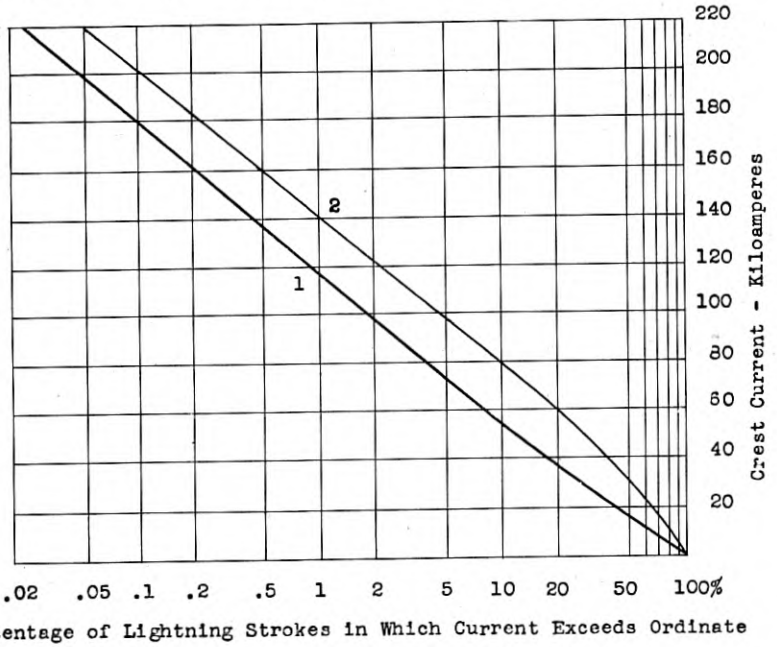

Figure 1—Distribution of crest currents in lightning strokes.

Curve 1: Currents in strokes to transmission line ground structures, based on 4410 measurements, 2721 in U. S. and 1689 in Europe.

Curve 2: Currents in strokes to buried structures, derived from curve 1.

There may then be a second leader, which does not exhibit the stepped character of the first leader and always proceeds from the cloud, and a second return stroke. This may be followed by a third leader and so on, the average number of strokes in multiple discharges being about 4 and the average time interval between strokes about $\frac{1}{10}$ second. Single-stroke discharges are, however, most common, discharges having more than 6 strokes being quite rare although discharges with as many as 40 strokes have been observed.

The crest value of currents in lightning discharges varies over wide limits.

Measurements of current in the ground structure of transmission lines[4,5] indicate that a relationship as shown in Fig. 1 exists between the crest currents and the percentage of discharges in which they occur. In the same figure is shown the crest current distribution for strokes to buried structures, which is derived in Part II from the curve for strokes to transmission line ground structures. Although measurements of wave shape are not extensive, they indicate that the current reaches its crest value in 5 to 10 microseconds and that it decays to half its maximum in 25 to 100 microseconds, the average being about 50 microseconds.[6] An average wave shape is assumed in this investigation.

In some 80 per cent of all lightning discharges the cloud is negative, so that the flow of current is from the earth toward the cloud. Further details about lightning discharges are summarized in recent surveys[6,7] which also contain an extensive list of references.

1.2 *Direct Strokes—Current Propagation Along Sheath*

As mentioned in the introduction and discussed further in Part II, a lightning stroke to ground may arc to a buried cable in the vicinity, in which case virtually all of the current will enter the sheath near the stroke point.

When a sinusoidal current J enters the sheath at $x = 0$ and the sheath is assumed to extend indefinitely in opposite directions from this point, the sheath current at the distance x is given by the following approximate expression

$$I(x) = \frac{J}{2} e^{-\Gamma x} \tag{2}$$

where Γ is the propagation constant of the sheath-earth circuit and is given by the following expression, derived in a previous paper.[8]

$$\Gamma = \frac{1}{v} [i\omega(i\omega + 1/\rho\kappa)]^{\frac{1}{2}} \tag{3}$$

where: v = Velocity of propagation along sheath
$= (2/\nu\kappa)^{\frac{1}{2}}$ meters per second
ν = Inductivity of earth $= 1.256 \cdot 10^{-6}$ hy/meter
κ = Capacitivity of earth $= \epsilon \cdot 8.858 \cdot 10^{-12}$ fd/meter
ϵ = Dielectric constant of earth
ρ = Earth resistivity, meter-ohms

In deriving the above formula the resistance of the sheath is neglected in comparison with its external reactance, which is permissible for frequencies in the range of importance, and the sheath is assumed to be half buried, that is, with its axis in the plane of the earth's surface. The latter assumption gives rise to a comparatively small error when the formula is applied

to cables buried at depths up to one meter or so, the propagation constant for a cable buried at infinite depth being larger than that given above by a factor of $\sqrt{2}$.

It is assumed that the current is propagated from the cable up the lightning channel with infinite velocity. The voltage between the cable conductors and the sheath obtained in this manner reaches a crest value after some 50 to 100 microseconds, or after the current in an actual lightning channel has traveled from the ground to the cloud. The error due to this assumption is thus probably quite small as regards the crest voltage, although the wave front will be somewhat slower when the actual velocity of propagation is considered.

1.3 *Direct Strokes—Voltage for Sinusoidal Current*

The current along the sheath gives rise to an electric force along the latter. The electric force along the inner surface of the sheath is given by:

$$E(x) = zI(x) = \frac{J}{2} ze^{-\Gamma x} \tag{4}$$

where z is the mutual-impedance of the sheath-earth and core-sheath circuits.

The latter mutual impedance is equal to the ratio of electric force along the inner surface of the sheath at any point, to the total current along the sheath at the same point, and for low frequencies equals the direct-current resistance of the sheath. It is given by the following slightly approximate formula:[9]

$$Z = R(i\omega\gamma)^{\frac{1}{2}}/\sinh\,(i\omega\gamma)^{\frac{1}{2}} \tag{5}$$

where: $\omega = 2\pi f$ and
R = Unit length d-c resistance of sheath, ohms/meter
$\gamma = \nu\delta/2\pi aR$
δ = Thickness of sheath, meter
a = Radius of sheath, meter
ν = Intrinsic Inductivity of sheath
$= 1.256 \times 10^{-6}$ henrys/meter

The current in the core-sheath circuit and the voltage between core and sheath due to an impressed field $E(x)$ along the core (inner surface of sheath) are obtained from the following equations, which are the general solutions of the transmission line equation for the core-sheath circuit.

$$J(x) = [A + P(x)]e^{-\Gamma_0 x} - [B + Q(x)]e^{\Gamma_0 x} \tag{6}$$

$$U(x) = K_0[A + P(x)]e^{-\Gamma_0 x} + K_0[B + Q(x)]e^{\Gamma_0 x} \tag{7}$$

where Γ_0 and K_0 are the propagation constant and the characteristic impedance of the core-sheath circuit and

$$P(x) = \frac{1}{2K_0}\int_0^x E(x)e^{\Gamma_0 x}\,dx = \frac{z}{2K_0}\,\frac{1 - e^{-(\Gamma-\Gamma_0)x}}{\Gamma - \Gamma_0} \tag{8}$$

$$Q(x) = \frac{1}{2K_0}\int_0^x E(x)e^{-\Gamma_0 x}\,dx = \frac{z}{2K_0}\,\frac{1 - e^{-(\Gamma+\Gamma_0)x}}{\Gamma - \Gamma_0} \tag{9}$$

Since the current must be zero at $x = 0$, it is necessary that $A = B$. To make the curent vanish when x becomes infinity, B must equal $-Q(\infty) = -\frac{z}{2K_0}\,\frac{1}{\Gamma + \Gamma_0}$. With these boundary conditions the voltage between core and sheath becomes:

$$U(x) = \frac{J}{2}\,\frac{z}{\Gamma^2 - \Gamma_0^2}\,(\Gamma e^{-\Gamma x} - \Gamma_0 e^{-\Gamma_0 x}) \tag{10}$$

The propagation constant Γ_0 is much smaller than Γ, and may be taken as:

$$\begin{aligned}\Gamma_0 &= [(R_0 + i\omega L_0)i\omega C_0]^{\frac{1}{2}} \\ &= \frac{1}{v_0}\,[i\omega(i\omega + R_0/L_0)]^{\frac{1}{2}}\end{aligned} \tag{11}$$

R_0 = Unit length resistance of core-sheath circuit, ohms/meter
L_0 = Unit length inductance of core-sheath circuit, hy/meter
C = Unit length capacitance of core-sheath circuit, fd/meter
$v_0 = (1/L_0C_0)^{\frac{1}{2}}$

1.4 *Direct Strokes—Lightning Voltage at Stroke Point*

The largest voltage between sheath and core conductors is obtained for $x = 0$, and for this case (10) becomes:

$$\begin{aligned}U(0) &= \frac{J}{2}\,\frac{z}{\Gamma + \Gamma_0} \\ &= \frac{J}{2}\,\frac{R\gamma^{\frac{1}{2}}/\sinh\,(i\omega\gamma)^{\frac{1}{2}}}{\frac{1}{v}\,(i\omega + 1/\rho\kappa)^{\frac{1}{2}} + \frac{1}{v_0}\,(i\omega + R_0/L_0)^{\frac{1}{2}}}\end{aligned} \tag{12}$$

For sufficiently high frequencies, so that $(i\omega\gamma)^{\frac{1}{2}} \gg 1$, $i\omega > 1/\rho\kappa$, $i\omega > R_0L_0$, and $\sinh\,(i\omega\gamma)^{\frac{1}{2}} \cong \frac{1}{2}\exp\,(i\omega\gamma)^{\frac{1}{2}}$ expression (12) becomes

$$U(0) = JR\gamma^{\frac{1}{2}}\,\frac{vv_0}{v + v_0}\,(i\omega)^{-\frac{1}{2}}e^{-(i\omega\gamma)^{\frac{1}{2}}} \tag{13}$$

For sufficiently low frequencies, so that $(i\omega\gamma)^{\frac{1}{2}} < 1$, $i\omega < i/\rho\kappa$, $i\omega < R_0/L_0$, and $\sinh (i\omega\gamma)^{\frac{1}{2}} \leqq (i\omega\gamma)^{\frac{1}{2}}(1 + i\omega\gamma/6)$, expression (12) becomes

$$U(0) = \frac{J}{2} \frac{R}{\alpha^{\frac{1}{2}} + \beta^{\frac{1}{2}}} \frac{1}{(i\omega)^{\frac{1}{2}}(i + \omega\gamma/6)^{\frac{1}{2}}} \tag{14}$$

where

$$\alpha = \nu/2\rho, \qquad \beta = R_0C_0$$

For small values of time, corresponding to large values of $i\omega$, the function $S'(t)$ defined before, as obtained by operational solution of (13) is [10]

$$S'(t) = R\gamma^{\frac{1}{2}} \frac{vv_0}{v + v_0} \left(\frac{1}{\pi t}\right)^{\frac{1}{2}} e^{-\gamma/4t} \tag{15}$$

For large values of time, corresponding to small values of $i\omega$, the function is obtained by operational solution of (14) and equals: (Reference 10, pair 542)

$$S'(t) = \frac{R}{2(\alpha^{\frac{1}{2}} + \beta^{\frac{1}{2}})} \left(\frac{6}{\gamma}\right)^{\frac{1}{2}} h(\sqrt{6t/\gamma}) \tag{16}$$

where, with $(6t/\gamma)^{\frac{1}{2}} = u$:

$$h(u) = -ie^{-u^2} \operatorname{erf} (iu) = \frac{2}{\sqrt{\pi}} e^{-u^2} \int_0^u e^{\tau^2}\, d\tau \tag{17}$$

erf being the error function.

Values of the function $h(u)$ are given in Table I.

In Fig. 2, curve 1 shows the function $S'(t)$ calculated from (15), and curve 2 that calculated from (16), for a cable of 1.4" diameter, using constants as indicated in figure. The constants apply to a cable on which measurements have been made of the voltage between sheath and core conductors, at a location where the measured earth resistivity was 400 meter-ohms. The function $S'(t)$ corresponding to equation (12) is obtained with sufficient accuracy by drawing a transition curve, 3, between curves 1 and 2.

If the impedance z is taken equal to the direct-current resistance R of the sheath and if the velocity of propagation along the sheath and along the core are assumed to be infinite, so that $\Gamma = (i\omega\alpha)^{\frac{1}{2}}$ and $\Gamma_0 = (i\omega\beta)^{\frac{1}{2}}$, the following expression is obtained

$$S'(t) = \frac{R}{2(\alpha^{\frac{1}{2}} + \beta^{\frac{1}{2}})} \left(\frac{1}{\pi t}\right)^{\frac{1}{2}} \tag{18}$$

In the following it will be shown that (18) is accurate enough for practical purposes.

The wave shape of the current in lightning strokes may be approximated by an expression of the form:

$$J(t) = I(e^{-at} - e^{-bt}). \tag{19}$$

With $a = .013 \cdot 10^6$, $b = .5 \cdot 10^6$, a current of the wave shape used in the measurements referred to above is obtained. This current reaches its crest in 10 microseconds and decays to its half-value in 65 microseconds, and is fairly representative of the average wave shape of lightning stroke currents. In the following, the voltages are for convenience referred to a crest value of 1000 amperes, which is obtained when $I = 1150$ amperes, the latter current being the initial value of each of the two exponential component currents included in (19).

TABLE I

$$\sqrt{\frac{\pi}{2}}\, h(u) = e^{-u^2} \int_0^u e^{\tau^2}\, d\tau = -\sqrt{\frac{\pi}{2}}\, ie^{-u^2}\, erf(iu)$$

$$\cong u \text{ when } u < .1$$

$$\cong \frac{1}{2u} \text{ when } u > 10$$

u	$\sqrt{\frac{\pi}{2}}\, h(u)$	u	$\sqrt{\frac{\pi}{2}} \cdot h(u)$
0	0	1.5	.4283
.1	.0993	2.	.3014
.2	.1948	2.5	.2232
.3	.2826	3.0	.1782
.4	.3599	3.5	.1496
.5	.4244	4.	.1293
.6	.4748	4.5	.1141
.7	.5105	5.	.1021
.8	.5321	6.	.0845
.9	.5407	8.	.0630
1.0	.5381	10.	.0503

A more complete table for the range between $u = 0$ and $u = 4$ is published in *Berichteverhandlungen Akademie der Wissenschaften, Leipzig, Math-Phys. Klasse*, Vol. 80, 1928, pages 217 to 223.

In Fig. 3, the dashed curve shows the measured voltage and curves 1 and 2 that calculated for the above surge current for two conditions. In calculating curve 1, $S'(t)$ was taken as curve 3 of Fig. 2, the voltage being obtained by numerical integration in accordance with (1); in calculating curve 2, z is taken as the direct-current resistance of the sheath and the velocities of propagation are assumed to be infinite, so that $S'(t)$ is given by (18). In the latter case the following expression is obtained for the voltage by solution of (1):

$$V(t) = \frac{JR}{2(\alpha^{\frac{1}{2}} + \beta^{\frac{1}{2}})} \left[a^{-\frac{1}{2}} h(\sqrt{at}) - b^{-\frac{1}{2}} h(\sqrt{bt})\right] \qquad (20)$$

where the function $h(u)$, $u = \sqrt{at}$ or $\sqrt{bt}$, is defined as before.

Comparison of curves 1 and 2 of Fig. 3 shows that (20) is accurate enough for practical purposes, so that the voltage may be taken proportional to the direct-current resistance of the sheath. Since $\beta^{\frac{1}{2}}$ is only 2.5 per cent of $\alpha^{\frac{1}{2}}$, propagation in the core-sheath circuit may be neglected in comparison with propagation along the sheath-earth circuit, so that it is permissible to take the voltage proportional to the square root of the earth resistivity.

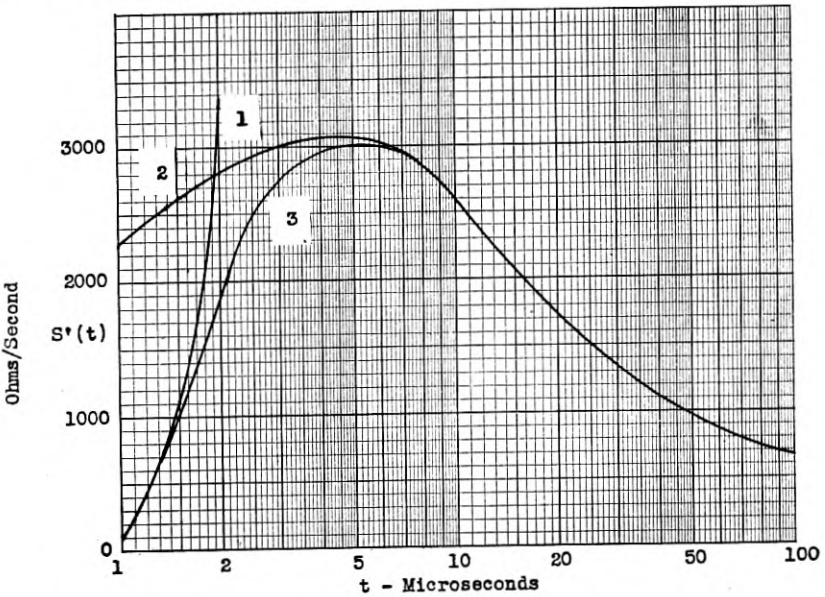

Figure 2—Approximate solution for $S'(t)$.

1: Calculated from formula for small times.
2: Calculated from formula for large times.
3: Transition curve giving approximate solution for $S'(t)$.
Earth resistivity, $\rho = 400$ meter-ohms.
Radius of cable, $a = 1.75$ cm.
Sheath thickness, $\delta = 2.4$ mm.
Sheath resistance, $R = .92 \cdot 10^{-3}$ ohms/meter.
Core-sheath cap. $C_0 = .96 \cdot 10^{-9}$ fd/meter.
Core-sheath resist. $R_0 = R \cong .92 \cdot 10^{-3}$ ohm/meter.
Velocity $v_0 = 2 \cdot 10^8$ meter/sec.
Velocity $v = 1 \cdot 10^8$ meter/sec.

Furthermore, from (20) it is seen that when a and b are divided by the same factor k, so that the wave shape of the current remains the same but the duration of the current is increased k times, the voltage is increased $\sqrt{k}$ times. Thus, if the surge current had reached its crest value in 20 microseconds and its half-value in 130 microseconds, the voltage would be increased by $\sqrt{2}$, and the crest voltage would have been reached after 120 rather than 60 microseconds.

If the breakdown voltage of the core insulation is assumed to be 2000 volts, the above cable would be able to withstand a stroke current of about 30,000 amperes before the insulation is punctured. From Fig. 1 it is seen

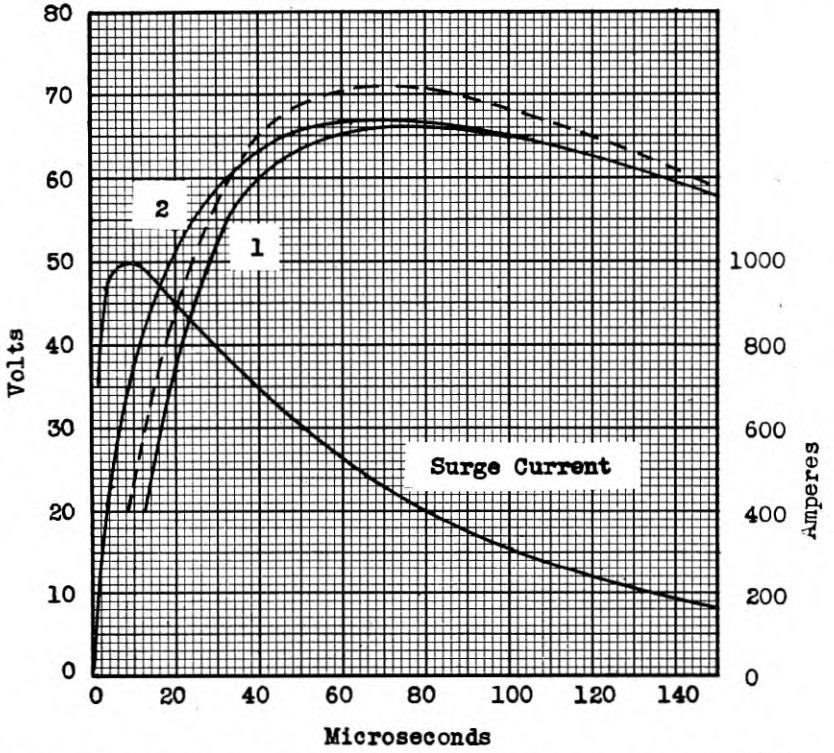

Figure 3—Comparison of measured, shown by dashed curve, and calculated voltage between sheath and core conductors, shown by curves 1 and 2, for surge current as shown and cable constants as given in Fig. 2.

1: Calculated from formula including skin-effect in sheath and finite velocity of propagation.

2: Calculated from formula based on d-c resistance of sheath and assuming infinite velocity of propagation.

that in about 50 per cent of all strokes the crest current exceeds 30,000 amperes.

When there are two cables, each will provide shielding for the other, and the shielding effect may be calculated as for shield wires (Sec. 3.3). Frequently the cables are of equal or nearly equal size and are close together. It is then accurate enough to use the parallel resistance of the two sheaths in calculating the voltage, which will be practically the same in both cables.

1.5 *Direct Strokes—Lightning Voltages Along Cable*

It was shown above that with only a minor error the impedance z may be taken equal to the direct-current resistance of the sheath and that the propagation constants may be taken as

$$\Gamma = (i\omega\alpha)^{\frac{1}{2}}, \qquad \Gamma_0 = (i\omega\beta)^{\frac{1}{2}}$$

With this modification expression (10) becomes:

$$U(x) = \frac{J}{2}\frac{R}{\alpha - \beta}\left[\alpha^{\frac{1}{2}} e^{-(i\omega\alpha)^{\frac{1}{2}}x} - \beta^{\frac{1}{2}} e^{-(i\omega\beta)^{\frac{1}{2}}x}\right](i\omega)^{-\frac{1}{2}} \tag{21}$$

The corresponding function S' is:[10]

$$S'(x, t) = \frac{R}{2(\alpha - \beta)}\left(\frac{1}{\pi t}\right)^{\frac{1}{2}}(\alpha^{\frac{1}{2}} e^{-\alpha x^2/4t} - \beta^{\frac{1}{2}} e^{-\beta x^2/4t}) \tag{22}$$

The voltage due to a surge current $J(t)$, as obtained from (1), may be expressed as:

$$V(x, t) = \frac{R}{2(\alpha - \beta)}\left[\alpha^{\frac{1}{2}} g(\alpha^{\frac{1}{2}}x, t) - \beta^{\frac{1}{2}} g(\beta^{\frac{1}{2}}x, t)\right] \tag{23}$$

where, with $\sigma = \alpha^{\frac{1}{2}}x$ or $\beta^{\frac{1}{2}}x$,

$$g(\sigma, t) = \int_0^t J(t - \tau)\left(\frac{1}{\pi\tau}\right)^{\frac{1}{2}} e^{-\sigma^2/4\tau}\, d\tau \tag{24}$$

For a current as given by (19), the latter integral may be expressed in terms of error functions of complex arguments, for which, however, no tables are available at present. Curves for the function g, as obtained by numerical integration are shown in Fig. 4.

When the core conductors are connected to the sheath at $x = 0$, the constants A and B of (6) and (7) are obtained from the following boundary conditions: At $x = 0$, $V(0) = 0$ so that $A = -B$. As before, $B = -Q(\infty)$. The voltage between core and sheath is then given by:

$$\begin{aligned} U_0(x) &= \frac{J}{2}\frac{R\Gamma}{\Gamma^2 - \Gamma_0^2}(e^{-\Gamma x} - e^{-\Gamma_0 x}) \\ &= \frac{JR\alpha^{\frac{1}{2}}}{\Gamma^2 - \Gamma_0^2}\left[e^{-(i\omega\alpha)^{\frac{1}{2}}x} - e^{-(i\omega\beta)^{\frac{1}{2}}x}\right] \end{aligned} \tag{25}$$

In this case the derivative of the voltage due to unit step current is:

$$S_0'(x, t) = \frac{R\alpha^{\frac{1}{2}}}{2(\alpha - \beta)}\left(\frac{1}{\pi t}\right)^{\frac{1}{2}}\left[e^{-\alpha x^2/4t} - e^{-\beta x^2/4t}\right] \tag{26}$$

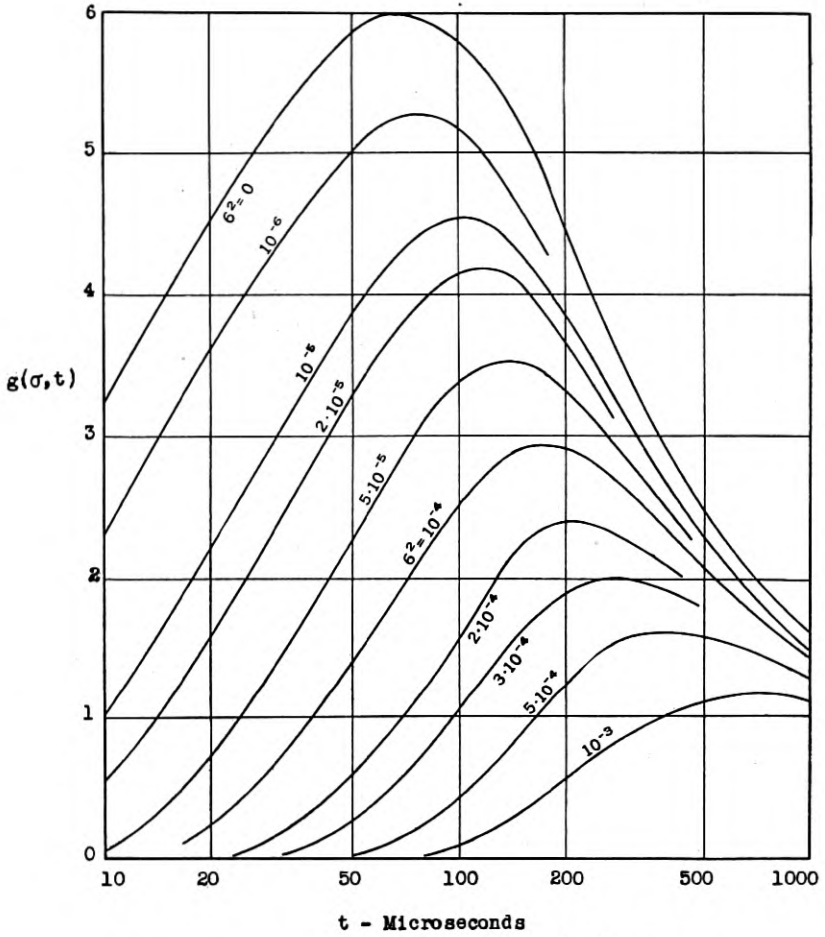

Figure 4—Function $g(\sigma, t) = \int_0^t J(t-\tau)\left(\frac{1}{\pi\tau}\right)^{\frac{1}{2}} e^{-\sigma^2/4\tau}\, d\tau$

$J(t) = I(e^{-at} - e^{-bt})$

$a = 1.3 \cdot 10^4$, $b = 5 \cdot 10^5$ $I = 1150$ amperes

and

$$V_0(x, t) = \frac{R\alpha^{\frac{1}{2}}}{2(\alpha - \beta)} [g(\alpha^{\frac{1}{2}}x, t) - g(\beta^{\frac{1}{2}}x, t)] \tag{27}$$

In Fig. 5 the crest values of $V(x, t)$ and $V_0(x, t)$, calculated for the cable considered before, are plotted against x, together with those observed in the tests. When the voltage $V(0, t)$ at the point where current enters the sheath is great enough to break down the insulation of a core conductor, the

latter will be in contact with the sheath by virtue of arcing. Under this condition, the voltage $V_0(x, t)$ between this conductor and the sheath will increase with distance along the cable as shown in Fig. 5. A maximum is reached a fairly short distance from the original fault, and beyond this point the voltage slowly decreases. After a puncture of the insulation where current enters the sheath, other failures may therefore occur, not necessarily at the point where $V_0(x, t)$ is largest, but sometimes at points nearer or much farther away where the insulation may be weaker. A single lightning stroke may thus cause insulation failures over a considerable distance along the cable.

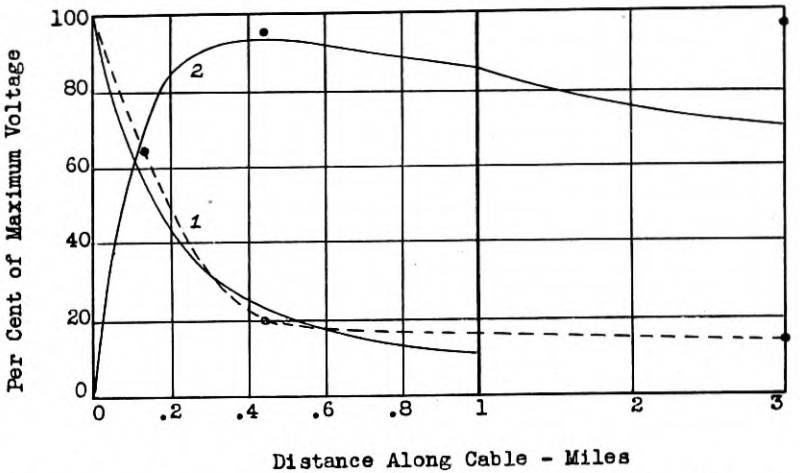

Figure 5—Comparison of measured variation of voltage between sheath and core, along cable, as shown by points and dashed curve, with calculated variation shown by curves 1 and 2.
1: Conductor not connected to sheath.
2: Conductor connected to sheath at point where surge current enters sheath.

1.6 *Direct Strokes—Voltage Due to Long Duration Current*

As mentioned before, a current of low value and long duration may exist on the lightning channel after the main discharge. This current is usually of such long duration that the resistance of the sheath must be considered in calculating the current propagation along the cable. The propagation constant in that case becomes

$$\Gamma = [(R + i\omega L)G]^{\frac{1}{2}} = \left(\frac{R}{L} + p\right)^{\frac{1}{2}} \left(\frac{\nu}{2\rho}\right)^{\frac{1}{2}} \tag{28}$$

R, L and G being the unit length resistance, inductance and leakance of the sheath-earth circuit. Neglecting propagation in the core-sheath circuit,

the voltage between core and sheath at the stroke point due to a sinusoidal current J_1 becomes,

$$U_1(0) = \frac{J_1 R}{2\Gamma} = J_1\left(\frac{\rho}{2\nu}\right)^{\frac{1}{2}} R(p + R/L)^{-\frac{1}{2}} \tag{29}$$

The corresponding voltage for a unit step current J_1 is:

$$V_1(0, t) = J_1 R\left(\frac{\rho L}{2\nu R}\right)^{\frac{1}{2}} \text{erf } (Rt/L)^{\frac{1}{2}} \tag{30}$$

where erf is the error function.

For large values of time, when $Rt/L > 1$, (30) becomes

$$V_1(0, t) = J_1 R\left(\frac{\rho L}{2\nu R}\right)^{\frac{1}{2}} \tag{31}$$

The latter expression is valid when t exceeds about 2 milliseconds and thus applies for the long duration current of a lightning stroke, since the latter usually lasts for about 100 milliseconds. For a current of 1000 amperes, the core-sheath voltage for a cable of 1.4″ diameter is about 700 volts. In many strokes the long duration current may be several hundred amperes, and a substantial voltage may then exist between core and sheath for .1 second or so. Thus, while this current component does not increase the crest voltage, it substantially increases the likelihood of permanent failure when the insulation is punctured by prolonging the current through the puncture.

1.7 *Strokes to Ground Not Arcing to Cable*

Let it be assumed that the current enters the ground at the distance y from a buried cable and that conditions are such that it does not arc to the latter. The flow of current in the ground gives rise to an electric force in the ground along the cable, and thus to currents in the sheath and to voltages between core and sheath. When the earth is assumed to have uniform conductivity, the earth potential at the distance r from the point where current enters the ground is given by:

$$Ve = JQ_0(r) = J\rho/2\pi r \tag{32}$$

where

ρ = Earth resistivity in meter-ohms
$r = (x^2 + y^2)^{\frac{1}{2}}$ = Distance in meters

The sheath current and the voltage between sheath and core may in this case be obtained from published formulas,[11] provided propagation along

the core-sheath circuit is neglected in comparison with propagation along the sheath-earth circuit, which is permissible. The voltage between sheath and core conductor differs by the factor z/Z from the voltage between sheath and ground as given in Table II, case 3 of the paper referred to, z being defined as before and Z being the unit length self-impedance of the sheath-earth circuit. At a point opposite the lightning stroke, $x = 0$, the voltage between core and sheath is in this case given by:

$$U(0, y) = J\frac{R\Gamma}{Z}\int_0^\infty Q_0(r)e^{-x}\,dx = J\frac{R}{Z}\frac{\rho}{2\pi}\Phi(\Gamma y) \tag{33}$$

where $Z = \Gamma^2/G$ and G is the unit length leakance of the sheath-earth circuit. The leakance is given by the approximate expression:

$$G = \left(\frac{\rho}{\pi}\log\frac{1}{\Gamma a}\right)^{-1} \tag{34}$$

a being the radius of the sheath and $\log = \log_\epsilon$.

The function $\Phi(\Gamma y)$ is given by the approximate formula:

$$\Phi(\Gamma y) \backsimeq \log\frac{1 + \Gamma y}{\Gamma y} \tag{35}$$

Inserting (34) and (35) in (33), the latter expression may be written:

$$U(0, y) = U(0, a)\lambda(\Gamma y) \tag{36}$$

where $U(0, a) = U(0)$ is the voltages when the current enters the sheath directly ($y = a$) and:

$$\lambda(\Gamma y) = \left(\log\frac{1 + \Gamma y}{\Gamma y}\right)\Big/\log 1/\Gamma a \tag{37}$$

where $\Gamma = (i\omega\nu/2\rho)^{\frac{1}{2}} = (i\omega\alpha)^{\frac{1}{2}}$.

The rigorous solution of the time function corresponding to (36) would be rather complicated. Since, however, λ is the ratio of two functions, each of which varies logarithmically with Γ, and thus varies only slightly with $i\omega$, an approximate solution is obtained by replacing $i\omega$ with $1/t$ in (37). For instance, the solution of an operational expression p^{-n} is $t^n/n!$ while the solution of $p^{-n}\log p$ is $[\psi(1 + n) + \log 1/t]t^n/n!$, ψ being the logarithmic derivative of the gamma function. For representative values of n and $t(n < 1, t < 10^{-4})$, ψ is less than 5% of $\log 1/t$, so that a good approximation is obtained by replacing p by $1/t$ in $\log p$, which in this illustration simulates the factor $\lambda(\Gamma y)$. With this approximation:

$$V(0, y, t) = V(0, a, t)\lambda[y(\alpha/t)^{\frac{1}{2}}] \tag{38}$$

In Fig. 6 is shown the variation in the voltage calculated from (38), together with that observed in the tests referred to before. That the measured decrease in the voltage is smaller than calculated is due to the fact that the earth resistivity at the test location increases with depth. Earth resistivity measurements made by the four-electrode method show that the resistivity is about 400 meter-ohms for electrode spacings up to about 20 feet and then gradually increases, reaching about 700 meter-ohms at 300 feet, 1200 meter-ohms at 1000 feet and approaching 1500 meter-ohms for

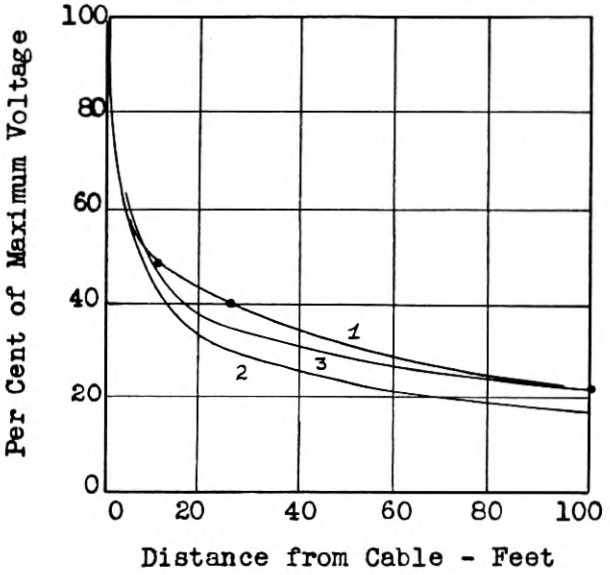

Figure 6—Reduction in voltage between sheath and core with increasing distance from cable to point where current enters the ground.
1: Measured when remote ground representing cloud is at a distance of 1000 ft.
2: Calculated for uniformly conducting earth with remote ground at distance of 1000 ft.
3: Calculated for uniformly conducting earth with remote ground at infinity.

large electrode spacings. The measured variation in voltage with separation is in substantial agreement with that calculated for an earth structure of this type in the manner outlined in Section 1.9.

1.8 *Discharges Between Clouds*

In considering voltages due to discharges between clouds, the lightning channel is assumed to parallel the cable. Due to magnetic induction, the lightning current will give rise to an impressed electric force along the cable sheath. Without much error it may be assumed that there is no impressed force outside the exposed section of the sheath and that the electric force in the exposed section due to a sinusoidal current J is $E^0(x) =$

JM, where M is the unit length mutual impedance of the lightning channel and the sheath. The resulting sheath current $I(x)$ is obtained from (6) and (7), when E is replaced by E^0, Γ_0 by Γ and K_0 by K, the characteristic impedance of the sheath-earth circuit. The constants A and B are found by observing the voltage between sheath and ground is zero at $x = s/2$. The electric force along the core is given by $E(x) = RI(x)$, and the voltage between the core conductors and the sheath is obtained by a second application of (6) and (7), the constants A and B being determined from the condition that the latter voltage must equal zero at $x = s/2$. The voltage between the core conductors and the sheath at the distance x along the cable beyond one end or the other of the lightning channel projection on the cable is then:

$$U(x) = \frac{JRM\Gamma^2 s}{2Z(\Gamma^2 - \Gamma_0^2)}\left[\frac{e^{-\Gamma_0 x}}{\Gamma_0 s}(1 - e^{-\Gamma_0 s}) - \frac{e^{-\Gamma x}}{\Gamma s}(1 - e^{-\Gamma s})\right] \quad (39)$$

the sign of the voltage beyond one end of the channel being opposite to that beyond the other end.

Since $\Gamma \gg \Gamma_0$, the last bracket term may be neglected. It was shown previously, that attenuation along the core-sheath circuit within a distance of one mile, which is representative of the length s, is quite small, so that $1 - e^{-\Gamma_0 s} \cong \Gamma_0 s$. With these modifications:

$$U(x) = \frac{JRM\Gamma^2 s}{2Z(\Gamma^2 - \Gamma_0^2)} e^{-\Gamma_0 x} \quad (40)$$

The earth-return impedances M and Z are given by the following approximate expressions:[12]

$$M = \frac{i\omega\nu}{2\pi} \frac{\sqrt{2}h}{(h^2 + y^2)(i\omega\alpha)^{\frac{1}{2}}} \quad (41)$$

$$Z = \frac{i\omega\nu}{2\pi} \log \frac{\sqrt{2}}{a(i\omega\alpha)^{\frac{1}{2}}} \quad (42)$$

where α is defined as before, $\log = \log_\epsilon$ and:

h = height of lightning channel above ground
y = horizontal separation of lightning channel from cable

The expression for M holds when $\alpha(h^2 + y^2)^{\frac{1}{2}} > 5$, a condition which is satisfied in the important part of the frequency range.

Inserting (41) and (42) in (40):

$$U(x) = \frac{JR\alpha^{\frac{1}{2}}}{2(\alpha - \beta)} \mu \left(\frac{1}{i\omega}\right)^{\frac{1}{2}} e^{-(i\omega\beta)^{\frac{1}{2}}x} \quad (43)$$

where

$$\mu = \frac{\sqrt{2}hs}{(h^2 + y^2) \log \frac{\sqrt{2}}{a(i\omega\alpha)^{\frac{1}{2}}}} \tag{44}$$

Comparison with (21) and (23) shows that in this case:

$$V(x, t) = \frac{R\alpha^{\frac{1}{2}}}{2(\alpha - \beta)} \mu g(\beta^{\frac{1}{2}} x, t) \tag{45}$$

In the above solution, μ was assumed constant. Actually it changes slightly with frequency and, for reasons mentioned before, it is accurate enough for practical purposes to replace $i\omega$ with $1/t$ when calculating μ.

The maximum voltage is obtained at $x = 0$, i.e., at a point opposite one end or the other of the lightning channel, and comparison with (22) shows that this voltage differs from that obtained in the case of a direct stroke by the factor μ, since $\beta^{\frac{1}{2}} \ll \alpha^{\frac{1}{2}}$ so that the second term may be neglected in (23). The above factor has the following approximate value:

$$\mu = .14 \frac{sh}{h^2 + y^2} \tag{46}$$

Since each cloud has an equal and oppositely charged image at the distance h below the surface of the ground, the electric field between cloud and ground is substantially equal to that between the clouds when $s = 2h$. For a discharge to take place between clouds, rather than to the earth, the length s would, therefore, have to be less than $2h$; so that with $y = 0$ the factor would not be expected to exceed $\mu = .28$. Thus, for the cable previously considered, failures due to discharges between clouds would not be expected except for currents in excess of 100,000 amperes in a lightning channel approximately above and parallel to the cable.

Maximum voltages of opposite signs are obtained at the two ends of the lightning channel, the voltage at the mid-point being zero. As the distance x from one end of the lightning channel increases, the voltage diminishes rather slowly in the same manner as shown in Fig. 5 for $V_0(x, t)$.

1.9 *Stratified Earth Structures*

In the foregoing, the earth was assumed to have a uniform resistivity ρ. In many cases the average resistivity near the surface along a route may be substantially greater or smaller than the resistivity at greater depths, and this condition may affect the nature of lightning troubles, as will be shown below.

The function $Q_0(r)$ appearing in equation (33) represents the earth

potential at a point due to unit current entering the earth at a distance r from the point; i.e. $Q_0(r)$ is the mutual resistance between two points on the earth's surface separated by the distance r. In the case of a two-layer horizontally stratified earth the function $Q_0(r)$ may be approximated by the following expression:

$$Q_0(r) = \frac{1}{2\pi r}[\rho_2 + (\rho_1 - \rho_2)e^{-\gamma_0 r}] \tag{47}$$

where

ρ_1 = Resistivity of upper layer, meter-ohms
ρ_2 = Resistivity of lower layer, meter-ohms
$\gamma_0 = k/2d$
d = Depth of upper layer, meters
k = Constant depending on the ratio ρ_1/ρ_2

When r is sufficiently small compared to d, the above expression approaches the limit $Q_0(r) = \rho_1/2\pi r$ and when r is sufficiently large compared to d the expression becomes $Q_0(r) = \rho_2/2\pi r$. Expression (47) gives a fair approximation to the function $Q_0(r)$ as given by curves calculated from rather complicated integrals.[13] Earth resistivity measurements by the so-called "four-electrode measurements" are based on measurements of $Q_0(r)$ and the results of such measurements may usually be approximated to the same degree of accuracy by (47) as by the curves applying accurately for two-layer earth, for the reason that the earth structure usually departs considerably from an ideal two-layer earth. For various ratios ρ_1/ρ_2 the constant k is about as follows:

$\rho_1/\rho_2 =$	100	10	1	.1	.02
$k =$	2	1.84	1.16	.4	.12

Inserting (47) in (33) and proceeding as before, the voltage between core and sheath due to a stroke at the distance y may be written:

$$V(0, y, t) = V(0, a, t)\frac{\rho_2\lambda(y) + (\rho_1 - \rho_2)\mu(y)}{\rho_2\lambda(a) + (\rho_1 - \rho_2)\mu(a)} \tag{48}$$

where $V(0, a, t)$ is the voltage for a direct stroke calculated for an equivalent earth-resistivity:

$$\rho_e = \rho_2\lambda(a) + (\rho_1 - \rho_2)\mu(a) \tag{49}$$

and where

$$\lambda(y) = \log[(1 + \Gamma y)/\Gamma y] \tag{50}$$

$$\mu(y) = \int_0^\infty \frac{1}{r} e^{-\alpha r} e^{-\Gamma x} dx \tag{51}$$

$$\backsimeq \log \frac{1 + y(\gamma_0 + \Gamma)}{y(\gamma_0 + \Gamma)} \quad \text{when} \quad \gamma_0 y \ll 1 \tag{52}$$

$$\backsimeq e^{-\gamma_0 y} \lambda(y) \quad \text{when} \quad \gamma_0 y \gg 1 \tag{53}$$

In applying the above expressions, a rough value of ρ_e is first assumed in calculating $\lambda(a)$ and $u(a)$ and a more accurate value next obtained from

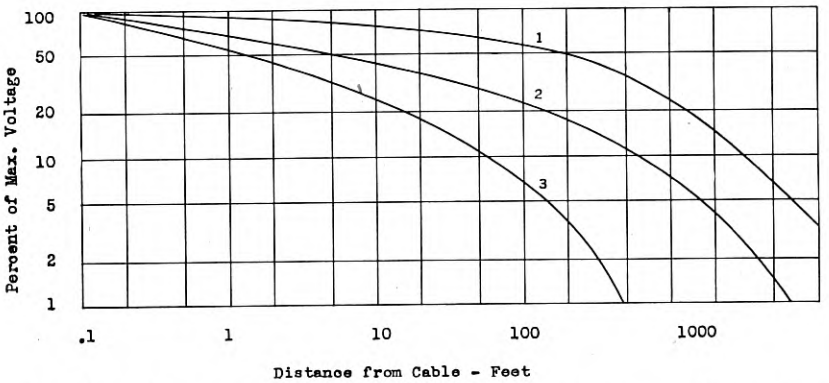

Figure 7—Reduction in voltage between sheath and core with increasing distance from cable to point where current enters ground.
1: Upper layer of 400 meter-ohms and 30 ft. depth. Lower layer of 4000 meter-ohms and infinite depth.
2: Uniformly conducting earth.
3: Upper layer of 1500 meter-ohms and 30 ft. depth.
Lower layer of 150 meter-ohms and infinite depth.

(49). If the value of ρ_e thus obtained differs materially from the assumed value, a second calculation may be required. In the expressions for λ and μ the resistivity ρ_e is to be used in calculating Γ, the latter being taken as $(\nu/2\rho_e t)^{\frac{1}{2}}$ where t is the time to crest value of the voltage as before.

In Fig. 7 is shown the manner in which the voltage decreases with increasing separation for three assumed earth structures. The resistivities and the depth of the upper layer were selected such that the equivalent earth-resistivity, and thus the voltage in the case of a direct stroke, is the same in all cases and equal to 1000 meter-ohms. It will be noticed that in the case where the resistivity of the lower layer is high, the voltage due to a stroke at a distance of 200 ft. is 50% and at a distance of 1000 ft., 25% of the voltage due to a direct stroke. When the cable is small, insulation failures may thus be occasioned by strokes to ground at considerable

distances from the cable, although the resistivity near the surface up to depths of say 50 ft. is only moderately high.

It is seen, however, that when the earth resistivity of the lower layer is low, failures due to strokes to ground not arcing to the cable are rather unlikely, even when the earth resistivity near the surface is rather high. On account of the higher surface resistivity, however, a greater number of strokes would be expected to arc to the cable for a given equivalent resistivity, than when the conductivity is uniformly distributed. On the other hand, many strokes which would arc to the cable if the earth were uniformly conducting may channel through the surface layer to the good conducting lower layer, so that the incidence of direct strokes is reduced on this account. Experience indicates that the latter factor tends to predominate, so that lightning damage is not ordinarily severe when the resistivity is low at depths beyond 20 ft. or so.

In the case of discharges between clouds the coupling between the lightning channel and the cable depends, in the frequency range of importance, to a great extent on the resistance of the lower layer. Thus, when the resistivity of the lower layer is very high the voltages may possibly give rise to insulation failures in the case of small cables, while this is not likely to occur when the resistivity of the lower layer is small or when the earth structure is uniform and of moderately high resistivity.

1.10 *Cables with Insulated Sheaths*

Assume that a short length Δx of insulated sheath is placed on the ground and that a voltage is applied between the sheath and a remote ground. When the applied voltage is greater than the breakdown voltage of the insulation, arcing to ground will take place at numerous equidistant points, provided the insulation and the earth are assumed to be uniform. The voltage between the sheath and adjacent ground increases from zero at a point where arcing takes place to a maximum value midway between two points at which arcing occurs, the maximum value being equal to the breakdown voltage of the insulation. Midway between two arcing points the potential in the earth (referred to infinity) may with negligible error be calculated as though the leakage current through the numerous arcs were uniformly distributed along the sheath. This potential in the ground would then be $\Delta I/G\Delta x$, where ΔI is the total leakage current and $1/G\Delta X$ the resistance to ground of the sheath without insulation, G being the unit length leakage conductance. Midway between the arcing points the potential of the sheath to a remote ground is then:

$$V = V_0 + \Delta I/\Delta x G \tag{54}$$

Let dI_0/dx be the leakage current through the arcs and dI_1/dx the leakage current due to capacity C between the sheath and the adjacent ground. For sinusoidal currents the following equations then hold, when Z is the unit length impedance and G the unit length leakance for a sheath in direct contact with the earth:

$$-\left(\frac{dI_0}{dx} + \frac{dI_1}{dx}\right)\frac{1}{G} + V_0 = V \tag{55}$$

$$-(I_0 + I_1)Z = \frac{dV}{dx} \tag{56}$$

$$-\frac{1}{i\omega C}\frac{dI_1}{dx} = V_0 \tag{57}$$

In the last equation it is assumed that the voltage between sheath and ground is equal to the breakdown voltage of the insulation, although this is not true in the immediate vicinity of the arcs.

Eliminating V the following equation is obtained:

$$\left(\frac{d^2 I_0}{dx^2}\frac{1}{G} - I_0 Z\right) + \left(\frac{d^2 I_1}{dx^2}\frac{1}{Y} - I_1 Z\right) = 0 \tag{58}$$

where:

$$\frac{1}{Y} = \frac{1}{G} + \frac{1}{i\omega C} \quad \text{or:} \quad Y = \frac{i\omega CG}{G + i\omega C}$$

Equation (58) is satisfied when:

$$\begin{aligned} I_0 &= A_0 e^{-\Gamma x} + B_0 e^{\Gamma x} \\ I_1 &= A_1 e^{-\Gamma_1 x} + B_1 e^{\Gamma_1 x} \end{aligned} \tag{59}$$

where Γ and Γ_1 are the propagation constants for a sheath in direct contact with the ground and for an insulated sheath without breakdown, respectively.

$$\Gamma = (GZ)^{\frac{1}{2}}, \qquad \Gamma_1 = (YZ)^{\frac{1}{2}}$$

For a sheath of infinite length the B_0 and B_1 terms vanish, so that:

$$I(x) = I_0 + I_1 = A_0 e^{-\Gamma x} + A_1 e^{-\Gamma_1 x} \tag{60}$$

The constants A_0 and A_1 are obtained from the following boundary conditions:

$$\text{At } x = 0 \qquad I(x) = I(0) = A_0 + A_1 \tag{61}$$

$$\text{As } x \to \infty \qquad I(x) \to A_1 e^{-\Gamma_1 x} = \frac{V_0}{K_1} e^{-\Gamma_1 x} \tag{62}$$

where $K_1 = (Z/Y)^{\frac{1}{2}}$ is the characteristic impedance of the insulated sheath without breakdown.

From (61) and (62)

$$A_1 = \frac{V_0}{K_1} \qquad A_0 = I(0) - \frac{V_0}{K_1} \tag{63}$$

So that:

$$I(x) = I(0)e^{-\Gamma x} + \frac{V_0}{K_1}(e^{-\Gamma_1 x} - e^{-\Gamma x}) \tag{64}$$

For a rubber insulated cable the breakdown voltage V_0 would be in the order of 30,000 volts and the characteristic impedance K_1 would be in the order of 100 ohms. The maximum current which could flow on the sheath without breakdown, V_0/K_1, is then about 300 amperes, while in the case of an average lightning stroke the current $I(0)$ would be about 15,000 amperes (i.e. 30,000 amperes total). The first term in (64) gives the attenuation along a sheath in direct contact with the ground. The current given by this term would diminish from 15,000 amperes to about 2,000 amperes within a distance of $\frac{1}{2}$ mile or so, for a typical lightning stroke wave shape and an earth resistivity of 1000 meter-ohms. At distances of several miles from the stroke point the first term will vanish and the current will be determined by the second term, since exp $(-\Gamma_1 x)$ will vanish much more slowly than exp $(-\Gamma x)$.

In the case of a stroke to ground the impressed electric force in the ground along the sheath is

$$E_0(x) = -dV_e(x)/dx \tag{65}$$

where V_e is the earth potential due to the lightning stroke current and is given by

$$V_e(x) = \frac{J\rho}{2\pi(x^2 + y^2)^{\frac{1}{2}}} \tag{66}$$

Instead of equation (58), the following equation is obtained for the currents in the sheath

$$\left(\frac{d^2 I_0}{dx^2}\frac{1}{G} - I_0 Z\right) + \left(\frac{d^2 I_1}{dx^2}\frac{1}{Y} - I_1 Z\right) = -E_0(x) \tag{67}$$

Writing $E_0(x) = cE_0(x) + (1 - c)E_0(x)$, the solution of the latter equation may be written as the sum of two solutions of the form given by (6) and (7). After the constants A_0, B_0 applying to the current I_0 and the constants A_1 and B_1 applying to the current I_1 have been determined from the boundary

conditions, in the same manner as before, the total sheath current may be written in the form:

$$I(x) = cI_g(x) + (1 - c)I_i(x) \tag{68}$$

where I_g is the current for a grounded sheath, I_i the current entering a perfectly insulated sheath by virtue of its capacity to ground and c is given by:

$$c = V_0/V^0 \cong V_0/V_e(0) \tag{69}$$

where V^0 is the potential difference between sheath and adjacent ground without breakdown at $x = 0$, which is substantially equal to the earth potential. The above relationship for the constant c is obtained by applying equation (57) at $x = 0$ to the general solution for I_1, V^0 being given by:

$$V^0 = \frac{G}{G + i\omega c} \int_0^\infty E_0(x)e^{-\Gamma_1 x}\, dx \tag{70}$$

The voltage between core and sheath of an insulated cable may be written in a similar manner when I_g is replaced by V_g, the voltage for a cable in direct contact with the ground, and I_i replaced by V_i, the voltage for a cable insulated from ground.

From (68) and (69) it will be seen that when $V_e(0)$ is much greater than the breakdown voltage of the insulation, the current entering the sheath is nearly the same as for a sheath in direct contact with the ground. Thus, when the earth resistivity is 1000 meter-ohms, and the stroke current 30,000 amperes, the earth-potential at a distance of 30 meters (100 feet) is 160,000 volts. The impulse breakdown of the insulation may be in the order of 30,000 volts, so that the current entering the sheath will be substantially the same as for a cable in direct contact with the soil. When the earth-potential at $x = 0$ is only slightly larger than the breakdown voltage of the insulation, however, the current entering the sheath through punctures in the insulation is fairly small.

In the above derivation the voltages and currents were assumed to vary sinusoidally which, of course, is a rather rough approximation in a phenomenon where breakdown occurs after the voltage reaches a certain instantaneous value. While the derivation is not accurate, it does indicate under what conditions an insulated cable behaves like a cable in direct contact with the ground.

1.11 *Oscillographic Observations of Lightning Voltages*

To obtain data on the characteristics of lightning voltages in buried cable, five magnetic string oscillographs were installed for one lightning

season along a 50-mile section of the Stevens Point-Minneapolis route. The oscillographs, which were arranged to trip where the voltage exceeded 100 volts, recorded lightning voltages due to some 600 strokes on 38 days, the Weather Bureau average being 33 thunderstorm days for this region in the same months. The character of the voltages varied widely from sharp transients of a few millisecond duration to slowly changing voltages lasting .2 seconds from one zero value to the next, voltages due to multiple discharges being quite common, the interval between voltage peaks in such cases being in the order of .1 second. Of the disturbances, 90% lasted for more than .1 second, 50% for more than .4 and 10% for more than 1.25 second, the maximum duration being 2.3 seconds. By way of comparison, the observed duration of discharges to a tall structure (3) were, in respectively 90, 50 and 10% of all cases, in excess of .08, .3 and .6 second, the maximum duration being 1.5 second. The maximum voltage recorded was 940 volts and was probably due to a stroke to ground near the cable. About 2% of the voltages were in excess of 500 volts, most of these and the lower voltages being due to discharges between clouds, as indicated by the opposite polarity of the voltages at the two ends of the test section. The wave shape of the voltages at the ends of the section were much the same as at intermediate points, even for the sharpest surges recorded, the attenuation along the core-sheath circuit being quite small. It is possible that substantially higher voltages than observed may obtain in the case of severe discharges along a path parallel to and directly above the cable, and that such voltages may produce cable failure if the core insulation is below normal.

While the oscillographs were arranged to trip on 100 volts, a smaller voltage was recorded in 40% of all cases, as the peaks were too fast to be recorded by the type of oscillograph used. It is also possible that for this reason fast voltage peaks in excess of the maximum given above may have escaped measurement.

II. Lightning Trouble Expectancy

2.1 *General*

In estimating the liability of a cable to lightning damage, it is assumed below that once the core insulation is punctured, as it is likely to be at several points, at least one permanent failure will occur. The lightning trouble expectancy curves presented here thus give the number of times lightning damage is likely to occur, without consideration of the extent of the damage on each occasion. Each case of lightning damage usually involves several pairs and, based on experience, repair of each such case would require about four sheath openings. Damage due both to direct strokes and strokes to ground is included. Discharges between clouds have been neglected as a

source of lightning damage, however, as the voltages are likely to be insufficient unless the insulation is below normal.

The curves of lightning trouble expectancy calculated here are significant only if troubles on a long cable route are considered over a period of several years, so that the mile-years covered are in the order of 1000 or more.

2.2 *Incidence of Strokes to Ground*

To estimate the lightning trouble expectancy it is necessary to consider the incidence of strokes to ground in the vicinity of the cable, the number

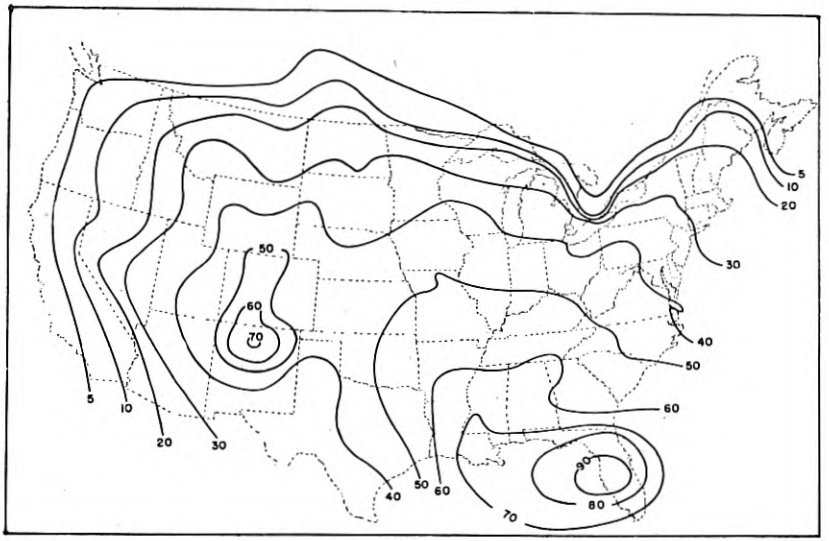

Figure 8—Map showing the average number of thunderstorm days per year.

of such strokes that will arc to the cable and cause damage in this manner and the number that will give rise to failure without arcing to the cable.

Magnetic link measurements (14) indicate that high tension transmission lines will be struck by lightning about 113 times per 100 miles per year, on the average, the minimum incidence in one year being about one half and the maximum about 1.6 times the average value. The above average incidence is based on observations covering about 1600 mile-years and applies for lines traversing areas where some 35 thunderstorm days are expected per year, as indicated by data issued by the U. S. Weather Bureau and collected over a period of 30 years,[15] and shown in Fig. 8. The above data on strokes to transmission lines may be used to estimate the rate of lightning strokes to ground, provided the width of the zone within which a transmission line will attract lightning can be determined.

Based on laboratory observations on small-scale models[16, 17, 18, 19], a line above ground will attract lightning strokes within an average distance on each side of the line which is about 3.5 times the height of the line when the cloud is positive and about 5.5 times the height when the cloud is negative. When the average height of a transmission line ground structure above ground is taken as 70 feet, a 100-mile line will thus attract positive strokes (i.e., strokes originating from a positive cloud) within an area of about 9.3 square miles and negative strokes within an area of approximately 14.5 square miles.

About 15% of the strokes to transmission line ground structures have positive polarity,[4, 5] so that the average rate of positive strokes to ground would be about 1.8 and that of negative strokes about 6.6 per square mile per year. The rate of positive and negative strokes to ground would thus be about 8.4 per square mile per year in areas where the yearly number of thunderstorm days is about 35, corresponding to about 2.4 strokes per square mile per 10 thunderstorm days.

Based on the above date, the ratio of negative to positive strokes to ground in open country would be 3.6. The ratio of negative to positive strokes has been determined by various investigators in different ways.[7] The ratio derived from measurement of field changes during thunderstorms varies between 2.1 and 6.5, that obtained from voltages observed in antennas is about 2.9, while point discharge recorder measurements indicate a ratio of 3.5 and the magnetization of basalt rocks struck by lightning indicates a ratio of 2.25. The above data were obtained in the temperate zone; in the tropics nearly all strokes have negative polarity.

2.3 *Arcing to Cable of Strokes to Ground*

As the stepped leader of a lightning discharge approaches the earth, charges accumulate in the ground under the leader and the resulting flow of current in the ground will give rise to a potential difference between points in the ground under the leader and remote points. Thus, when the tip of the leader has approached within 10 meters off the ground and the leader current is assumed to be as high as 500 amperes and the earth resistivity to be 1000 meter-ohms, a point directly under the leader will have a potential of 8000 volts with respect to a remote ground. The potential gradient along the surface of the ground would, of course, be affected by the presence of a buried cable. The total potential involved is, however, so small that the effect of a buried cable on the path of the leader would be entirely negligible compared to the effect of irregularities in the surface of the earth. As the tip of the leader contacts the ground, the potential may be large enough so that the leader may arc to a cable located within 2 ft. or so of the leader. Only

after the return stroke is initiated, however, is the potential large enough so that arcing will occur for appreciable distances.

When a stroke current J enters the ground, the electric force in the ground at the distance r from the stroke point is given by

$$E(r) = J\rho/2\pi r^2 \tag{71}$$

ρ being the earth resistivity. If the breakdown voltage gradient of the soil is e_0, breakdown of the soil will take place until $E(r) = e_0$, or for a distance:

$$r_0 = (J\rho/2\pi e_0)^{\frac{1}{2}} \tag{72}$$

For a distance r_0 around the stroke point the soil may then be regarded as a conductor of negligible resistivity.

The resistance encountered by the lightning channel in the ground is then

$$R_0 = \frac{\rho}{2\pi r_0} = \left(\frac{\rho e_0}{2\pi J}\right)^{\frac{1}{2}} \tag{73}$$

Measurements of the surge characteristics of grounds of fairly small dimensions[20, 21] indicate that the breakdown voltage of the soil may vary from roughly 1000 volts per cm to some 5000 volts/cm. The data are, however, quite limited and there is no assurance that the above values represent the limits. In the first of the papers referred to, measurement was made of the resistance encountered when a current of 10,000 amperes crest value was discharged into the ground from an electrode suspended above the ground. The measured resistance is in satisfactory agreement with that obtained from (73) using the earth resistivity and breakdown voltage determined from other measurements in the paper referred to. In connection with the present study some small scale measurements were made of the breakdown voltage of sand between plane electrodes, and of the resistance encountered in discharges into the sand over point electrodes. These measurements indicated a breakdown voltage of 5000 volts per cm for dry sand having a resistivity of 3700 meter-ohms and 2400 volts/cm when sufficient water was added to reduce the resistivity to 100 meter-ohms. The measured resistance of point electrodes was a satisfactory agreement with that calculated from (73) on the basis of the measured resistivities and breakdown voltages. These experiments were made with currents having crest values from 1 to 50 amperes.

Measurements of the breakdown voltage of various types of soil between completely buried spherical electrodes indicate substantially higher voltages than those given above, from about 11 to 23 kv/cm.[22] It is possible that for surface electrodes, breakdown at the lower voltage gradients occurs along the surface of the ground, so as to form a conducting plane of radius

r_0. This circumstance would change the preceding formulas only to the extent that 2π would be replaced by 4. For a given e_0, the resistance would then be about 25% higher.

The radius r_0 is not necessarily the same as the distance across which a lightning stroke would arc to a cable in the vicinity. Streamers will extend in various directions beyond r_0 so that ionization of the soil increases the conductivity for a greater distance, r_0 being the effective radius of an equivalent hemisphere of infinite conductivity.

The potential difference between the conducting sphere of radius r_0 and a point at the distance r_1 is

$$V_{01} = \frac{J\rho}{2\pi}\left(\frac{1}{r_0} - \frac{1}{r_1}\right) = \frac{J\rho}{2\pi}\frac{r_1 - r_0}{r_1 r_0} \tag{74}$$

Let it be assumed that streamers extend beyond r_0 until the average voltage gradient between r_0 and r_1 equals e_1. The potential difference is then:

$$V_{01} = e_1(r_1 - r_0) \tag{75}$$

From (74) and (75):

$$r_1 = \frac{J\rho}{2\pi r_0 e_1} = r_0\frac{e_0}{e_1} \tag{76}$$

The latter expression applies when the field is assumed to have a radial symmetry about the lightning channel. When a buried cable is present, however, this symmetry is disturbed. Calculations indicate that the potential of the cable at the point nearest to the lightning stroke will be less than 20% of the earth potential at the same point if the cable were absent. As a first approximation the cable may, therefore, be considered to have zero potential. The potential difference between the sphere considered above and the cable is then:

$$V_{02} = \frac{J\rho}{2\pi}\frac{1}{r_0} \tag{77}$$

If r_2 is the distance from the channel to the cable, the potential difference is also given by:

$$V_{02} = e_1(r_2 - r_0) \tag{78}$$

From (77) and (78):

$$r_2 = r_0\left(1 + \frac{e_0}{e_1}\right) \tag{79}$$

The arcing distance calculated in this manner will be the maximum, while that calculated from (76) will be the minimum distance.

From measurements made of the effective corona radius of a conductor in air,[22] it is found that the latter may be determined on the assumption that

breakdown occurs until $e_0 \leqq 14000$ volts/cm. On the other hand it is known that arcing between two conductors a considerable distance apart will occur when the average gradient is about 10,000 volts/cm. For air the ratio e_0/e_1 is thus about 1.4. For breakdown in the air, the ionization need not be very dense in order that the corona envelope may be regarded as conducting as regards displacement currents. For breakdown in the earth, however, the ionization must be much more complete in order to provide substantially better conductivity than the soil. The ratio e_0/e_1 is, therefore, likely to be greater, and has been taken as 2 in the following.

If the latter ratio is assumed for soil, it is seen by comparison of (76) and (79) that the presence of a cable may increase the arcing distance as much as 50%.

The arcing distance may be written in the form

$$r_1 = (J\rho)^{\frac{1}{2}} q_1, \qquad r_2 = (J\rho)^{\frac{1}{2}} q_2 \tag{80}$$

where:

$$q_1 = \left(\frac{1}{2\pi e_0}\right)^{\frac{1}{2}} \frac{e_0}{e_1}, \qquad q_2 = \left(\frac{1}{2\pi e_0}\right)^{\frac{1}{2}} \left(1 + \frac{e_0}{e_1}\right) \tag{81}$$

With $e_0/e_1 = 2$ the following values are obtained

$e_0 =$	250,000	500,000 volts/meter
$q_1 =$	$1.6 \cdot 10^{-3}$	$1.13 \cdot 10^{-3}$
$q_2 =$	$2.4 \cdot 10^{-3}$	$1.7 \cdot 10^{-3}$

Values of q_1 and q_2 about 25% greater than those given above are obtained by assuming that breakdown does not take place in the soil, but that a conducting plane of radius r_0 is formed by ionization of the air near the ground. Expression (71) is in this case replaced by $E(r) = J\rho/4r^2$ and the expressions for q become

$$\begin{aligned} q_1 &= \left(\frac{1}{4e_0}\right)^{\frac{1}{2}} \frac{e_0}{e_1} \\ q_2 &= \left(\frac{1}{4e_0}\right)^{\frac{1}{2}} \left(1 + \frac{e_0}{e_1}\right) \end{aligned} \tag{82}$$

In the following $q = 2.5 \cdot 10^{-3}$ has been taken as representative for low-resistivity soil and $q = 1.5 \cdot 10^{-3}$ for high-resistivity soil. When the current is expressed in kiloamperes, the corresponding values are .08 and .047.

The distance to which a stroke may arc is accordingly taken as:

$\rho \leq 100$ meter-ohms	$\rho \geq 1000$ meter-ohms
$r = .08\ (J\rho)^{\frac{1}{2}}$ meter	$r = .047\ (J\rho)^{\frac{1}{2}}$ meter
$= .26\ (J\rho)^{\frac{1}{2}}$ feet	$= .15\ \ (J\rho)^{\frac{1}{2}}$ feet

where J is in kiloamperes.

These values are, of course, of an approximate nature, and are only indicative of what may be expected under average conditions. In some cases the breakdown voltage of high-resistivity soil may be substantially lower than assumed, while that of low-resistivity soil may be noticeably higher.

2.4 *Crest Current Distribution for Strokes to Ground*

When the earth resistivity is taken as high as 5000 meter-ohms and the breakdown voltage of the soil is taken as high as 5000 volts/cm, the resistance encountered by the channel on the ground for a current of 25,000 amperes is about 250 ohms. If the lightning channel were a long conductor already in existence at the initiation of the return stroke and capable of carrying the stroke current without being fused, the current would be propagated upward with the velocity of light and the surge impedance of the channel would be in the order of 500 ohms. Due to the resistance in the ground the current would then be some 30% smaller than for a stroke to an object of zero resistance to ground. However, the lightning channel may not be regarded in the above manner, but as a conductor which is gradually prolonged at about 1/10 the velocity of light, and the impedance of the channel is then much larger, perhaps 5000 ohms. The surge impedance of a long insulated conductor having unit length capacitance C is $(1/Cv)$, v being the velocity of propagation. When energy is required to create the conductor, so that the velocity of propagation is reduced, the impedance is increased. Because of the high impedance of the channel, the resistance encountered in the ground may, therefore, be neglected as regards the effect on the crest current. The crest current distribution curve for strokes to transmission line ground structures may thus be used also in the case of strokes to ground, although a different distribution curve is obtained for those of the strokes to ground which arc to buried cable (Section 2.7).

2.5 *Failures Due to Direct Strokes and Strokes to Ground*

In calculating the number of failures due to direct strokes and strokes to ground, the earth is assumed to be a plane surface. A tree placed at random may attract a lightning stroke toward a cable or it may divert it from the cable and the net effect of a large number of trees along a route of substantial length is likely to be small. This is also true for variations in the terrain.

When N is the number of lightning strokes to ground per unit of area, and s the length of the cable, the number of lightning strokes on both sides of the cable within y and $y + dy$ is:

$$dN = 2Ns\,dy \tag{83}$$

A lightning stroke at the distance y will cause cable failure when the crest current i exceeds a certain value which depends on the distance:

$$i = f(y) \tag{84}$$

The fraction of all lightning strokes which has a crest current larger than i will be designated $P_0(i)$. The fraction of the lightning strokes dN which will cause cable failures is then:

$$dn = dNP_0(i) = 2NsP_0(i)\,dy \tag{85}$$

The number of cable failures along the length s due to all lightning strokes to ground up to the maximum distance Y that need to be considered is:

$$n = 2Ns \int_0^Y P_0(i)\,dy \tag{86}$$

For the purpose of computation it is convenient to change the variable in the latter integral from y to i. With $y = f^{-1}(i) = y(i)$, $di = dy \cdot f'(y)$, $i_0 = f(0)$ and $I = f(Y)$, the following integral is obtained:

$$n = 2Ns\left[YP_0(i) - \int_{i_0}^{I} y(i)P_0'(i)\,di\right] \tag{87}$$

In (87), I is the maximum stroke current that needs to be considered and may actually be replaced by infinity, as will be evident later on. The current i_0, which is the minimum current that will cause insulation puncture in the case of a direct stroke, may readily be determined from the breakdown voltage of the insulation and the calculated voltage between core and sheath per kiloampere, in the manner illustrated in Section 2.4.

In order to evaluate the integral of (87), it is divided as follows:

$$n = 2Ns\left[YP_0(I) - \int_{i_0}^{i_1} y_1(i)P_0'(i)\,di - \int_{i_1}^{I} y_2(i)P_0'(i)\,di\right] \tag{88}$$

When $i < i_1$, failures of the cables will be due to arcing of the stroke to the cable and when $i > i_1$, failures will occur before arcing takes place, due to the leakage current entering the sheath. Within each of the above two ranges the relationship of y to i is different and is designated $y_1(i)$ and $y_2(i)$, respectively.

As already shown, failures due to arcing will take place when:

$$y_1(i) \leq q(\rho i)^{\frac{1}{2}} \tag{89}$$

where q is defined as before and ρ is the earth resistivity in meter-ohms.

In Section 1.7 it was shown that failures due to leakage current will occur when

$$i \geq i_0/\lambda(y)$$

where

$$\lambda(y) = \log\left(\frac{1 + \Gamma y}{\Gamma y}\right) \Big/ \log\,(1/\Gamma a)$$

Γ being the propagation constant of the sheath-earth circuit and a the radius of the sheath. The solution of the latter equation for y is:

$$y = y_2(i) = \frac{1}{\Gamma(e^{mi_0/i} - 1)} \backsimeq \left(\frac{2\rho t}{\nu}\right)^{\frac{1}{2}} \frac{1}{e^{mi_0/i} - 1} \tag{90}$$

where

$m = \log\,(1/a\Gamma)$
$\Gamma \backsimeq (\nu/2\rho t)^{\frac{1}{2}}$ per meter
$\nu = 1.256 \cdot 10^{-6}$ henries per meter
$t \backsimeq 10^{-4}$ sec. $\backsimeq$ time to crest of core-sheath voltage.

When (89) and (90) are equated, the following expression is obtained:

$$i^{\frac{1}{2}}(e^{mi_0/i} - 1) = \left(\frac{2t}{\nu q^2}\right)^{\frac{1}{2}} \tag{91}$$

The value of i which satisfies the latter equation is the value i_1 defined above, and is shown in Fig. 9 as a function of mi_0 for various values of $(2t/\nu q^2)^{\frac{1}{2}}$.

When (89) and (90) are inserted in (88), the latter integral may be expressed as follows:

$$n = 2Ns\rho^{\frac{1}{2}}\left(q[H(i_0) - H(i_1)] + \left(\frac{2t}{\nu}\right)^{\frac{1}{2}} G(i_1, mi_0)\right) \tag{92}$$

where the current is in kiloamperes and:

N = Number of strokes to ground per square meter
s = Length of cable in meters
$q \backsimeq .08$ when $\rho \leq 100$, $q \backsimeq .047$ when $\rho \geq 1000$.

$$H(i) = -\int_i^I i^{\frac{1}{2}} P_0'(1)\, di \tag{93}$$

$$G(i, mi_0) = \frac{P_0(I)}{e^{mi_0/I} - 1} - \int_i^I \frac{P_0'(i)\, di}{e^{mi_0/i} - 1} \tag{94}$$

The first term in (94) equals $YP_0(I) = y_2(I)P_0(I)$. Since $P_0'(i)$ is negative, the above integrals will have positive values.

The term $q[H(i_0) - H(i_1)]$ of (92) gives the portion of failures due to direct strokes while the term involving the function G gives the portion of failures due to ground strokes not necessarily arcing to the cable although

they may do so (i.e. many of the currents in excess of i_1 may arc to the cable, although this is not essential in order to produce cable failure).

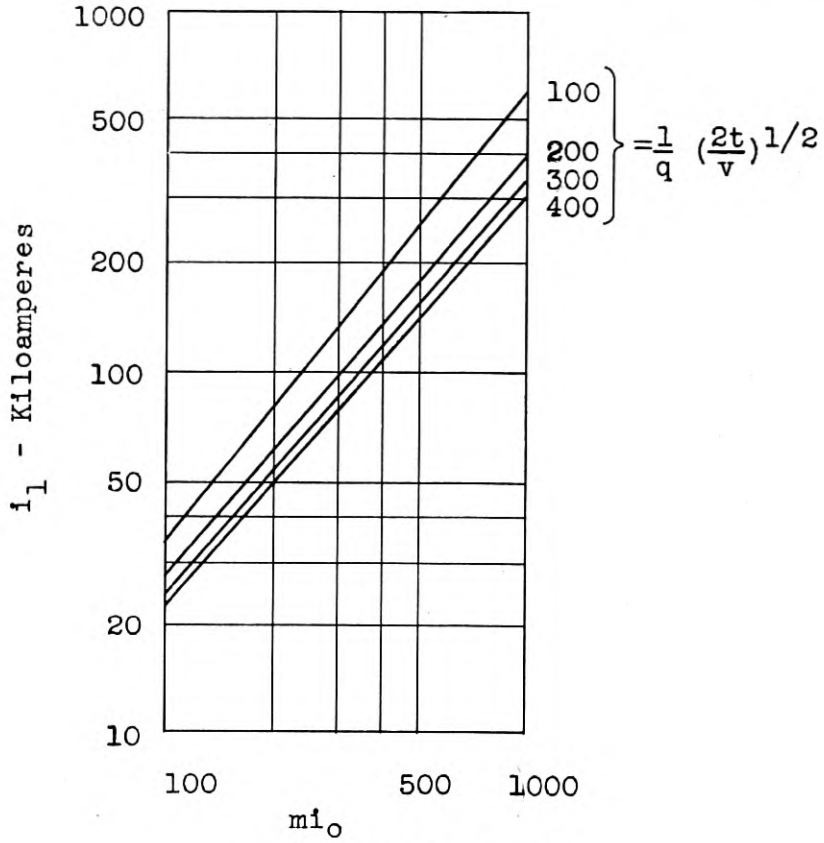

Figure 9—Solution of the equation:

$$i_1^{\frac{1}{2}}(e^{mi_0/i_1} - 1) = \frac{1}{q}\left(\frac{2t}{\nu}\right)^{\frac{1}{2}}$$

If strokes to ground not arcing to the cable were neglected as a source of failures, the number of failures would equal:

$$n_d = 2Ns\rho^{\frac{1}{2}}qH(i_0) \tag{95}$$

If, on the other hand, the dielectric strength of the earth were assumed to be infinite, so that none of the strokes to ground would arc to the cable, the number of failures would equal

$$n_g = 2Ns\rho^{\frac{1}{2}}\left(\frac{2t}{\nu}\right)^{\frac{1}{2}} G(i_1, mi_0) \tag{96}$$

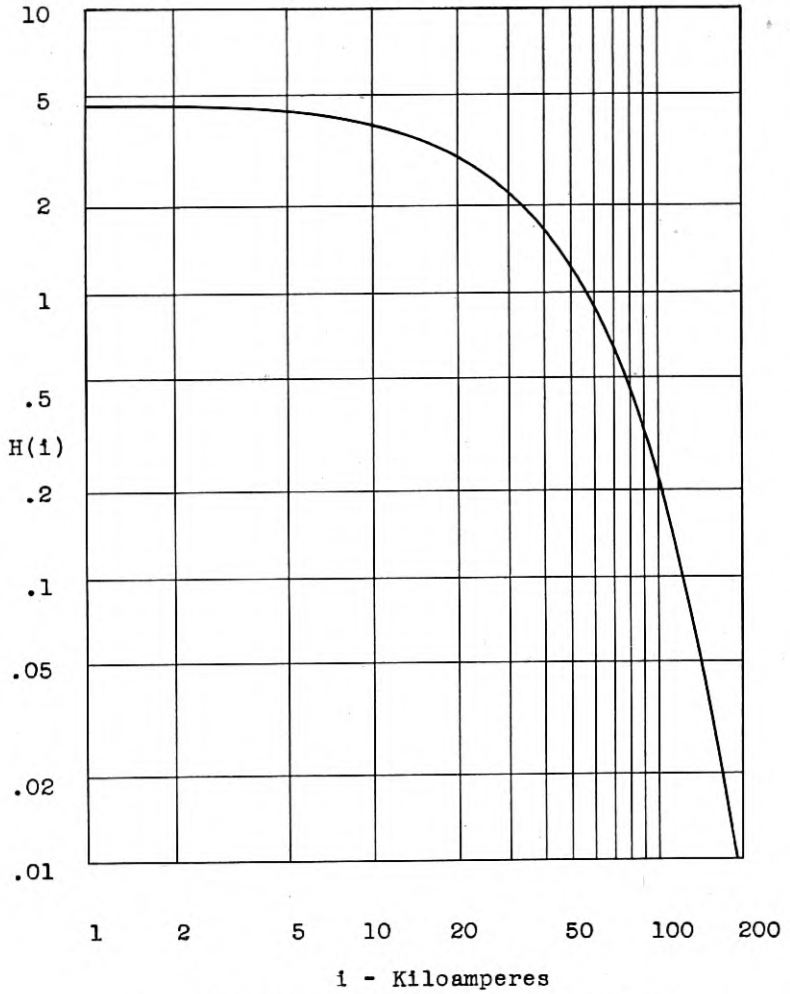

Figure 10—Function $H(i)$ when $P_0(i)$ is approximated by:
$P_0(i) = \exp(-ki)$, $k = .038$ per kiloampere.
$H(i) = k^{-\frac{1}{3}}[(ki)^{\frac{1}{3}}e^{-ki} + \frac{1}{2}\pi^{\frac{1}{3}}\operatorname{erfc}(ki)^{\frac{1}{3}}]$

From Fig. 1, it is seen that $P_0(i)$, as represented by curve 1, is nearly a straight line on semi-log paper and may, therefore, be approximated by:

$$P_0(i) \backsimeq e^{-ki} \tag{97}$$

With $k = .038$ per kiloampere, a straight line is obtained which coincides with curve 1 at $i = 0$ and $i = 100$ kiloamperes, and this value of k has been used in the following. The functions H and G obtained with this approximation are shown in Figs. 10 and 11. In obtaining these integrals, the up-

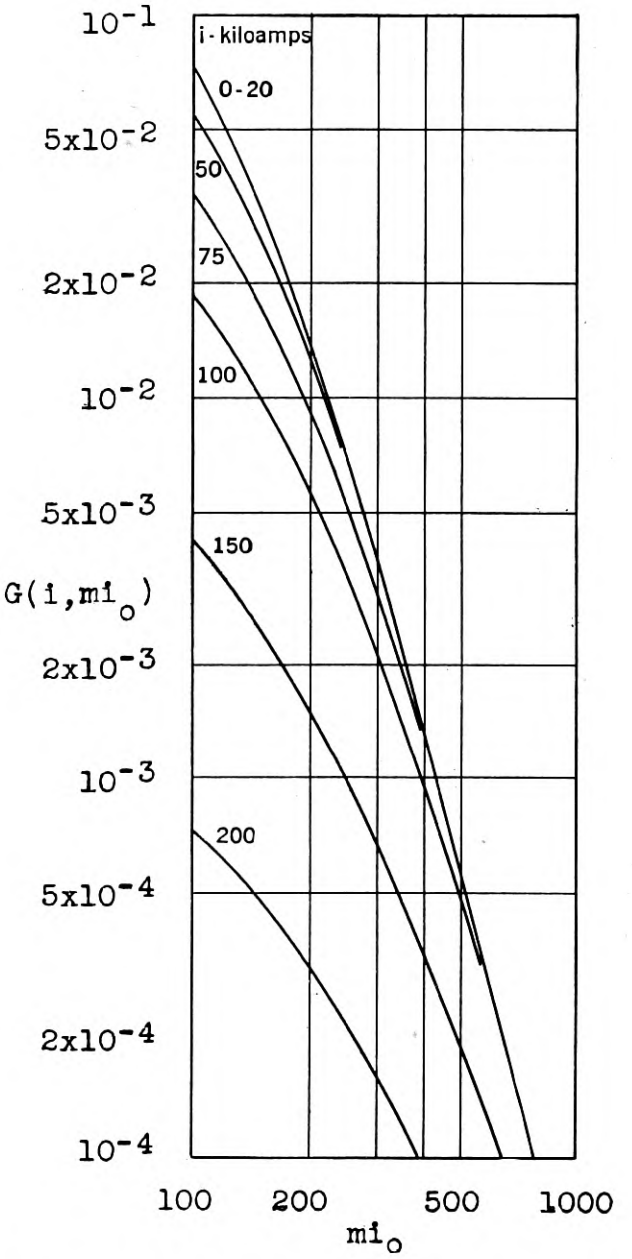

Figure 11—Function $G(i, mi_0)$ when $P_0(i)$ is approximated by: $P_0(i) = \exp(-ki)$; $k = .038$ per kiloampere.

$$G(i, mi_0) = k \int_i^\infty \frac{e^{-ki}\, di}{e^{mi_0/i} - 1}$$

per limit I may be replaced by infinity, and it is also seen that the first term in (94) then vanishes.

The lightning trouble expectancy as calculated from (92) is shown in Fig. 12 as a function of the earth resistivity for various sheath resistances. The curves are based on 2.4 strokes to ground per square mile, which is approximately the number of strokes per square mile during 10 thunderstorm days. The number of thunderstorm days per year along a given route is obtained from Fig. 8 and thus the number of times lightning failures would be expected during one year.

2.6 *Expectancy of Direct Strokes*

The incidence of direct strokes to the cable may be obtained from (96) with $i_0 = 0$ kiloamperes.

The number of strokes arcing to the cable is thus

$$n_a = 2Ns\rho^{\frac{1}{2}}qH(0) \tag{98}$$

The cable will thus attract strokes within an effective distance.

$$y = \rho^{\frac{1}{2}}qH(0) \tag{99}$$

$\rho \leq 100$ meter-ohms	$\rho \geq 1000$ meter-ohms
$y = .365\ \rho^{\frac{1}{2}}$ meters	$y = .22\ \rho^{\frac{1}{2}}$ meters
$= 1.2\ \rho^{\frac{1}{2}}$ feet	$= .7\ \rho^{\frac{1}{2}}$ feet

2.7 *Crest Current Distribution for Direct Strokes*

The fraction of the strokes to the cable having crest values in excess of i is given by:

$$\begin{aligned} P(i) &= H(i)/H(0) \\ &= 2\left(\frac{ik}{\pi}\right)^{\frac{1}{2}} e^{-ik} + \operatorname{erfc}(ik)^{\frac{1}{2}} \end{aligned} \tag{100}$$

and is shown by curve 2 in Fig. 1. It will be noticed that a buried cable attracts a greater proportion of heavy currents than a transmission line, because of the circumstance that heavy currents to ground arc for greater distances.

2.8 *Lightning Trouble Experience*

As mentioned before, lightning damage may be due to denting or to fusing of holes in the sheath, or to excessive voltages between the sheath and the cable conductors. Only the latter form of lightning failures have been considered here, since they predominate for cable of the size now being used, particularly in high-resistivity areas, and are likely to extend for a considerable distance to both sides of the point struck by lightning and are

thus more difficult to repair. For full-size cable in low-resistivity areas, however, insulation failures are more likely to occur as a result of sheath denting. For instance, along the 300-mile Kansas City-Dallas full-size cable route, where the earth resistivity is in the order of 100 meter-ohms, and where there are some 50 thunderstorm days per year, failures over a period of about 15 years have occurred about .5 times per 100 miles per year. Of these troubles 85% were due to sheath denting as a result of arcing between the tape armor and the sheath. Based on (99), 100 miles of cable would attract lightning strokes within an area of .5 square mile, so that the cable would be struck about six times per 100 miles per year, when the number of strokes per square mile per year is 2.4 per 10 thunderstorm days (Section 2.2). The rate of lightning failures experienced on this route may thus be accounted for by assuming that about 7% of the strokes, i.e. currents in excess of 90 kiloamperes as obtained from curve 2, Fig. 1, will produce sheath denting severe enough to cause insulation failure, while about 1%, i.e. currents in excess of 140 kiloamperes, will cause insulation failure due to excessive voltage. The latter value is in substantial agreement with that calculated for a full-size cable when the earth resistivity is assumed to be 100 meter-ohms. It is evident from the above examples that in low-resistivity areas lightning troubles will not be a problem, and this is also borne out by experience on other routes installed in such territory during the last few years.

All cable installed in high-resistivity territory since 1942 has been provided with doubled core insulation and with shield wires, in spite of which considerable damage has been experienced on some routes, as between Atlanta and Macon. This appears to have been due partly to the circumstance that in many cases the insulation in splices and accessories has not been equal to that obtained in the cable through the use of extra core wrap, and that in some cases damage has been due to holes fused in the sheath due to arcing between the sheath and the shield wires. As an example, along the Atlanta-Macon route there are some 70 thunderstorm days per year and the average effective earth resistivity is about 1300 meter-ohms. The corresponding estimated rate of direct strokes to the cable is about 20 per 100 miles per year. It is estimated, in the manner outlined in section 3.0, that only stroke currents in excess of 80 kiloamperes are likely to damage the cable, so that on the basis of curve 2, Fig. 1, cable failures would be expected to occur about 2 times per 100 miles per year. The actual rate of trouble experienced on this route over two years has been about five times higher, so that some 50% of the strokes to the cable; i.e., currents in excess of 30 kiloamperes or so, appear to have caused cable failures, most of which occurred in splices and accessories.

It is evident from the above examples that careful examinations of trouble records are required before the observed rate of lightning failures can be adequately compared with that obtained from theoretical expectancy curves. If the cable as well as splices and accessories actually have a dielectric strength as assumed in the calculations, it is likely that the average rate of failures due to excessive voltages experienced over a long period will not be any greater than estimated from these curves.

Based on experience, an average of 4 sheath openings is required to repair damage caused by excessive voltage between the sheath and the cable conductors, as compared to about 2 sheath openings when the damage is due mainly to denting and fusing of the sheath, as in the case of full-size, tape-armored cable in low-resistivity territory. Although the damage may be confined to one point, it cannot usually be located by a single sheath opening.

III. Remedial Measures

3.1 *General*

From Fig. 12 it is evident that the rate of cable failures to be expected, and hence the need for remedial measures, depend greatly on the earth resistivity. Experience has indicated that lightning damage is likely to be encountered even when the surface resistivity is fairly low, provided the resistivity beyond depths of 10 or 20 ft. or so is very high. Considerably less trouble has been experienced where the resistivity below this depth is low, even where the surface resistivity has been high. The lightning stroke may then channel through the surface layer to the good conducting lower layer, so that direct strokes are not experienced as frequently in spite of the high surface resistivity. As a guide in applying protective measures, earth resistivity measurements are usually made along new cable routes.[23]

The curves given in Fig. 12 may also be used to find the lightning trouble expectancy when extra core insulation, shield wires or both are used. Thus when the insulation strength is doubled the effect is the same as if the sheath resistance is halved. If the shield wires reduce the voltage by a shield factor η, the effect is the same as if the sheath resistance is multiplied by η. Considering direct strokes only, curve 2 in Fig. 1 may be used to find the percentage reduction in lightning strokes that will damage the cable, when the stroke current which the cable is able to withstand is increased by extra insulation or shield wires.

3.2 *Extra Core Insulation*

One method of reducing failures caused by lightning strokes to buried cables is to increase the insulation between the cable conductors and the

sheath, no extra insulation being required between individual cable conductors. This has already been done for most new installations. The cable itself, cable stubs, loading cases, and gas alarm contactor terminals are all provided with sufficient extra insulation to double the dielectric strength between cable conductors and sheath. For a cable like that on which the measurements referred to before were made, such a measure would increase the stroke current which would damage the cable from 30,000 to 60,0000 amperes and would reduce the number of direct lightning strokes that could cause failure by direct arcing to the sheath to about 20

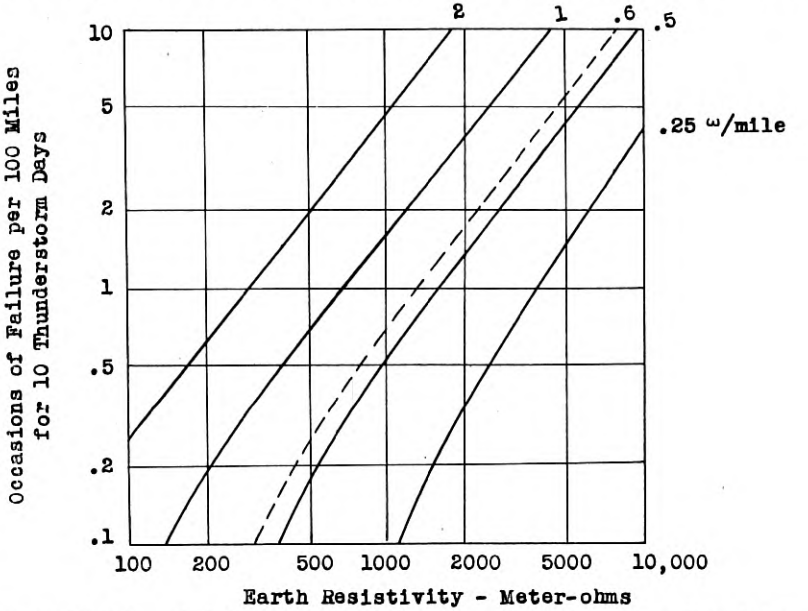

Figure 12—Theoretical lightning trouble expectancy curves showing number of times insulation failures due to excessive voltages would be expected per 100 miles for 10 thunderstorm days, for cables having sheath resistances as indicated on curves. Dashed line represents full-size cable.

per cent of the total instead of 50 per cent (see Fig. 1, curve 2). The number of failures due to direct strokes would thus have been reduced 2.5 times.

3.3 *Shield Wires*

Another method, employed in addition to the extra insulation where excessive lightning damage would otherwise be expected, is to bury shield wires over the cable. These conduct away part of the lightning current and thus reduce the amount that flows along the sheath. These wires may be plowed in with the cable, as has been done on several new routes, or may be installed afterward. When the wires and cables are plowed in

together, the arrangement shown in Fig. 13 has been used. The percentage of the current carried by the wires depends to a greater extent on their inductance relative to that of the sheath, than on their resistance. Two wires are employed, rather than a single wire of smaller resistance, in order to obtain a lower inductance than with a single wire.

On the route between Stevens Point and Minneapolis, where the shield wires were installed after the cable was in place, two 165-mil wires about twelve inches apart were plowed in some ten inches above the cable for a distance of eighty miles. Surge measurements made after these wires were installed indicated that the wires reduced the voltage between sheath and core conductors about 60 per cent, in substantial agreement with theoreti-

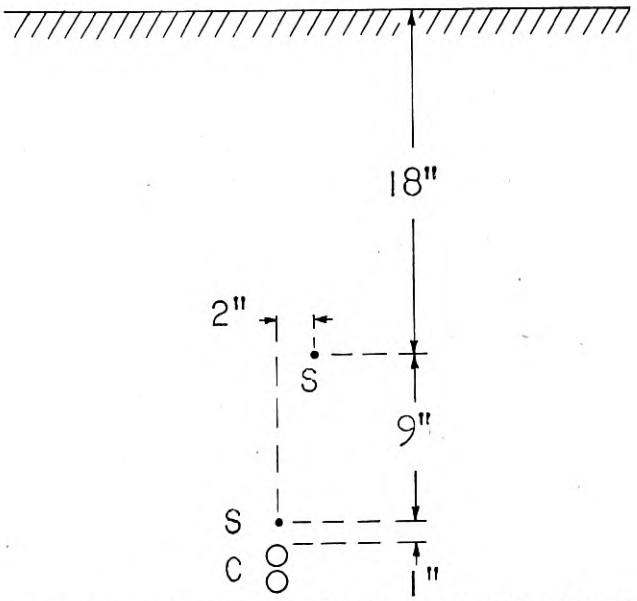

Figure 13—Position of shield wires, *S*, when they are plowed in with cable, *C*.

cal expectations. The cable would then withstand 75,000 amperes rather than 30,000 without shield wires. If a cable of normal construction were used on the above route, the shield wires would thus reduce the number of direct lightning strokes that would be expected to cause insulation failure about 3.3 times, from 50 per cent of the total without shield wires to about 15 per cent with shield wires (see Fig. 1, curve 2). If the insulation strength is only 1000 volts, however, about 80 per cent of all strokes would be expected to cause failure without shield wires and 40 per cent with shield wires, so that the reduction would be substantially smaller, as actually appears to be the case on the above route.

Aside from reducing core insulation failures, shield wires also minimize

damage to the sheath covering in the case of strokes to ground near the cable, particularly in the case of thermoplastic or rubber-covered cables. As mentioned in section 1.10, considerable current may enter the sheath of an insulated cable in the case of strokes to ground near the cable, due to numerous punctures in the insulation of the sheath. If conditions along the cable were uniform, the current through each puncture would be so small that the insulation would not be damaged. Due to variations in the resistivity of the soil and the presence of buried metallic structures, however, concentrated arcing may occur, and the insulation may then be damaged in spots, so that corrosion may be initiated. Shield wires reduce the voltage between the sheath and ground and thus the likelihood of damage to the sheath insulation.

It can be demonstrated theoretically, and has been proved by measurements, that when current enters shield wires next to a buried cable in good contact with the earth, the current in the sheath and the voltage between sheath and cable conductors is negligible. The reason for this is that current induced in the sheath by the shield wire current is equal and opposite to the current entering the sheath by virtue of leakage through the ground. Negligible voltages between sheath and core conductors would thus be obtained if shield wires were installed at such a distance that lightning strokes would be intercepted and direct strokes to the cable prevented. To prevent arcing to the cable of strokes to the shield wires, the separation between cable and shield wires would have to be at least 6 feet when the earth resistivity is 1000 meter-ohms, and greater for higher resistivities. Such wires cannot, therefore, be as easily installed in one plowing operation with the cable as shield wires at a smaller spacing. They are, therefore, not considered here, although they have been installed in one instance in a fairly short section where repeated lightning damage had been experienced.

When the sheath, as well as the shield wires, is in intimate contact with the earth, the propagation constant for the shield wires is the same as that for the sheath. In the case of a direct stroke to the cable or the shield wires, the voltage between sheath and shield wires will be so large that they will be in contact with each other at the stroke point by virtue of arcing. The current in the sheath is then:

$$I(x) = \frac{J}{2} \frac{Z_{22} - Z_{12}}{Z_{11} + Z_{22} - 2Z_{12}} e^{-\Gamma x} \tag{101}$$

where J is the total current at $x = 0$, and

$Z_{11} = R_1 + i\omega L_{11}$ = Unit length impedance of sheath

$Z_{22} = R_2 + i\omega L_{22}$ = Unit length impedance of shield wires

$Z_{12} = i\omega L_{12}$ = Unit length mutual impedance of sheath and shield wires

The voltage between sheath and core conductors at $x = 0$ then becomes:

$$\begin{aligned} V(0) &= \frac{J}{2}\frac{R}{\alpha^{\frac{1}{2}}+\beta^{\frac{1}{2}}}\frac{Z_{22}-Z_{12}}{Z_{11}+Z_{22}-2Z_{12}}\left(\frac{1}{i\omega}\right)^{\frac{1}{2}} \\ &= \frac{J}{2}\frac{R}{\alpha^{\frac{1}{2}}+\beta^{\frac{1}{2}}}\eta\left(\frac{1}{i\omega}\right)^{\frac{1}{2}}\frac{p+\alpha_0}{p+\beta_0} \end{aligned} \tag{102}$$

where

$$\eta = (L_{22} - L_{12})/(L_{11} + L_{22} - 2L_{12}) \tag{103}$$

$$\alpha_0 = R_2/(L_{22} - L_{12}) \tag{104}$$

$$\beta_0 = (R_1 + R_2)/(L_{11} + L_{22} - 2L_{12}) \tag{105}$$

The function S' is in this case

$$S'(0, t) = \frac{J}{2}\frac{R}{\alpha^{\frac{1}{2}}+\beta^{\frac{1}{2}}}\eta\left[\left(\frac{1}{\pi t}\right)^{\frac{1}{2}} + \frac{\alpha_0-\beta_0}{\beta_0^{\frac{1}{2}}}h(\beta_0^{\frac{1}{2}}t^{\frac{1}{2}})\right] \tag{106}$$

where the function h is defined as before.

When the shield wires are at a sufficient distance from the sheath, so that proximity effects may be neglected, the self and mutual inductances are as follows:

$$L_{11} - L_{12} = \frac{\nu}{2\pi}\log\frac{r_{12}}{r_{11}} \tag{107}$$

$$L_{22} - L_{12} = \frac{\nu}{2\pi}\log\frac{r_{12}}{r_{22}} \tag{108}$$

where

log = $\log_e$ and:

ν = $1.256 \cdot 10^{-6}$ henries per meter

r_{11} = Radius of sheath

r_{22} = Radius of shield wire

r_{12} = Distance between sheath and shield wire.

With more than one shield wire, r_{22} is the geometric mean radius and r_{12} their geometric mean separation from the sheath. When there are two cables, as is frequently the case, r_{11} is the geometric mean radius of the cables and R is their combined sheath resistance.

The surge voltage obtained by solution of (1), for a current as given by (19), is in this case:

$$\begin{aligned} V(0, t) = \frac{IR\eta}{2(\alpha^{\frac{1}{2}}+\beta^{\frac{1}{2}})}\Bigg[&\frac{a-\alpha_0}{a-\beta_0}a^{\frac{1}{2}}h(a^{\frac{1}{2}}t^{\frac{1}{2}}) \\ &- \frac{b-\alpha_0}{b-\beta_0}b^{-\frac{1}{2}}h(b^{\frac{1}{2}}t^{\frac{1}{2}}) + \frac{(\alpha_0-\beta_0)(b-a)}{(a-\beta_0)(b-\beta_0)}\beta_0^{-\frac{1}{2}}h(\beta_0^{\frac{1}{2}}t^{\frac{1}{2}})\Bigg] \end{aligned} \tag{109}$$

When $\alpha_0 = \beta_0$, the voltage with shield wires differs from that obtained without shield wires by the factor η. With two 165-mil wires 12 inches apart and 10 inches above the cable considered before, $\alpha_0 = 1.3 \cdot 10^3$, $\beta_0 = 1.5 \cdot 10^3$ and $\eta = .47$. In this case α_0 differs only slightly from β_0 so that the voltage is reduced by the factor η. Measurements made before and after the shield wires were installed indicated a reduction factor of .40 (i.e. the voltage with was .4 times the voltage without shield wires). The reasons for the smaller observed factor is partly that the shield wires are in more intimate contact with the earth than the sheath, and partly that the resistivity of the soil above the cable, where the shield wires are located, is somewhat smaller than the resistivity at the depth of the cable.

With 104-mil wires, $\alpha_0 = 3.2 \cdot 10^3$, $\beta_0 = 2.3 \cdot 10^3$ and $\eta = .49$. When the reduction factor is determined more accurately by calculating the crest voltage with shield wires from (109) and comparing it with the crest voltage without shield wires, a value of .52 is obtained as compared with .47 for 165-mil wires. It is thus seen that, within certain limits, the voltage reduction provided by shield wires depends to a comparatively small extent on the size of the wires, the resistance of 104-mil wires being about 2.5 times that of 165-mil wires.

3.4 *Lightning-Resistant Cable*

As mentioned before, buried cable may be covered by jute, thermoplastic, or rubber for protection against corrosion. The coating may be damaged by gophers or by lightning, and severe corrosion may be experienced at points where the coating is ruptured, particularly when thermoplastic or rubber coating is used. Even when the earth resistivity is low and protection against core insulation failures due to excessive voltage would not be required, the sheath coating may be damaged rather frequently.

Shield wires may effect a substantial reduction in core insulation failures and may also prevent damage to the coating in the case of strokes to ground at some distance from the cable. In the case of direct strokes, however, arcing between the shield wires and the sheath will damage the sheath coating and may also fuse a hole in the sheath, although there may be no insulation failures due to excessive voltage between the sheath and the cable conductors.

Reduction of damage to the coating and to the sheath occasioned by lightning, rodents, or corrosion and protection against core insulation failures occasioned by excessive voltage or crushing of the sheath may be secured by providing the sheath with a thermoplastic or rubber coating and an outside copper shield. If various auxiliary equipment connected to the sheath, such as load coils, gas pressure contactors and terminals are also properly

insulated from ground, currents will not then enter the sheath, except through the capacitance to the outside shield. The voltage across the core insulation will then be so small that core insulation failures will not occur, unless the voltage between the outside shield and the sheath is large enough to puncture the coating. Thus, if the resistance of the outside shield were 1.1 ohms per mile (10-mil copper shield around 1.2″ cable) and if the impulse breakdown voltage of the coating were 20,000 volts, breakdown of the insulation would not be expected except for currents in excess of 130 kiloamperes when the earth resistivity is as high as 4000 meter-ohms. For a cable of 2″ diameter with a 10-mil copper shield, breakdown of the thermo-

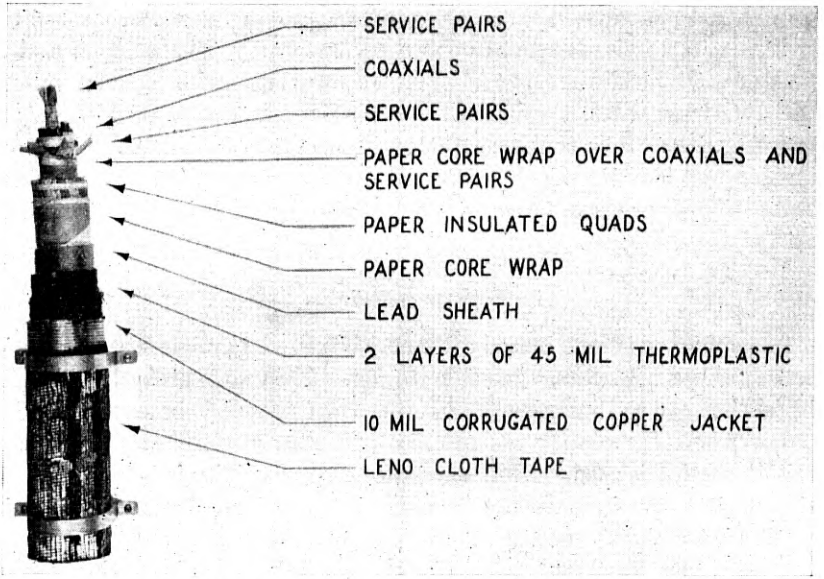

Figure 14—Thermoplastic covered, copper jacketed cable.

plastic insulation would not be expected except for currents in excess of 200 kiloamperes when the breakdown voltage of the coating is 20 kv and the earth resistivity is 4000 meter-ohms, or when the breakdown voltage is 10 kv and the earth resistivity 1000 meter-ohms. The above type of cable is also advantageous in that low-frequency induced voltages and noise due to static are reduced.

A cable of the above type is now being installed for a distance of about 180 miles along the Atlanta-Meridian route, where the effective earth resistivity varies between 1000 and 4000 meter-ohms and lightning storms occur frequently. The diameter of the lead sheath of this cable is about 2″, and the sheath is covered with two layers of thermoplastic each 45 mils

thick, with diametrically opposite seams having an overlap of about $\frac{1}{2}''$. The outside 10-mil copper shield is corrugated to facilitate bending and has a $\frac{1}{4}''$ overlap at the seam. The thermoplastic coating is flooded with thermoplastic cement to reduce moisture absorption. A photograph of this cable is shown in Fig. 14.

SUMMARY

Current in the sheath of buried cables, due to direct lightning strokes, strokes to ground near the cables or discharges between clouds, gives rise to voltages between the cable conductors and the sheath. The voltages are practically proportional to the square root of the earth resistivity and to the direct-current sheath resistance. For the latter reason they are substantially larger for carrier cables of the size now used than for the much larger voice-frequency cables. While direct strokes are usually most important, strokes to ground must be considered when the cables are of small size, even when the surface resistivity is low, provided the resistivity at greater depths is high. Under the latter conditions it is possible that for small cables, discharges between clouds over the cable may also cause failure.

For cables with thermoplastic or rubber coating the voltages between the sheath and the core conductors are much the same as for jute-covered cables. The coating of such cable is likely to be damaged by direct strokes and strokes to ground near the cable, in which case corrosion of the sheath may occur at such points.

Based on theoretical lightning expectancy curves, the incidence of lightning troubles increases faster than the sheath resistance or the earth resistivity. When the breakdown voltage of the core insulation is doubled by use of extra core wrap, or when shield wires are installed in situations where lightning damage is anticipated or has been experienced, a substantial reduction in lightning failures is to be expected. Shield wires will, however, not prevent damage to the sheath and the sheath coating.

Where the earth resistivity is very high and lightning storms occur frequently, doubled core insulation together with shield wires may not provide sufficient protection, even for cable of substantial size. Protection against various forms of lightning damage may then be secured by use of thermoplastic sheath coating of adequate dielectric strength together with an outside concentric copper shield.

REFERENCES

1. E. D. Sunde: "Lightning Protection of Buried Cable," *Bell Telephone Laboratories Record*, Vol. 21, No. 9, May 1943.
2. B. F. J. Schonland: "The Lightning Discharge," Clarendon Press, Oxford, England, 1938 or "Thunderstorms and Their Electrical Effects," *Proc. of the Phys. Soc.*, Vol. 55, Part 6, No. 312, Nov. 1, 1943.

3. K. B. McEachron: "Lightning to the Empire State Building," *Electrical Engineering*, Dec. 1938 and Sept. 1941.
4. W. W. Lewis and C. M. Foust: "Lightning Investigations on Transmission Lines" VIII—*A.I.E.E. Trans.*, Vol. 64, 1945, p. 107.
5. H. Grünewald: C.I.G.R.E. 1939, Report 323.
6. C. F. Wagner and G. D. McCann: "Lightning Phenomena," *Elec. Engg.*, Aug., Sept. and Oct. 1941.
7. C. E. R. Bruce and R. Golde: "The Mechanism of the Lightning Stroke and its Effect on Transmission Lines," *Jour. I.E.E.*, Part II, Dec. 1941.
8. E. D. Sunde: "Surge Characteristics of a Buried Bare Wire," *A.I.E.E. Transactions*, Vol. 59, 1940 or *Bell Telephone System Monograph* B-1279.
9. S. A. Schelkunoff: "Electromagnetic Theory of Coaxial Transmission Lines and Cylindrical Shield," *Bell System Technical Journal*, October, 1934. Equation (5) is equivalent to Equation (82) of the above paper.
10. G. A. Campbell and R. M. Foster: "Fourier Integrals for Practical Applications," *Bell Telephone System Monograph* B-584, pair 807.
11. E. D. Sunde: "Currents and Potentials Along Leaky Ground Return Conductors," *Elec. Engg.*, December 1936 or *B.T.S. Monograph* B-970.
12. J. R. Carson: "Wave Propagation in Overhead Wires with Ground Return," *Bell Sys. Tech. Jour.*, October 1926. Z obtained by use of (34) and (35) and M by use of (36) and (37) of the paper referred to.
13. J. Riordan and E. D. Sunde: "Mutual Impedance of Grounded Wires for Stratified Two-Layer Earth," *Bell System Technical Journal*, April 1933 or *B.T.S. Monograph* B-726.
14. E. Hansson and S. K. Waldorf: "An Eight-Year Investigation of Lightning Currents and Preventive Lightning Protection on a Transmission System" presented at A.I.E.E. 1944 Winter Convention.
15. W. H. Alexander: "The Distribution of Thunderstorms in the United States, 1904–33," *Monthly Weather Review*, Vol. 63, 1935, page 157.
16. A. Matthias: "Modellversuche über Blitzeinschläge," *E.T.Z.* Aug. 12 and Sept. 9, 1937.
17. A. Matthias and W. Burkhardtsmaier: "Der Schutzraum von Blitzfang-Vorrichtungen und seine Ermittlung durch Modellversuche," *E.T.Z.*, June 8 and June 15, 1939.
18. C. F. Wagner, G. D. McCann and G. L. MacLane, Jr.: "Shielding of Transmission Lines", *A.I.E.E. Trans.*, Vol. 60, 1941, p. 313–328.
19. C. F. Wagner, G. D. McCann and C. M. Lear: "Shielding of Substations," *A.I.E.E. Trans.*, Vol. 61, 1942, p. 196–200.
20. P. L. Bellaschi, R. E. Armington and A. E. Snowden: "Impulse and 60-cycle Characteristics of Driven Grounds—II," *A.I.E.E. Trans.*, Vol. 61, 1942, p. 349.
21. R. Davis and T. E. M. Johnston: "Surge Characteristics of Tower Footing Impedance," *J.I.E.E.* Vol. 88, Part II, No. 5, Oct. 1941.
22. I. R. Eaton: "Impulse Characteristics of Electrical Connections to the Earth," *General Electric Review*, Oct. 1944, p. 41–50.
23. G. D. McCann: "The Effect of Corona on Coupling Factors between Ground Wires and Phase Conductors," *A.I.E.E. Trans.*, Vol. 62, 1943, p. 818–826.
24. G. Wascheck: "Earth Resistivity Measurements," *Bell Telephone Laboratories Record*, Vol. 19, No. 6, Feb. 1941.

Abstracts of Technical Articles by Bell System Authors

Ultra-Short-Wave Receiver for the Cape Charles-Norfolk Multiplex Radiotelephone Circuit.[1] D. M. BLACK, G. RODWIN and W. T. WINTRINGHAM. The requirements for an ultra-short-wave receiver for use in a multiplex radiotelephone link circuit are outlined. The technical details of a receiver designed to meet such requirements in the circuit between Cape Charles and Norfolk, Virginia, are described.

Ultra-Short-Wave Multiplex.[2] CHARLES R. BURROWS and ALFRED DECINO. The technical requirements of a twelve-channel ultra-short-wave multiplex system are discussed and the means of meeting them are described. The intermodulation between channels in equipment based on this design has been reduced to the point where it is possible to use twelve-channel radio systems in the toll plant. By employing a sufficient amount of envelope feedback, the transmitter can be operated with a high modulation factor without the use of spread sidebands.

Airplane Vibration Reproducer.[3] G. R. CRANE. This paper describes a reproducer set designed for use in the reproduction for analysis of multiple track film recordings. It is capable of reproducing simultaneously 13 variable-area tracks recorded side by side on standard 35-mm. film. Recorded signals between 5 and 3000 cps are accurately reproduced and may be analyzed for frequency components, amplitude, and phase relation.

Airplane Vibration Recorder.[4] J. C. DAVIDSON and G. R. CRANE. This paper describes a portable film recorder capable of simultaneously recording 13 variable-area tracks on 35-mm. film. It is intended for use in the analysis of airplane vibration or similar studies in which it is desirable to record disturbances (mechanical, acoustical, or electrical) from a number of sources in such a manner that the resultant record can be analyzed for frequency, amplitude, and phase relation. Film speeds of 12, 6, or 3 in. per sec. are available.

Application of Sound Recording Techniques to Airplane Vibration Analysis.[5] J. G. FRAYNE and J. C. DAVIDSON. This paper describes methods which have been developed for analysis of the various vibration components present in airplane structures. The complex wave forms are recorded on standard motion picture sound negatives during flight. These films later,

[1] *Proc. I. R. E.*, February 1945.
[2] *Proc. I. R. E.*, February 1945.
[3] *Jour. S. M. P. E.*, January 1945.
[4] *Jour. S. M. P. E.*, January 1945.
[5] *Jour. S. M. P. E.*, January 1945.

after proper development, are analyzed electrically, making possible a complete analysis on the ground and thereby reducing materially the time devoted to flight test, and also simplifying the process of analysis of complex wave forms.

Ultra-Short-Wave Transmitter for the Cape Charles-Norfolk Multiplex System.[6] R. J. KIRCHER and R. W. FRIIS. Design features of an unattended ultra-short-wave double-sideband multiplex transmitter are described. Forty decibels of envelope feedback is utilized over the 12- to 60-kilocycle band of the twelve type-K carrier-signal channels which modulate the last stage of the transmitter. Accessibility of apparatus and ease in maintenance contribute toward obtaining maximum reliability of the equipment in commercial service.

Paper Capacitors Containing Chlorinated Impregnants. Stabilization by Anthraquinone.[7] D. A. MCLEAN and L. EGERTON. This paper shows anthraquinone to be an effective stabilizer for capcitors having paper dielectrics containing chlorinated impregnants when aluminum electrodes are used and d-c. potentials are applied. One half per cent of anthraquinone prevents formation of the usual carbonized brown spots in the paper, and diminishes corrosion of electrodes and instability of leakage current. It increases the life under accelerated testing conditions by factors of four to one hundred fold, depending upon materials used and conditions of test. This development has added appreciably to the reliability of paper capacitors containing chlorinated impregnants, particularly for military equipment where high temperatures and high voltages are often encountered simultaneously. Solubility of anthraquinone in the usual chlorinated impregnants is limited. Where greater solubility is desired, the more soluble chloro and methyl derivatives can be used.

Reflex Oscillators.[8] J. R. PIERCE. This paper discusses qualitatively the behavior of reflex oscillators. Power production, electronic tuning, variation of frequency with resonator voltage, effect of modulation coefficient, and influence of load are considered. Two brief mathematical appendixes are included.

Cape Charles-Norfolk Ultra-Short-Wave Multiplex System.[9] N. F. SCHLAACK and A. C. DICKIESON. This paper describes the general features of a radio multiplex system which has been installed between Cape Charles and Norfolk, Virginia. The radio-frequency equipment operates in the vicinity of 160 megacycles. The system employs the 12 telephone channels of the type K cable carrier system which are in the frequency range 12 to 60 kilocycles.

[6] *Proc. I. R. E.*, February 1945.
[7] *Indus. & Engg. Chem.*, January 1945.
[8] *Proc. I. R. E.*, February 1945.
[9] *Proc. I. R. E.*, February 1945.

Contributors to this Issue

I. E. FAIR, B.S. in Electrical Engineering, Iowa State College, 1929. Bell Telephone Laboratories, Radio Research Department, 1929–. Mr. Fair has been engaged in the study of piezoelectric crystals and crystal oscillators.

C. W. HARRISON, B.S. in Electrical Engineering, Purdue University, 1938; M.S., Lehigh University, 1940. Bamberger Broadcasting Service, 1939–41; Bell Telephone Laboratories, 1941–. Engaged in the development of communication circuits.

E. D. SUNDE, B.S., Haugesund, Norway, 1922; E.E., Darmstadt, Germany, 1926. American Telephone and Telegraph Company, 1927–33; Bell Telephone Laboratories, 1933–. Mr. Sunde has been engaged in studies of interference in telephone circuits from power lines and railway electrification and is now concerned with studies of protection of the telephone plant against lightning damage.